# The fate of benzo(*a*)pyrene-induced oxidative DNA damage in the testis of transgenic mice

by Silja Meier

Master thesis in Toxicology
Department of Toxicology and Ecophysiology
Institute of Biology
University of Oslo
August 2008

## Acknowlegdements

The work presented in this thesis was carried out at the Department of Chemical Toxicology, Division of Environmental Medicine, Norwegian Institute of Public Health during the time period from August 2006 to August 2008 for the Master's Degree in Toxicology. My primary supervisor has been scientist Ann-Karin Olsen PhD and my co-supervisors have been Department Director Gunnar Brunborg PhD and Scientist Nur Duale MSc. Professor Steinar Øvrebø PhD at the Department of Toxicology and Ecophysiology, Institute of Biology, University of Oslo has served as my supervisor at the University.

I would like to give my gratitude to Ann-Karin Olsen for being a great mentor and a source of inspiration and knowledge. Your enthusiasm and support have been of great value to me. Because of you, I now know what I want to do for the rest of my life.

My gratitude goes to Gunnar Brunborg for constantly pushing my boundaries, and forming me into a scientist. Your knowledge is irreplaceable. My big thanks to Nur Duale for giving me lots of help and encouragement in real-time.

My thanks go to everyone at the department, for the warm, cheerful and welcoming environment. You have been an inspiration, and I am grateful for all help in the laboratory and for all smiles and insightful conversations. PhD-student Siri Helland Hansen deserves my special thanks for invaluable help and support, and for being so caring. My thanks go to Christine Maass for our great discussions and conversations, I dearly value our friendship. I also want to thank my study companion Elin Ansok for all our laughs.

My love goes to my family and friends, for supporting and encouraging me, and for just being there. I am very grateful to my fiancée Henning Kulander, who has motivated and supported me during all my ups and downs and still wants to marry me.

Oslo, August 2008

Silja Meier

# Contents

# Summary

Disease in the male reproductive system seems to increase in industrialised countries. Examples are increasing rates of poor semen quality, and more cases of testicular cancer, - with Denmark and Norway having the World's highest rates. Male reproductive health is crucial for the ability to reproduce, and these changes gives rise to concern. This project studies whether - and how - environmental factors contribute to this development. In particular, we have investigated genotoxic effects of one specific compound, benzo(*a*)pyrene (BaP), using several experimental approaches.

BaP, which is a carcinogen present in cigarette smoke, is among the agents proposed to mediate negative effects on reproduction. Smoking causes DNA damage in sperm such as BaP DNA adducts, known to be transmitted to the early embryo. BaP can also lead to oxidised base damage through generation of reactive oxygen species (ROS).

One would expect the cells of the male germ line to be able to preserve the integrity of their DNA by exhibiting active DNA repair. This is however not the case with respect to excision repair. Human male germ cells exhibit low or non-functional nucleotide transition repair (NER) as well as limited repair of oxidised DNA such as 7,8-dihydro-8-oxodeoxyguanosine (8-oxoG) by base excision repair (BER). The consequences and importance of these characteristics in the testes are not known. In particular, it is essential to understand whether human male germ cells are particularly sensitive to genotoxic agents in the environment.

We have previously proposed a transgenic mouse line to be used as a model for human male reproductive toxicity. The enzyme 8-oxoguanine-DNA glycosylase (Ogg1; the mammalian homologue of *E. coli* Fpg) removes oxidised base lesions such as 8-oxoG. The functional homologue has been disrupted in the mouse line, giving rise to repair deficient ($Ogg1^{-/-}$) animals mimicking the normal human male with respect to repair of oxidative DNA lesions in the testis.

In this work we have examined whether exposure to BaP (150 mg/kg i.p.) leads to oxidative DNA lesions in the testes *in vivo,* in both $Ogg1^{-/-}$ and $Ogg1^{+/+}$ mice. A mechanical method for isolating nuclei was established, allowing analysis of DNA damage by the comet assay. To better understand the response in the testis, the expression of selected genes involved in the metabolism of BaP was measured with real-time RT PCR. The genes included *Akr1a4*

(required for induction of oxidised DNA) as well as *Cyp1a1*, *-1a2* and *-1b1* (required for induction of bulky DNA adducts). We found that BaP did indeed induce statistically increased levels of oxidative DNA damage in the testis of *Ogg1*$^{-/-}$ mice at day 17 after the exposure. DNA damage was also induced in somatic tissues such as the lung, and there were indications of damage in the liver (not significant). Such damage was not observed in wild type (*Ogg1*$^{+/+}$) mice. Gene expression analysis of *Akr1a4* and *Cyp1a1* showed that these gene products were induced in the testis and liver of both genotypes, to variable degrees, implying that BaP may be metabolised to induce DNA adducts as well as oxidised base damage in these tissues. Hence, the data corroborate the fact that increased levels of oxidised base damage were found in the testis. Both *Cyp1a2* and *-1b1* were induced in the liver of both genotypes. In the testis, a different pattern was observed; *Cyp1a2* was not clearly induced in the testis of *Ogg1*$^{-/-}$ mice, and was down-regulated in the testis of *Ogg1*$^{+/+}$ mice. *Cyp1b1* was induced neither in the testis of *Ogg1*$^{-/-}$ nor *Ogg1*$^{+/+}$ mice.

We also studied the *in vivo* repair of Fpg-sensitive DNA lesions in *Ogg1*$^{-/-}$ and *Ogg1*$^{+/+}$ mice exposed to X-rays (10 Gy), as part of evaluating the *Ogg1*$^{-/-}$ mouse model. Results from the *in vivo* repair experiment showed that repair of Fpg-sensitive sites was not detectable in the testis, liver or lung of *Ogg1*$^{-/-}$ mice following X-rays, indicating no significant back-up repair by alternative repair pathways in these tissues. As expected, *Ogg1*$^{+/+}$ mice did repair Fpg-sensitive sites.

Taken together, we have established experimental protocols for DNA damage analysis after *in vivo* exposure, that are highly suitable for large-scale animal experiments and inter-laboratory collaborations. Our results show that BaP gives rise to oxidative DNA lesions in testicular cells of *Ogg1*$^{-/-}$ mice; this could explain the elevated levels of such lesions observed in sperm of smoking men. The *Ogg1*$^{-/-}$ mouse model obviously requires further evaluation, but our results give strength to the belief that it could serve as a model for human male germ cells in the study of possible effects of genotoxic agents.

# Abbreviations

| | |
|---|---|
| 5-OHC | 5-hydroxycytosine |
| 8-oxoG | 7,8-dihydro-8-oxodeoxyguanosine |
| ABP | Androgen binding protein |
| AhR | Aryl hydrocarbon receptor |
| AKR | Aldo-keto reductase |
| AKR1A1 | Aldehyde reductase 1A1 |
| ANOVA | Analysis of variance |
| AP endonuclease | Apurinic/apyrimidinic endonuclease |
| AP site | Apurinic/apyrimidinic site (abasic site) |
| APS | Ammonium persulphate |
| ARNT | Aryl hydrocarbon receptor nuclear translocator |
| ATP | Adenosine triphosphate |
| BaP | Benzo(*a*)pyrene |
| BER | Base excision repair |
| BPDE | 7,8-dihydroxy-9,10-epoxy-7,8,9,10-tetrahydrobenzo(*a*)pyrene |
| BSA | Bovine serum albumin |
| CG | Cytosine glycol |
| CT | Cycle threshold |
| CYP | Cytochrome P450 |
| dATP | Deoxyadenosine triphosphate |
| dCTP | Deoxycytosine triphosphate |
| dGTP | Deoxyguanine triphosphate |
| $dH_2O$ | Distilled water |
| DMSO | Dimethyl sulphoxide |

| | |
|---|---|
| DNA | Deoxyribonucleic acid |
| dRP | 5´-deoxyribose phosphate |
| DSB | Double strand break |
| dTTP | Deoxythymidine triphosphate |
| *E. coli* | *Escherichia coli* |
| EDTA | Ethylenediaminetetraacetic acid |
| ESCODD | European Standards Committee on Oxidative DNA Damage |
| EtBr | Ethidium bromide |
| FaPyG | 2,6-diamino-4-hydroxy-5-formamidopyrimidine |
| FCS | Foetal calf serum |
| FEN1 | Flap endonuclease 1 |
| Fpg | Formamidopyrimidine-DNA glycosylase, also called MutM |
| FSH | Follicle stimulating hormone |
| GC-MS | Gas chromatgraphy-mass spectrometry |
| GGR | Global genome repair |
| GST | glutathione S-transferase |
| Gy | Gray |
| HAP1 | Human AP-endonuclease 1 |
| HPG | Hypothalamus-pituitary-gonadal |
| HPLC-EC | High performance liquid chromatography-electrochemical detection |
| HR | Homologous recombination |
| i.p. | Intraperitoneal |
| ICSI | Intracellular sperm injection |
| IVF | *in vitro* fertilisation |
| kDa | kiloDalton |

| | |
|---|---|
| $LD_{50}$ | Lethal dose 50% |
| LET | Linerar energi transfer |
| LH | Luteinising hormone |
| LPR | Long-patch repair |
| MGMT | $O^6$ methylguanine-DNA transferase |
| MMR | Mismatch repair |
| MRP1 | Multidrug-resistance-associated protein 1 |
| MutM | See Fpg |
| MutT | 8-oxoGTPase |
| MutY | Adenine-DNA glycosylase |
| NADPH | Nicotinamide adenine dinucleotide phosphate |
| NEIL | Nei-like protein |
| NER | Nucleotide excision repair |
| NHEJ | Non-homologous end joining |
| NTH1 | Thymine glycol-DNA glycosylase 1 (human version of endonuclease III/Nth) |
| OGG1 | 8-oxoguanine-DNA glycosylase |
| PAGE | Polyacrylamide gel electrophoresis |
| PAH | Polycyclic aromatic hydrocarbon |
| PBS | Phosphate buffer solution |
| PCNA | Proliferating cell nuclear antigen |
| PCR | Polymerase chain reaction |
| Polβ | DNA polymerase β |
| RCF | Replication Factor C |
| RNA | Ribonucleic acid |
| ROS | Reactive oxygen species |
| RPMI | Roswell Park Memorial Institute |

| | |
|---|---|
| rRNA | Ribosomal RNA |
| RT | Reverse transcriptase |
| SDS | Sodium dodecyl sulphate |
| SLS | Sodium lauryl sarcosinate |
| SOD | Superoxide dismutase |
| SPR | Short-patch repair |
| SSB | Single strand break |
| TCDD | 2,3,7,8-tetrachlorodibenzo-*p*-dioxin |
| TCR | Transcription-coupled repair |
| TDS | Testicular dysgenesis syndrome |
| Temed | N,N,N',N'-Tetramethylethylenediamine |
| TG | Thymine glycol |
| Tris | Tris(hydroxymethyl)aminomethane |
| XRE | Xenobiotic responsive element |

**Note: The names of proteins will in this thesis be denoted with capital letters for humans (e.g. OGG1), and with large initial and then low-case letters (e.g. Ogg1). The same rules apply to genes, but they are in addition written in *italic*.**

# 1 Introduction

## 1.1 General background

In today's industrialised community there is reason for concern about the reproductive state of the male, due to increased rates of poor sperm quality as well as testicular cancer. We are engaged in searching for possible explanations to this health problem. We believe that some answers can be identified through studying some harmful environmental mutagens, commonly found in the industrialised environment that humans are exposed to in their daily life. Several such substances are found in cigarette smoke, which we are almost daily exposed to, and we are studying one of those compounds, namely benzo(*a*)pyrene (BaP).

Testicular cancer is probably the best documented and most well-known indicator of an altered male reproductive state. Norway and Denmark have the highest incidence rates of testicular cancer in the world (Adami *et al.* 1994; Richiardi *et al.* 2004; Jacobsen *et al.* 2006), and there is a decrease in semen quality and number in Norwegian and Danish men, contrary to Finnish and Estonian men. This correlates with the higher testicular cancer incidents in Norway and Denmark compared to Finland and Estonia (Jorgensen *et al.* 2002). Testicular cancer is strongly correlated with cryptorchidism (undescended testis), hypospadias (abnormally placed urinary opening) and poor semen quality. These conditions have been proposed to constitute a syndrome called testicular dysgenesis syndrome (TDS) (Skakkebaek *et al.* 2001). They exhibit various degrees of severity, and poor semen quality represents the most common symptom.

The causes of these trends are largely unknown, but lifestyle and environmental factors are assumed to be partly responsible, along with genetic and epigenetic effects (Skakkebaek *et al.* 2001). There are a number of recent studies on maternal smoking as source for the foetal exposure *in utero*, but there is still controversy on the significance of maternal smoking for the high incidences of testicular cancer in some countries (Clemmesen 1997; Pettersson *et al.* 2004; Pettersson *et al.* 2007). The paternal impact is still unknown. Exposure to environmental agents after birth is likely to accelerate the onset and severity of testicular cancer. Inherent mutations in the foetus in tumour suppressor genes such as p53 would also accelerate the carcinogenic process. Such mutations could arise both from the father and the mother.

At the molecular level, smoking has been shown to correlate with higher levels of DNA damage, both adducts and oxidative DNA damage, in sperm (Zenzes *et al.* 1999a; Zitzmann *et al.* 2003). It has also been shown that DNA adducts from cigarette smoke can be transferred from sperm to the early embryo (Zenzes *et al.* 1999b). Furthermore, controversial results suggests that paternal smoking may be linked to childhood cancer (Ji *et al.* 1997; Chang *et al.* 2006).

New mutations arising in the germ line (*de novo* mutations) lead to a significant portion (~20%) of the genetic disorders occurring in infants (Crow and Denniston 1981; Nelson and Holmes 1989). *De novo* mutations can arise both in the mother and the father. Chromosomal aberrations and aneuploidies, which can give rise to conditions like Down syndrome, commonly originate from the mother, whereas point mutations commonly originate from the father (Chandley 1991). *De novo* mutations represent a high percentage of mutations associated with genetic diseases such as neurofibromatosis (Riccardi *et al.* 1984). Several autosomal dominant disorders, including achondroplasia (dwarfism) (Tiemann-Boege *et al.* 2002) and Waardenburg syndromes (Vogel and Rathenberg 1975) are exclusively associated with *de novo* male germ line mutations and advanced paternal age.

Not only genetic damage in the germ line, but also epigenetic abnormalities can affect the health of the offspring. Epigenetic abnormalities are changes in gene expression that occur without a change in the sequence of coding bases. They are rather achieved through methylation of DNA, post-translational modifications of histone proteins and RNA-based silencing. Such abnormalities can occur as a consequence of environmental exposure, and cause aberrant epigenetic programming in early embryos (Barton *et al.* 2005; Anway *et al.* 2005). It has been shown that exposure to the endocrine disrupting substance vinclozolin during the time of sex determination reduced the fertility of the male offspring through four consecutive generations. The effect was associated with altered DNA methylation and was transmitted through the male germ line only. It was observed among more than 90% of the offspring (Anway *et al.* 2005). It has also been shown that paternal exposure to ionising radiation and chemical mutagens can lead to transgenerational genomic instability (Dubrova *et al.* 2008; Verhofstad *et al.* 2008).

There is an increasing use of assisted fertilisation such as *in vitro* fertilisation (IVF) and intracellular sperm injection (ICSI). It is generally assumed that the reduced fecundity (ability to reproduce) in both sexes is linked to socioeconomic changes in our society such as an

increased age of the mother. Little focus has been on the father, and the role of poor semen quality for the changing fertility pattern is not known. Poorly motile or immotile spermatozoa can be used to fertilise the oocyte when using the ICSI technique. Fertilisation can also be achieved using ICSI when the spermatozoon contains heavily damaged DNA (Twigg *et al.* 1998). In a recent study that used both IVF and ICSI techniques, it was shown that male smokers had a significantly decreased clinical pregnancy success rate by as much as 40% compared to non-smokers (Zitzmann *et al.* 2003).

Obviously, reproduction is essential for the existence of man, and the integrity of the DNA (deoxyribonucleic acid) in the germ line is of great importance for generating a healthy offspring and maintaining the species. Oxidative DNA damage, such as the oxidative lesion 7,8-dihydro-8-oxodeoxyguanosine (8-oxoG), is commonly present in human sperm, and are strongly correlated with poor semen quality, disturbed embryonic development and high rate of early pregnancy loss (Ahmadi and Ng 1999). There are several mechanisms for repairing such DNA lesions. We have previously shown that lesions such as 8-oxoG are poorly repaired in humans compared to rodents (Olsen *et al.* 2003). Smoking can cause oxidative stress which can negatively influence the sperm quality, and metabolites can induce DNA adducts. Testicular cells from both human and rodents also exhibit limited abilities to repair bulky adducts (Brunborg *et al.* 1995; Jansen *et al.* 2001). Hence, DNA damage in male germ cells may disrupt the ability to achieve conception because of decreased sperm quality and number, mutated spermatozoa and apoptosis.

In this project we have addressed the consequences of one environmental mutagen (BaP) in male germ cells of wild type and repair deficient mice. We have measured the generation and removal of DNA lesions as well as the response on the level of gene expression on genes involved in BaP metabolism, using protocols that were established for the purpose. The ultimate aim has been to better understand the effects of environmental mutagens on male germ cells.

## 1.2 Male germ cells

### 1.2.1 The testicle

The testicle is a vital part of the male reproductive organ. It produces sperm cells and steroid hormones such as testosterone, in separate adjacent compartments. The testis is physically

enclosed by a capsule (tunica albuginea) (Figure 1-1), and display two major compartments; the intertubular/interstitial compartment and the seminiferous tubule compartment. The interstitial compartment contains Leydig cells, mast cells, macrophages and the blood- and lymphatic-vessels. The Leydig cells are the primary source of androgens and other steroids. Testosterone is the major male hormone and is required for male differentiation of the foetus and sperm production. The testosterone production is dormant until the onset of puberty. The production is regulated through the hypothalamus-pituitary-gonadal (HPG) axis, where hormones such as the luteinising hormone (LH) and the follicle stimulating hormone (FSH) work as positive stimulators of the Leydig cells. Testosterone and oestrogen have a negative feedback effect on the pituitary gland.

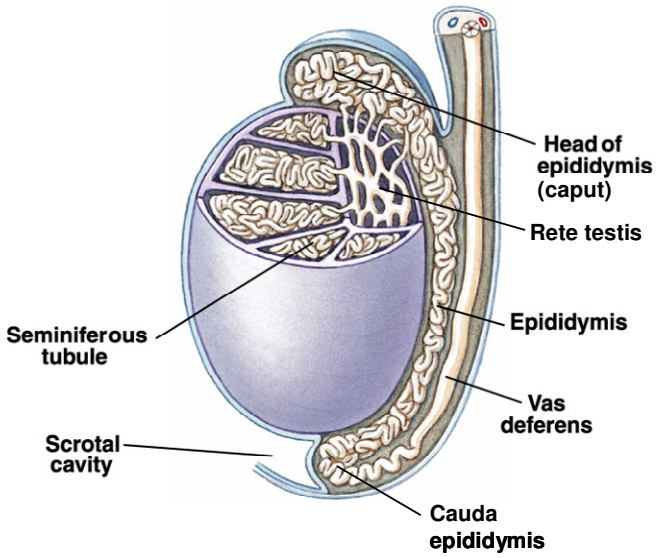


**Figure 1-1 Anatomy of the testis. The seminiferous tubules are coiled loops connected to the rete testis, which leads to the epididymis. The epididymis consists of the caput (head) and cauda (tail) epidydimis, that leads to the vas deferens. Adapted from (Silverthorn and Ober 2007).**

The seminiferous tubules are convoluted loops connected to the rete testis, which leads to the caput epididymis and cauda epididymis and further to vas deferens (Figure 1-1). The seminiferous tubules contain the germ cells and the Sertoli cells, and this is where spermatogenesis takes place. The seminiferous tubule tissue is organised as shown on Figure 1-2. Sertoli cells are somatic cells that provide the structural framework in the seminiferous epithelium, nursing the germ cells and forming the basal and adluminal compartment. The basal compartment includes spermatogonia and spermatocytes to the stage of early leptotene in meiosis, and they are separated from the adluminal compartment cells by tight junctions

between adjacent Sertoli cells and between Sertoli-cells and capillary endothelial cells, constituting the blood-testis barrier (Russell L.D. *et al.* 1990; Bart *et al.* 2002). To ensure that this barrier is not disrupted during transit of cells from the basal to the adluminal compartment, an intermediate compartment is temporarily formed. The function of the blood-testis barrier is to protect developing germ cells from harmful agents and immunologic attack. The barrier is generated as the first rounds of spermatogenesis are initiated at puberty.

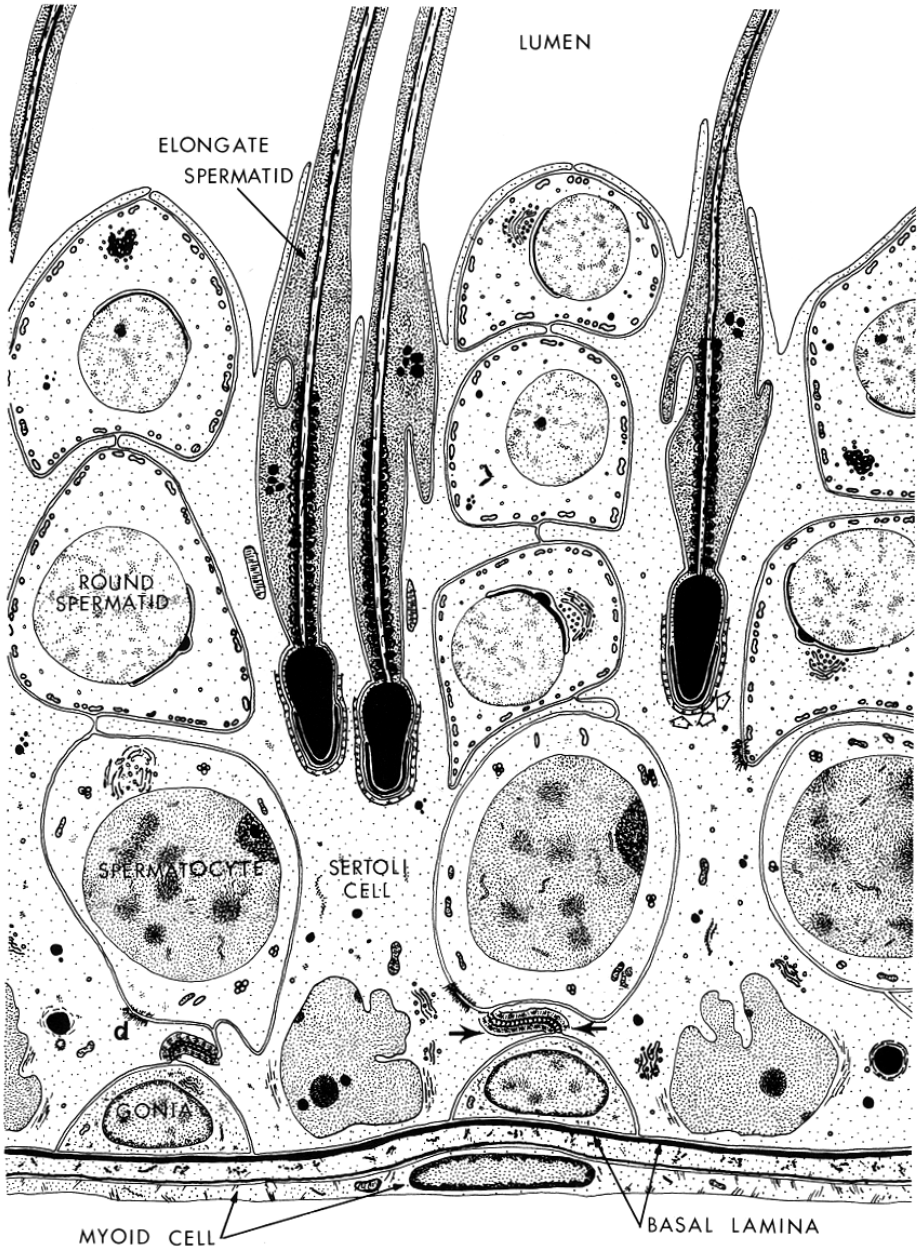


**Figure 1-2 General description of the seminioferous tubules showing spermatogonia, spermatocytes and spermatids. The bold arrows indicate tight junctions that form the blood-testis barrier (Russell L.D. *et al.* 1990).**

The physicochemical properties of the blood-testis barrier prevent large and hydrophilic molecules to cross the barrier, but small and lipophilic molecules can enter via diffusion or active transport. And even if some compounds have the physicochemical properties to cross, there are pumps present such as the P-glycoprotein and multidrug-resistance-associated protein 1 (MRP1) present that keep the concentration of the compounds at a lower level than in other tissues. These pumps are specific for some compounds, but other compounds still penetrate the barrier. For example, BaP can cross the barrier and is not removed. Furthermore, Sertoli cells can eliminate T lymphocytes via the Fas-Fas-ligand system, thus protecting the germ cells from the immune system when germ cells produce proteins that can serve as foreign antigens (Bart *et al.* 2002; Sutovsky P. and Manandhar G. 2006).

As a further protection against xenobiotica, the testis exhibit both phase I and phase II biotransformation enzymes such as CYP-enzymes (cytochrome P450) and glutathione S-transferases (GST), enzymes that could increase the xenobiotic hydrophilicity and promote excretion. In general, the expression and activity of the biotransformation enzymes may vary in different male germ cell types and between germ cells and somatic cells. GST activity, as an example, is highest in caput epididymis and decreases towards the vas deferens (Gandy *et al.* 1996). Some of the CYP-enzymes are further described in chapter 1.3.2.1.

Sertoli cells are important for maintaining the integrity of the epithelium, the blood-testis barrier, and the delivery of energy substrates such as lactate to the developing germ cells. Furthermore, Sertoli cells contribute to the regulation of spermatogenesis; they communicate with adjacent Sertoli and germ cells and have receptors for both FSH and testosterone. They secrete inhibin that is part of the negative feedback loop in the HPG axis. They also produce androgen binding protein (ABP) that binds testosterone, making it more hydrophilic in order to concentrate it in the seminiferous tubule lumen. Sertoli cells also contribute to the translocation of germ cells from the intermediate to the adluminal compartment, and to the delivery of spermatozoa to tubular lumen (spermiation). Spermatozoa are immotile in the seminiferous tubular lumen, and are transported to the seminal vesicle by peristaltic contractions made by myofibroblasts in the peritubular tissue (Russell L.D. *et al.* 1990; Holstein *et al.* 2003).

Blood vessels are just located between the seminiferous tubuli, and oxygen reaches the tubular lumen by diffusion only. Therefore the oxygen partial pressure are low, with a

dropping pressure gradient from the blood vessel and towards the seminiferous tubule lumen (Klotz *et al.* 1996; Wenger and Katschinski 2005).

### 1.2.2 Spermatogenesis

Spermatogenesis is the process of cell differentiation by which spermatozoa are generated from spermatogonia, a process that progresses from puberty and throughout life. Spermatogenesis is essentially similar in all mammals, and can be divided into three phases: 1) the proliferative phase, in which spermatogonia undergo rapid successive mitotic divisions, 2) the meiotic phase and 3) differentiation of the haploid spermatids (spermiogenesis) (Figure 1-3). Spermatozoa, the final product of spermatogenesis, are transported to and stored in seminal vesicles until ejaculation. The duration of spermatogenesis is 64 days in humans and 35 days in mice, the transport of spermatozoa to the seminal vesicle takes additionally 8-17 days in humans and ~7 days in mice (Adler 1996).

Spermatogonial stem cells originate from primordinal germ cells that proliferate *in utero*. After birth they initiate the proliferating phase when they undergo mitotic division to generate two diploid daughter cells, one gives rise to a type A spermatogonium and the other remains as a stem cell. Type A spermatogonia undergo further mitotic divisions where pale and dark type A and type B spermatogonia can be distinguished by their position in the basal compartment of the epithelium, their morphology and stainability. Type B spermatogonia represent the onset of germ cell development to spermatids, they enter the lengthy meiosis and are called primary spermatocytes (Russell L.D. *et al.* 1990; Holstein *et al.* 2003).

Meiosis takes 25 days in humans and 14 days in mice, with the first meiotic division (reduction division) occupying the majority of the time. Meiosis of spermatocytes starts in the basal compartment, where the leptotene stages of the prophase occurs. After crossing the blood-testis barrier via an intermediate compartment and reaching the adluminal compartment, the spermatocytes continue with the next prophase stages; the zygotene, pachytene and diplotene stage (Figure 1-3). Reduplication of DNA, condensation of chromosomes, the pairing of homologous chromosomes and homologous crossing-over (genetic recombination) occurs during prophase. Primary spermatocytes have two sets of chromosomes (4C), but are still diploid (2n). They undergo the first meiotic division to become secondary spermatocytes. Secondary spermatocytes consist of one pair of chromosomes (2C), and are diploid. The second meiotic division is rapid and results in four

haploid round spermatids. The round spermatids undergo a series of changes, spermiogenesis, where the acrosome and the flagellum develops, the nuclei condensate and cytoplasmic constituents are eliminated. At this point they have become spermatozoa that are ready for release into the seminiferous tubular lumen for transport to the seminal vesicle (Russell L.D. *et al.* 1990; Holstein *et al.* 2003; Sutovsky P. and Manandhar G. 2006). During the chromatin condensation histones are replaced by transition proteins, and finally by small, highly basic protamines bound to each other with extensive disulfide crosslinks, resulting in the formation of a compact chromatin structure which is devoid of transcriptional activity (Hecht 1990).

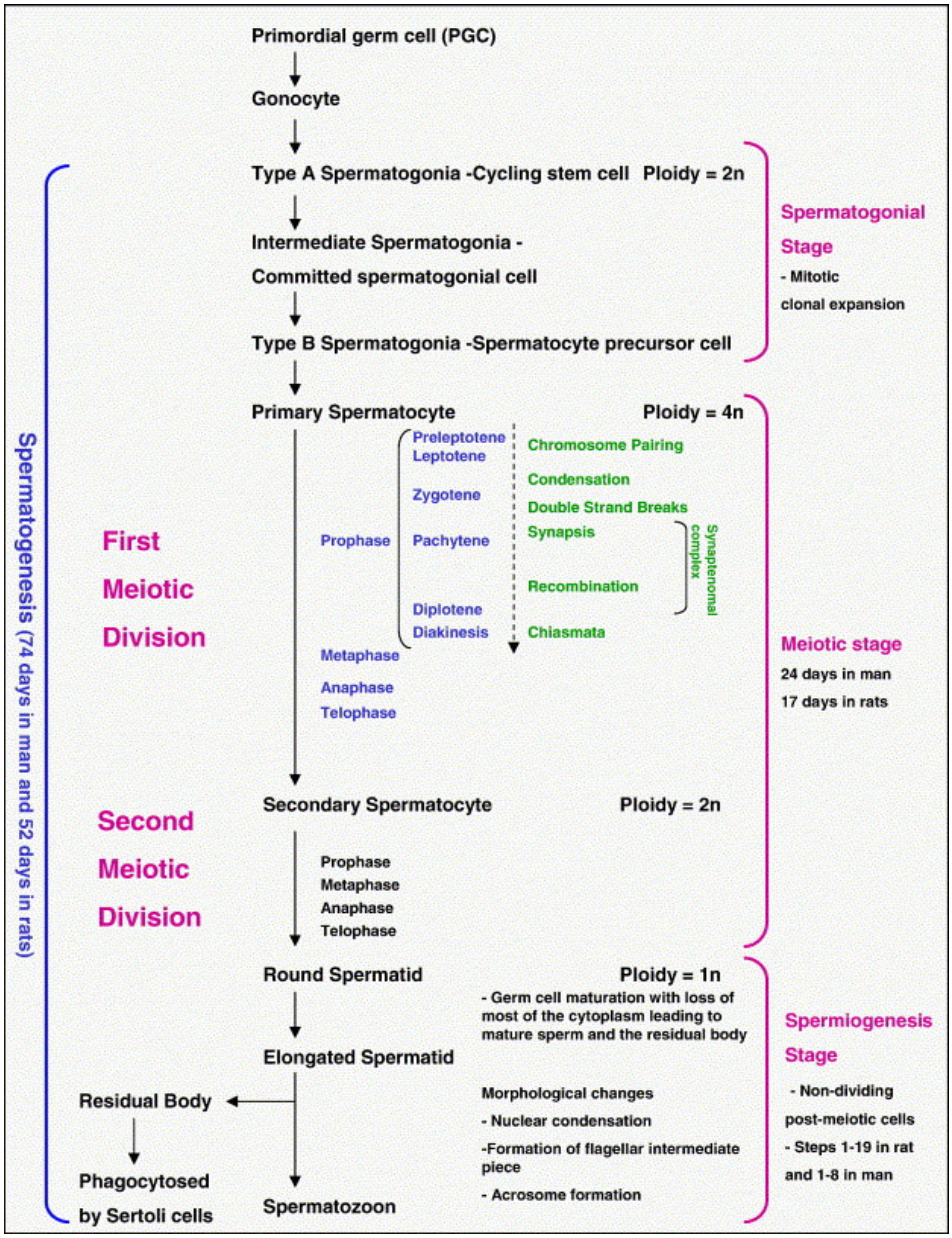


**Figure 1-3 Spermatogenesis (Olsen *et al.* 2005).**

The efficiency of the spermatogenesis is severalfold lower in humans than in non-primates. Mice spermatogonia go through eight mitotic steps before entering meiosis as spermatocytes. Humans on the other hand, pass only two mitotic steps before entering meiosis (Ehmcke *et al.* 2006). Furthermore, germ cell loss during spermatogenesis and number of malformed spermatozoa are extremely high, approximately 12% of the spermatogenetic potential is available for reproduction in humans. In addition, one Sertoli cell can only manage 3-4 germ cells in humans, compared to 12 germ cells in the rat (Holstein *et al.* 2003).

## 1.3 DNA damage

Cellular DNA is constantly attacked by endogenous as well as environmental agents. It is commonly accepted that DNA damage is a major factor during mutagenesis, carcinogenesis and ageing (Lindahl 1993). DNA is susceptible to temperature, pH, to chemical compounds, oxidation, irradiation, spontaneous hydrolysis and to errors introduced during replication, recombination and repair. Spontaneous damage occurs by processes such as hydrolysis (depurination is most prevalent), oxidative damage, or non-enzymatic methylation. DNA in one human cell is subject to approximately 20,000 lesions every day due to normal metabolism alone. On top of that DNA damage occur as a consequence of environmental factors such as ionising irradiation, UV irradiation or chemical agents such as alkylating agents, cross-linking agents, intercalating agents and electrophilic reactants.

### 1.3.1 Oxidative DNA damage

Attack from reactive oxygen species (ROS) on DNA is considered a major source of spontaneous damage to the DNA as well as other macromolecules such as proteins and lipids. There are various intra- and extracellular sources of oxygen radicals. The major intracellular source is believed to be electron leakage from the cellular respiration process in mitochondria. Also peroxisomal metabolism, lipid peroxidation and enzymatic synthesis of nitric oxide contribute. Extracellular sources include ionising and near-UV radiation, heat, various drugs and redox cycling compounds. Inflammation caused by endogenous and environmental agents can lead to ROS production as well. The most common ROS are hydroxyl radicals ($OH^{\bullet}$), singlet oxygen ($^1O_2$), oxygen radicals ($O_2^{\bullet-}$) and hydrogen peroxide ($H_2O_2$). $H_2O_2$ is relatively inert, but gives rise to the highly reactive $OH^{\bullet}$ in a process catalysed by transition metals (typically $Fe^{2+}$), a reaction known as the Fenton reaction or the metal-catalysed Haber-Weiss reaction (Friedberg E.C. *et al.* 2006). There are antioxidant enzymes such as superoxide

dismutase (SOD) and catalase together with radical scavengers such as glutathione, spermine (Ha *et al.* 1998) and vitamins C and E that protect DNA from damage caused by ROS. Extracellular SOD is expressed in the epididymis, lung, brain, testis, heart, kidney and liver, but not in spleen and uterus. Germ cells express SOD, but only one-third of that in Sertoli cells (reviewed in; (Mruk *et al.* 2002)).

ROS can induce strand breaks, modifications of bases and abasic sites (AP sites) in DNA. All of the four bases can be oxidised, but guanine has the lowest oxygen potential, and is therefore most prone to oxidation (Kovacic and Wakelin 2001). Over 80 aberrant bases caused by ROS are known, and around 15 oxidised forms of guanine have been identified. The most common are 7,8-dihydro-8-oxodeoxyguanosine (8-oxoG; Figure 1-4) and 2,6-diamino-4-hydroxy-5-formamidopyrimidine (FaPyG). FaPyG is an imiidazole ring-opened derivative of guanine and is prominent among the base damage formed by $H_2O_2$ (Friedberg E.C. *et al.* 2006). Other oxidised pyrimidines (cytosine and thymine) are also common. Pyrimidine residues have a 5-6-double bond that oxidises easily to generate glycols such as thymine glycol (TG) and cytosine glycol (CG). CG is unstable and is readily dehydrated to form 5-hydroxycytosine (5-OHC) (Bjelland and Seeberg 2003; Friedberg E.C. *et al.* 2006). 8-oxoG is generated by oxidation of the C8-position of guanine in DNA or incorporation of 8-oxodGTP. It can pair with adenine as well as cytosine during DNA synthesis and induces GC → TA transversions (Cheng *et al.* 1992). 8-oxoG can either form a stable Watson-Crick base pair with cytosine, or it can form a stable Hogsteen mispair with adenine which establishes the structural basis for 8-oxoG mutagenicity (Figure 1-4, B and C) (Bjelland and Seeberg 2003; Hsu *et al.* 2004). There have been controversies to the normal levels of 8-oxoG in different sources. The background levels has been estimated with at least 10 times difference according to which method that was used, and the problem lies in that the method used itself generates additional levels of 8-oxoG in the DNA (Gedik and Collins 2005). The background levels of 8-oxoG in a normal human cell is now estimated to be approximately one per $10^6$ guanine (Collins 2005; Gedik and Collins 2005).

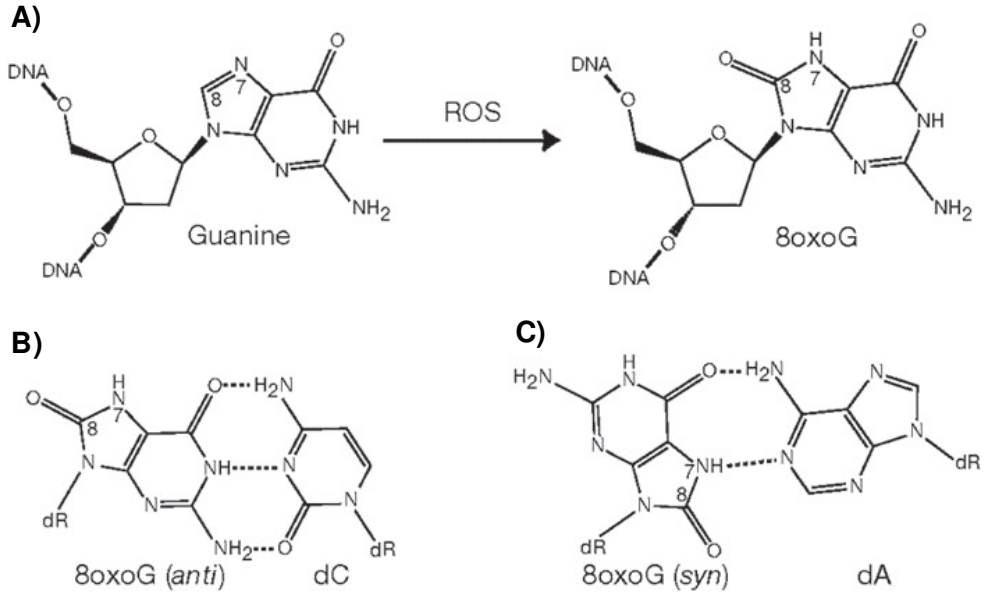


**Figure 1-4 Base pairing properties of 8-oxoG. A) Oxidation of guanine to 8-oxoG at C8-position by ROS. B) 8-oxoG is base paired with cytosine, the normal *anti* conformation forming a stable Watson-Crick base pair with three hydrogen bonds (dashed lines). C) 8-oxoG base paired with adenine in the *syn* conformation forming a stable Hogsteen mispair with two hydrogen bonds. The figure is taken from (Hsu *et al.* 2004).**

### 1.3.2 Benzo(*a*)pyrene

Polycyclic aromatic hydrocarbons (PAHs) such as benzo(*a*)pyrene (BaP) (Figure 1-5) are ubiquitous environmental toxicants, generated by incomplete combustion of organic material.

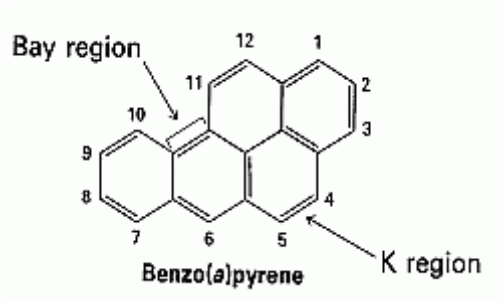


**Figure 1-5 Benzo(*a*)pyrene.**

The major natural sources are forest fires and volcanic eruptions. Anthropogenic sources include heating, car outlet, car tyre and asphalt wear, wood burning and industrial applications (Bostrom *et al.* 2002; Baird *et al.* 2005). The largest emission sources of total PAHs in Norway in 2005 were industry (mainly aluminium smelters) (68%) and wood heating (18%). The Norwegian environmental authorities have agreed that PAH emissions should be reduced

within 2010. There will be a ban on the use of PAH in car tyres from 1. January 2010. The aluminium smelters were required to reduce PAH emissions from 2007, and the authorities expect that the total levels of PAH will be reduced with 50% from 1995 to 2010 (SFT 2008).

The general population is exposed to BaP and other PAHs through the diet, soil, water and air, but the main exposure route is through the diet accounting for over 90% of the daily intake (Hattemer-Frey and Travis 1991; Phillips 1999). Grilling or charring meat at high temperatures increases the amount of BaP and other PAHs in the food. Estimated daily intake of BaP from food ranged from 0.1 – 1.6 µg/day per person in the 1980s – early 1990s. BaP-concentrations as high as 130 µg/kg have been found in fatty meat and around 50 µg/kg in charcoal-grilled T-bone steak, but the levels are usually around 1 µg/kg in meat. Levels at 130 µg/kg has been found in mussels, but normally the levels are up to 3.5 µg/kg in most seafood (WHO 1998). The background air concentrations measured at a station in Sweden ranged from 0.06 to 0.12 ng/m$^3$ air for 1995-1998, whereas at a station in Northern Finland the concentration was reduced by a factor 3-5 (Bostrom *et al.* 2002). In European cities in the 1960s the BaP levels were sometimes higher than 100 ng/m$^3$, but during the last 30 years the concentrations have decreased considerably (WHO 1998). In the centre of Stockholm the levels of BaP were between 0.4 and 2 ng/m$^3$, measured during spring 1994-2000 three meter above street level, which corresponded to 1% of total amounts of the PAHs measured (Bostrom *et al.* 2002). In Norway necessary precautions should be taken to ensure that air concentrations of BaP do not exceed 1 ng/m$^3$/year within 1. January 2013 (Ministry of the Environment 2004).

Tobacco smoke is an important source of exposure to BaP. Levels of 11 ng of BaP per cigarette were found in mainstream smoke and 103 ng per cigarette in sidestream smoke have been reported (WHO 1998). For smokers this is a significant contribution to the exposure to BaP. Occupational exposure also represents a source of high exposure, for example in coal industries, offshore and smelter industries. Exposure to BaP could be as high as 100 ng/l air at workplaces (Straif *et al.* 2005). In an electrode paste plant the workers was exposed to 0.8 ng BaP/l (Ovrebo *et al.* 1994).

#### 1.3.2.1 Metabolism and disposition

PAHs are lipophilic compounds, that can easily cross membranes and enter the cells. The respiratory passage and lungs are the main uptake routes for inhaled PAHs, the digestive tract for ingested PAHs and skin for PAH containing materials (ATSDR 1995). There is almost

complete absorption of inhaled BaP (Sun *et al.* 1982). Inhaled radioactive BaP were quickly distributed (within 60 minutes) to the liver, kidneys, intestines, blood, bones, testis and muscles (Sun *et al.* 1982; Weyand and Bevan 1986). In the liver it reached a maximum level of 21% of the 1 µg BaP/kg bodyweight dose within 10 minutes. After 6 hours 45% of administered dose were in the intestinal contents (Weyand and Bevan 1986). The oral availability of BaP after exposure of rats to 100 mg BaP/kg bodyweight dissolved in peanut oil was approximately 40%, derived from oral and intravenous plasma concentrations of BaP (Ramesh *et al.* 2001).

Metabolism of BaP and other PAHs occur in all tissues, and through several pathways. The metabolising routes either detoxify or activate the PAHs, although the cells "intention" always is towards detoxifying and elimination of the xenobiotica. Both phase I and phase II enzymes are involved, adding a functional group or conjugate to elevate the hydrophilic property of the xenobiotic and thereby facilitating excretion. The enzymes can react with available hydrogens on BaP. For activation of BaP three major routes are described (Figure 1-6) (reviewed by; (Xue and Warshawsky 2005)). **1)** A BaP radical cation is formed by the peroxidase activity of CYP (Cytochrome P450 superfamily), a one-electron mediated oxidation. This BaP-radical have the potential to induce DNA adducts, but this radical anions are probably not long-lived enough to cause DNA damage in living cells (Cavalieri and Rogan 1995). CYP1A1, -1A2 or -1B1 convert BaP to BaP-7,8-oxide which is hydrolysed by epoxide hydrolase to yield *trans*-dihydrodiols such as (±)-*trans*-7,8-dihydroxy-7,8-dihydroBaP (BaP-7,8-diol). Only (-)-BaP-7,8-diol is formed *in vivo* (Gelboin 1980). BaP-7,8-diol is substrate for the two remaining activation routes. **2)** It can either undergo a second epoxidation by CYP1A1/1A2/1B1 to yield 7,8-dihydroxy-9,10-epoxy-7,8,9,10-tetrahydroBaP ((+)-*anti*-BPDE), which readily forms adducts with DNA (mainly (+)-*anti*-BPDE-$N^2$-dGuo adducts) (Xue and Warshawsky 2005). The epoxide is located at the sterically hindered bay region of BaP where epoxide hydrolase does not easily react, and BPDE is regarded as an ultimate carcinogen. **3)** The other alternative is $NADP^+$-dependent oxidation of the *trans*-dihydrodiols catalysed by enzymes in the aldo-keto reductase (AKR) superfamily to produce *o*-quinones such as BaP-7,8-dione (Figure 1-6) (Penning 2004). Initially, a catechol is produced that undergoes subsequent oxidation to yield an *o*-semiquinone anion radical and $H_2O_2$, followed by a second one-electron oxidation yielding the fully oxidised *o*-quinone. This *o*-quinone can then either undergo a reduction in the presence of a reducing cofactor such as NADPH back to catechol, or form covalent DNA adducts. Redox cycles may be established through this AKR-mediated

pathway, by which ROS are generated until cellular reducing equivalents are depleted (Penning *et al.* 1996).

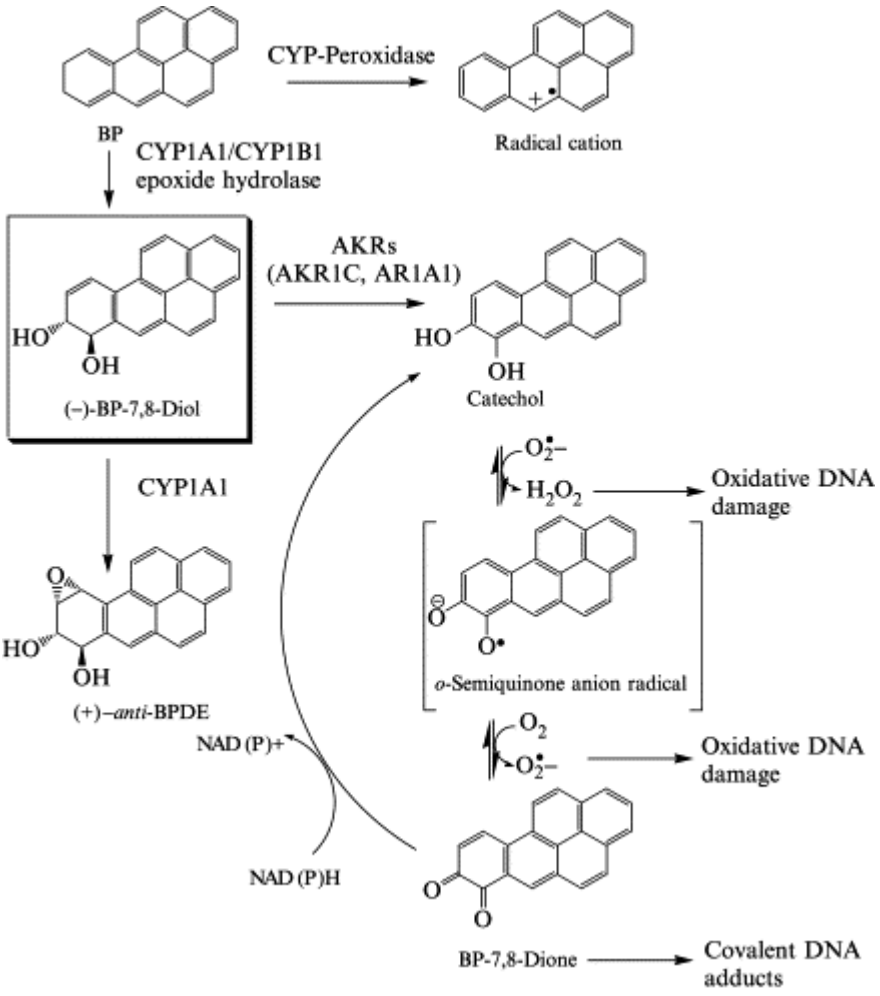


**Figure 1-6 Metabolic routes for activation of BaP and other PAHs (Penning 2004).**

CYP1A1, -1A2 and -1B1 are induced through the aryl hydrocarbon receptor (AhR) pathway. 2,3,7,8-tetrachlorodibenzo-*p*-dioxin (TCDD) and similar substrates such as BaP bind as ligands to AhR, which changes its conformation and mediate active transport into the nuclei. In the nuclei AhR associates with ARNT (AhR Nuclear Translocator). AhR-ARNT binds to xenobiotic responsive elements (XRE), regulator sequences in DNA located in the promoter regions of *CYP1A1, -1A2, -1B1* and other genes. The binding leads to enhanced transcription of these genes (Schmidt and Bradfield 1996; Nebert *et al.* 2004). PAH *o*-quionones can also induce the CYP enzymes through AhR (Burczynski and Penning 2000; Jiang *et al.* 2005). CYP1A1 is the most active member of the CYP1 family that metabolises PAHs. The enhancer region of *CYP1A1* contains multiple XREs that give rise to large increases of mRNA and

protein levels after BaP or other ligands binds to AhR (Casarett *et al.* 2001). *Cyp1a1* from C57BL/6J mice are constitutively expressed at low levels in several tissues such as the liver and testis, but is strongly induced after BaP exposure (Shimada *et al.* 2003). In absence of an inducer, transcription of *CYP1A1* is suppressed by a repressor protein in most species (Casarett *et al.* 2001). CYP1A2 is not believed to be expressed in extrahepatic tissues (Landi *et al.* 1999; Choudhary *et al.* 2003) and is induced at lower levels than *CYP1A1* in the liver (Casarett *et al.* 2001). m*Cyp1b1* is expressed at significant levels in several organs including the liver and testis in C57BL/6J mice after induction with BaP. Constitutively the liver expressed lower amounts of Cyp1b1 than other organs (Shimada *et al.* 2003).

AKRs constitute a superfamily of NADPH linked oxidoreductases that reduce aldehydes and ketones to their corresponding primary and secondary alcohols. They are generally located in the cytosol and are monomeric proteins of 37 kDa. AKR1A1 (aldehyde reductase) and -1C1-1C4 are the AKRs that metabolise BaP and other PAHs (Jez *et al.* 1997a; Jez *et al.* 1997b; Penning 2004). Akr1a4 is the mouse homologue to the human AKR1A1 (Allan and Lohnes 2000). AKR1A1 is ubiquitously expressed in almost all tissues. It is highly expressed in liver and kidney, compared to lower levels in the testis (O'Connor *et al.* 1999; Barski *et al.* 1999). The mouse homologue Akr1a4 is expressed in all tissues analysed, with highest amounts in the kidney, whereas the levels in the testis was not measured (Allan and Lohnes 2000). AKRs are, like CYPs, phase I xenobiotic-metabolising enzymes (Casarett *et al.* 2001). *AKR1A1* has XREs in its promoter region, suggesting a possible regulation through the AhR mediated mechanism (Penning and Drury 2007). Recently it has been shown that AKRs can effectively compete with CYP1A1 and -1B1 for BaP-*trans*-dihydrodiol activation in human lung adenocarcinoma (A549) cells given that the quinones can redox cycle. Both CYP1A1 and -1B1 have a 100-fold higher catalytic activity in metabolising BaP-7,8-diol in the redox state of A549 cells. But formation of *o*-quinones by AKRs can lead to redox-cycling, which can alter the redox state favouring the AKR pathway (Quinn and Penning 2008). Furthermore, in another recent study it was observed that activation of BaP-7,8-diol by AKRs in the same lung cells (A549) could lead to BaP-7,8-dione formation, ROS formation and increased 8-oxoG levels. Using a hOGG1-coupled comet assay and a catechol *O*-methyl transferase (COMT) inhibitor (which can metabolise catechols to 7-hydroxy-8-methoxy-BaP instead of the AKR mediated quinone-pathway), the investigators observed a further increase of 8-oxoG lesions than without this inhibitor, showing that ROS formation was produced during the

redox-cycling of BaP-7,8-dione produced by the AKR pathway. This could again contribute to ROS mediated genotoxicity and carcinogenesis (Park *et al.* 2008b).

BaP and its metabolites are mainly excreted through bile (elimination in faeces) and urine, with faeces dominating at early time points of excretion and urinary excretion dominating later. Approximate excretion half-life is 24 hours (Ramesh *et al.* 2001). After inhalation of 4.8 mg/m$^3$ radiolabeled BaP in rats, approximately 96% of the administered dose was excreted in the faeces, with an excretion half-life of 22 hours (ATSDR 1995). There is evidence of enterohepatic circulation; 6 hours after oral exposure of rats to 1 µg BaP/kg bodyweight, 53% of the administered dose was recovered in intestine contents of animals lacking a bile cannula (when the enterohepatic circulation functions as normal), whereas 77% of the administered dose was recovered in bile, intestines and intestine contents of animals with a bile cannula (Weyand and Bevan 1986).

#### 1.3.2.2 Toxicity

Acute and subchronic toxicities of BaP are relatively low. A study showed that BaP affects both blood elements and organs, and that male rats are more sensitive than female rats (Knuckles *et al.* 2001). The intraperitoneal (i.p.) $LD_{50}$ for the mouse is 232 mg BaP/kg bodyweight (Salamone 1981). Targets for BaP toxicity are cells (cytotoxicity), the immune system, the blood, the kidneys and the reproductive system (ATSDR 1995; Knuckles *et al.* 2001). Subchronic exposure of F-344 rats to 75 µg BaP/m$^3$, 4 hours daily for 60 days contributed to reduced testicular and spermatogenic function (Ramesh *et al.* 2008; Archibong *et al.* 2008).

#### 1.3.2.3 Carcinogenesis

BaP was previously categorised as an IARC group 2B carcinogen (possibly carcinogenic to humans), but is now considered as an IARC group 1 carcinogen (carcinogenic to humans) "based on sufficient evidence in animals and strong evidence that the mechanisms of carcinogenesis in animals also operate in exposed human beings" (Straif *et al.* 2005).

BaP is a known potent experimental skin carcinogen and is often used as positive control in bioassays of other agents. BPDE is known as a complete and ultimate carcinogen meaning that it is involved in both initiation, promotion and progression of cancer. Tumour formation

has been observed in several organs including lungs, the respiratory tract and forestomach in rodents after exposure to high doses of BaP (ATSDR 1995).

*o*-quinones are metabolising products of BaP, and they can form stable and depurinating DNA-adducts (McCoull *et al.* 1999; Balu *et al.* 2004; Balu *et al.* 2006). Further, ROS generated during *o*-quinone production and redox-cycling, as explained above, creates oxidative DNA lesions, such as 8-oxoG. 8-oxoG may lead to mutations in genes such as the *p53* tumour suppressor gene inducing carcinogenesis (Yu *et al.* 2002) because the normal cell-cycle regulation function of *p53* is disrupted. Furthermore, the mutations generated by BaP *o*-quinones were mainly G-T transversions (Yu *et al.* 2002). Several recent studies from Trevor Penning's group shows that *o*-quinones genereated by AKRs can have an important role in lung carcinogenesis, because the pattern of *p53* mutations is driven by 8-oxoG formation, while the mutation spectrum observed in *p53* lung cancer is determined by biological selection for dominance (Jiang *et al.* 2005; Shen *et al.* 2006; Park *et al.* 2008a; Park *et al.* 2008b). This is for the time being shown *in vitro* in yeast and human lung A549 cells, but may prove important in carcinogenesis studies.

## 1.4 DNA Repair

DNA damage can be fatal to cells. DNA double strand breaks (DSBs) are lethal to the cell, and modified bases and AP sites can interfere with DNA replication and transcription. Mutated genes can lead to the production of aberrant proteins. The cells have therefore acquired several lines of defence against the induction and persistence of DNA damage. There are agents that prevent the formation of DNA damage, such as the antioxidant enzymes and oxyradical scavengers. When present in DNA, lesions can be removed via various DNA repair pathways, or the damaged cell itself can be eliminated by apoptosis. In this chapter one major form of DNA repair will be described; excision of DNA damage. Other DNA repair pathways are mismatch repair (MMR), homologous recombination (HR) and non-homologous end joining (NHEJ). MMR is an important pathway for removing replication errors that lead to mismatches, as well as deaminations and small deletions/insertions (Li 2008). Direct reversal of lesions and ligation of single strand breaks (SSB) are the simplest forms of DNA repair. During direct reversal, specific enzymes such as AlkB in *E. coli* (Falnes *et al.* 2002) or $O^6$ methylguanine-DNA transferase (MGMT) (Pegg 2000) remove alkyl groups from bases without removing the base itself, and reconstitutes the normal base. DSBs arise from DNA damaging agents such as ionising radiation, or from stalled or broken

replication forks. DSBs are also induced endogenously in germ cells undergoing meiosis, since they serve as sites for initiation of genetic recombination. DSBs can be repaired via HR or NHEJ (O'Driscoll and Jeggo 2006).

Excision repair can be subdivided into base excision repair (BER) and nucleotide excision repair (NER). BER remove a range of base damages such as 8-oxoG, introduced endogenously as a part of cellular respiration, but also introduced by environmental agents (described in more detail in chapter 1.4.1). NER predominantly repair helix-distorting DNA lesions such as those caused by UV-light or by a range of exogenous agents such as BaP, cisplatin and aflatoxin $B_1$. NER excises and restores larger parts of DNA, up to 30 bases in length. NER is divided into two sub-pathways; global genome repair (GGR) and transcription-coupled repair (TCR). GGR maintains the whole genome, whereas TCR repair lesions blocking elongating RNA polymerases in actively transcribed genes (reviewed in; (van Hoffen *et al.* 2003)).

### 1.4.1 Base excision repair (BER)

BER is the major pathway for repairing lesions (one to ten bases) induced by endogenous and exogenous agents, such as 8-oxoG induced by ROS. These are DNA lesions that cause minor structural changes in DNA. As first reported by Lindahl (1974) BER is initiated with the release of a damaged base by DNA glycosylases via hydrolytic cleavage of the N-C1´ glycosylic bond between the base and deoxyribose (incision; Figure 1-7). The excision of the aberrant bases by DNA glycosylases forms baseless AP sites, which could also form spontaneously by hydrolysis. There are mono-functional and bi-functional DNA glycosylases; mono-functional DNA glycosylases only removes the damaged base, whereas bi-functional DNA glycosylases cleaves the AP sites (AP-lyase). Subsequent to incising the damaged base, an AP endonuclease (HAP1) produces a nick in the backbone of the phosphodiester 5´ to the AP site, which creates a 5´-deoxyribose phosphate (dRP) group with DNA ends that are suitable substrates for new DNA synthesis. To further complete the BER process two sub-pathways have been characterised: During the predominant pathway, short patch repair (SPR), DNA polymerase β (Polβ), which also exhibit dRPase activity that creates a dRP group, incorporate one nucleotide and the nick is sealed by a DNA ligase III/XRCC1 heterodimer (X-ray cross complementing protein 1). During long patch repair (LPR) DNA polymerase δ or ε together with proliferating cell nuclear antigen (PCNA) and Replication Factor C (RFC) incorporates several nucleotides. This generates a 5´ flap structure that is removed by flap

endonuclease FEN1, and the resulting nick is sealed by DNA ligase 1. BER has been reviewed in detail in (Krokan *et al.* 2000; Barnes and Lindahl 2004).

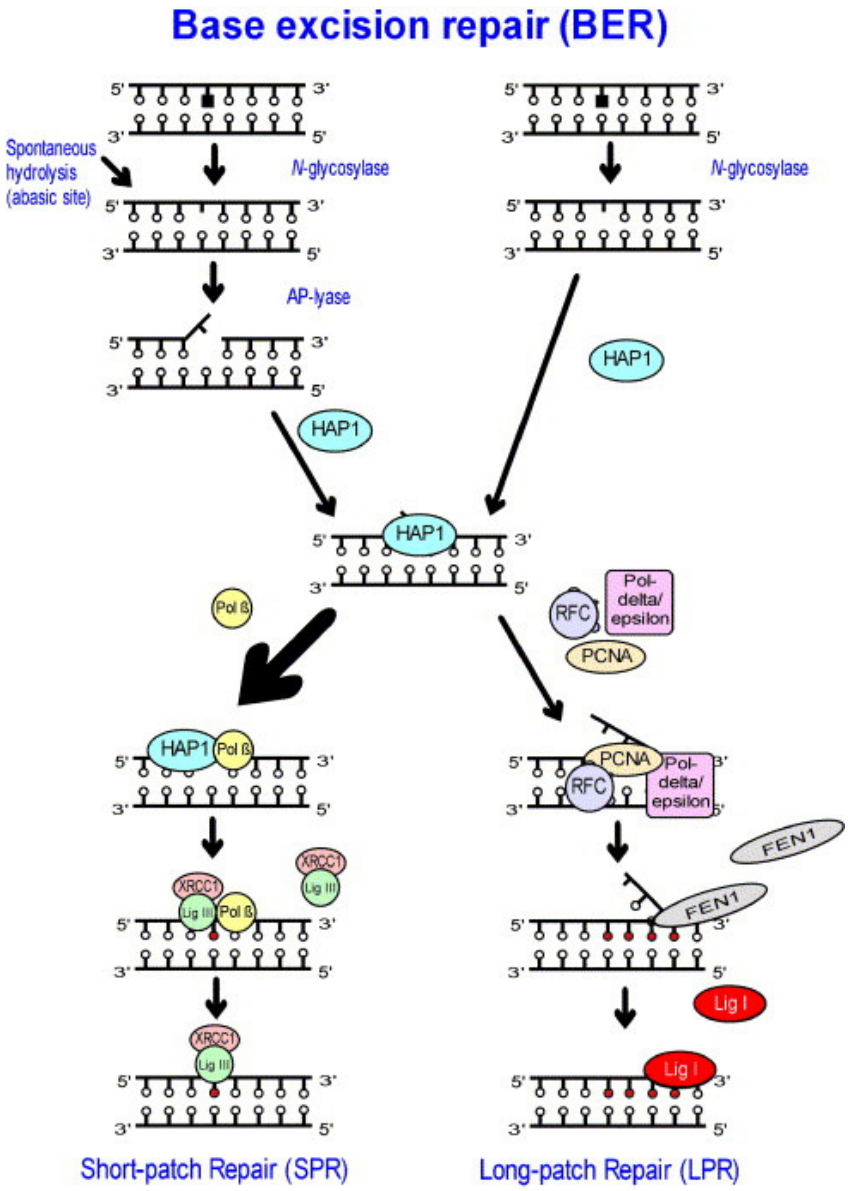


**Figure 1-7 The base excision repair (BER) pathway. Refer to text for details. Abbreviations: HAP1, human AP-endonuclease 1; Polβ, DNA polymerase β, XRCC1, X-ray cross complementing protein 1; LigIII, DNA ligase III; PCNA, proliferating cell nuclear antigen; RFC, replication factor C; Polδ-ε, DNA polymerase δ-ε; FEN1, Flap endonuclease 1; Lig1, DNA ligase 1 (Olsen *et al.* 2005).**

### 1.4.2 DNA glycosylases excising oxidative DNA lesions

In mammalians, eleven different DNA glycosylases are described. Here the focus is on the DNA glycosylases that removes oxidative DNA lesions (Table 1-1). *E. coli* have three important enzymes for avoiding genotoxic effects from 8-oxoG lesions; 8-oxoGTPase

(MutT), Formamidopyrimidine-DNA glycosylase (Fpg/MutM) and Adenine-DNA glycosylase (MutY). MutT hydrolyses 8-oxodGTP in the nucleotide pool and thus minimises the incorporation of 8-oxodGTP. Fpg removes 8-oxoG paired with cytosine whereas MutY removes erroneously incorporated adenine paired with 8-oxoG in DNA (Michaels and Miller 1992).

**Table 1-1 Mammalian DNA glycosylases that excise oxidative DNA lesions.**

| Enzyme | Main substrates |
|---|---|
| 8-oxoguanine-DNA glycosylase (OGG1) | 8-oxoG basepaired with C, FaPyG |
| Human MutY homologue (MYH) | Adenine basepaired with 8-oxoG |
| Thymine glycol-DNA glycosylase 1 (NTH1) | Oxidised pyrimidines, FaPyG |
| NEIL1 | 8-oxoG, Oxidised pyrimidines, FaPyG, FaPyA |
| NEIL2 | 8-oxoG, Oxidised pyrimidines, FaPyG, FaPyA |

Mammalian cells have similar error-avoiding mechanisms with MTH1 and MYH as orthologs for MutT and MutY respectively (Sakumi *et al.* 1993; Sekiguchi 1996; Slupska *et al.* 1996). OGG1 is a functional homologue for Fpg, and it removes 8-oxoG and FaPyG lesions, creating an AP site (van der Kemp *et al.* 1996; Bjoras *et al.* 1997; Arai *et al.* 1997; Aburatani *et al.* 1997; Rosenquist *et al.* 1997; Radicella *et al.* 1997; Roldan-Arjona *et al.* 1997; Lu *et al.* 1997; Prieto Alamo *et al.* 1998; Tani *et al.* 1998), reviewed by Klungland and Bjelland (2007). There are two major variants of the enzyme in humans, one localised in the nucleus and the other in mitochondria (Nishioka *et al.* 1999). They are expressed in all tissues examined, but the levels vary between tissues. A very high level of *Ogg1* mRNA in mouse testis has been reported (Rosenquist *et al.* 1997), whereas in human tissues, including the testis, *OGG1* mRNA is ubiquitously expressed (Radicella *et al.* 1997; Nishioka *et al.* 1999). Our previous studies showed that the expression of OGG1 in human testis varied markedly between individuals. The expression was at higher levels in testicular cells than in mononuclear blood cells, but lower than in human fibroblasts. The nuclear variant of hOGG1 dominated, and the expression was highest in spermatocytes and lowest in elongating/elongated spermatids. The expression of Ogg1 in the rat male germ cells was different from the expression in humans and Ogg1 was expressed in markedly lower amounts in germ cells than in somatic cells.

hNTH1 and Nth1 was used as positive controls for human and rat expression, respectively (Olsen *et al.* 2003).

The mammalian homologue of *E. coli* endonuclease III (Nth) is denoted NTH1, and has been characterised in both humans and mice (Aspinwall *et al.* 1997; Hilbert *et al.* 1997; Sarker *et al.* 1998). NTH1 excises oxidised pyrimidines such as thymine glycols (TG), 5-hydroxycytosines (5-OHC) and FaPy residues, and exhibits an AP-lyase activity (Aspinwall *et al.* 1997; Dizdaroglu *et al.* 1999; Luna *et al.* 2000; Eide *et al.* 2001). Both OGG1 and NTH1 belong to the Nth group of enzymes based on base homology. In addition there are two enzymes belonging to the Fpg/Nei group of enzymes, NEIL1 and NEIL2, that excise a variety of oxidised DNA bases and overlaps with both OGG1 and NTH1 (Bandaru *et al.* 2002; Morland *et al.* 2002; Takao *et al.* 2002; Hazra *et al.* 2002a; Hazra *et al.* 2002b; Bandaru *et al.* 2006). NEIL1 excises lesions such as 8-oxoG, 5-OHC and FaPy, but the activity of 8-oxoG removal is weaker than that of OGG1 (Bandaru *et al.* 2002; Morland *et al.* 2002; Takao *et al.* 2002; Hazra *et al.* 2002a). NEIL2 excises primarily oxidative products of cytosine, and exhibit its highest transcript levels in skeletal muscle and testis (Morland *et al.* 2002; Hazra *et al.* 2002b). Furthermore, a role for NEIL1 in processing clustered DNA lesions generated by gamma radiation is suggested. NEIL1 excises 8-oxoG located in close proximity to the 3´ end of a DNA single strand break more efficiently than OGG1 and NTH1 (Parsons *et al.* 2005). NEIL1 thus seems not only to be a backup-DNA glycosylase for OGG1 and NTH1, but to have its own substrate specificity different from both OGG1 and NTH1 (Rolseth 2007).

To learn more about the relevance of Ogg1 in mammals, *Ogg1*$^{-/-}$ null mice has been generated by Klungland and co-workers (1999). These mice have been used in this study. The mice were generated by replacing the highly conserved helix-hairpin-helix motif required for DNA glycosylase/AP lyase activity, with neomycin-resistance gen/polyadenylation signal (*Neo*). An embryonic stem cell (from 129SV mice) clone with homologous recombination in on allele of *Ogg1* was injected into blastocysts from C57BL/6J mice. Resultant confirmed heterozygous mice were interbred and homozygous *Ogg1*$^{-/-}$ mutants were recovered at frequencies consistent with Mendelian segregation (Klungland *et al.* 1999). These mice have a normal physical appearance with no overt phenotype, but 8-oxoG and Fpg-sensitive sites accumulate at abnormal levels in an age- and tissue-specific fashion (Minowa *et al.* 2000; Osterod *et al.* 2001). One study also reported that lung adenoma/carcinoma occurring spontaneously in 1.5 years old *Ogg1*$^{-/-}$ mice (Sakumi *et al.* 2003). Other mice models deficient in certain DNA glycosylases have also been constructed, with no severe phenotypes reviewed

in (Larsen *et al.* 2007), indicating the presence of overlapping specificities of DNA glycosylases or alternative DNA repair mechanisms. Indeed, an Ogg1 independent global genomic repair pathway for removing 8-oxoG was identified (Le Page *et al.* 2000; Osterod *et al.* 2002), but this pathway may not be functional in humans or rodents which have impaired NER capacity in the testis (Brunborg *et al.* 1995; Jansen *et al.* 2001). It may also be so that exhibiting higher levels of base damage is not very dangerous through the lifespan of one individual.

### 1.4.3 Clustered DNA damage and repair

X-rays, a form of low linear energy transfer (low LET) ionising radiation, leads predominantly to single-strand breaks and base damage. 1 Gy produces approximately 1000 breaks per diploid mammalian cell (Friedberg E.C. *et al.* 2006). A high portion of all DNA damage from ionising radiation is formed via ROS produced by hydrolysis of water in the vicinity of DNA. Such DNA lesions are normally repaired by base excision repair (BER) (Wallace 1994). However, ionising radiation seems to have a unique ability to form clustered DNA damage, which are two or more elemental lesions induced within 10-20 base pairs or one to two helical turns of DNA after passage of one single radiation track (Goodhead 1994; Ward 1994; Nikjoo *et al.* 1999). This clustering of DNA damage arises when the ionising radiation produces clusters of $OH^{\bullet}$ radicals. Because these radicals are highly reactive and have a short range, several sites of damage can be produced within a few base pairs on both strands (Ward 1988; Friedberg E.C. *et al.* 2006). This type of DNA damage is a challenge to the BER pathway, and is less repairable (Goodhead 1994; Blaisdell and Wallace 2001; Wallace 2002; Lomax *et al.* 2002). A cluster of damage containing a SSB or an AP site within a few base pairs opposite an 8-oxoG lesion is one of the difficult types to repair (Weinfeld *et al.* 2001; Lomax *et al.* 2002; Pearson *et al.* 2004). Fpg activity is inhibited when the SSB/AP site is located in the vicinity of a 8-oxoG, particulary when the SSB/AP site is within 1-5 base pairs from the 8-oxoG in the complementary strand (David-Cordonnier *et al.* 2001; Pearson *et al.* 2004). Another type of clustered DNA damage that is difficult to repair is when one or several lesions exist in tandem on one strand (Cunniffe *et al.* 2007). Furthermore, there are evidence of increased mutation rates from closely spaced DNA lesions (Pearson *et al.* 2004).

### 1.4.4 DNA damage and repair in male germ cells

DNA damage in male germ cells is a matter of concern because it may lead to mutated spermatozoa, apoptosis and decline of fertile sperm, and therefore interfere with male ability to reproduce (Steinberger and Rodriguez-Rigau 1983; Aitken *et al.* 2004; Aitken and De Iuliis 2007). It may also lead to mutations in the offspring. As much as 20% of the total of 5% of children suffering from a genetic disease by early adulthood originates via *de novo* mutations. Sperm containing lesions such as 8-oxoG, is correlated with a decrease in sperm quality and number (Ni *et al.* 1997; Shen *et al.* 1997; Lopes *et al.* 1998; Irvine *et al.* 2000). DNA damage in spermatozoa is negatively associated with *in vitro* and *in vivo* fertilisation ability (Lopes *et al.* 1998; Sakkas *et al.* 1998). Sperm with X-ray induced DNA damage are still able to fertilise an oocyte, but extensive DNA damage result in impaired embryonic development and high rate of early pregnancy loss (Ahmadi and Ng 1999). Oxidative DNA damage in sperm has also been reported to be associated with childhood cancer and infertility, but there are controversies to these findings (reviewed in; (Aitken and Krausz 2001)).

DNA adducts from the sperm have been shown to be present in the fertilised oocyte and persist at least to the early embryo (Zenzes 1999a, 1999b). BPDE-adducts were first detected in sperm from smokers (Zenzes *et al.* 1999a), and relatively high levels were also detected in non-smokers, indicating that the environmental exposure is substantial. In a later work paternal transmission of BPDE-adducts from sperm to the early embryo was shown (Zenzes *et al.* 1999b).

There has been a growing interest in and knowledge concerning induction and repair of DNA damage in male germ cells during recent years. Methodology has improved, but still isolating, acquiring pure suspensions of specific cells and cultivating different male germ cell types remain a challenge.

Cells in the early stages of the spermatogenesis from rats and hamsters repair SSBs as efficient as many somatic cell types, whereas elongated spermatids exhibit no repair (Van Loon *et al.* 1991; Van Loon *et al.* 1993). This has been confirmed in our laboratory (Olsen *et al.* 2001; Jansen *et al.* 2001; Olsen *et al.* 2005).

For excision repair a number of studies have utilised unscheduled DNA synthesis (UDS) as a measure of repair. In general those agents that did induce UDS were largely agents that give rise to DNA damage repaired via the BER pathway, whereas agents leading to DNA adducts

repaired via NER did not induce UDS. We addressed these observations more in detail, and found that rat testicular cells with UV-C induced bulky adducts, normally repaired via NER, showed very low repair using the alkaline elution assay or the comet assay (Brunborg *et al.* 1995; Jansen *et al.* 2001). Both TCR and GGR were inefficient in male germ cells of both humans and rodents (Jansen *et al.* 2001; Olsen *et al.* 2005). Furthermore, studying BER we found that oxidative lesions such as 8-oxoG were efficiently repaired in testicular cells of rats (Olsen *et al.* 2003) and mice (unpublished). However, in human testicular cells such repair was very poor (Olsen *et al.* 2003; Olsen *et al.* 2005). Therefore, it appears that human male germ cells may be particularly susceptible to the possible negative effects of oxidised DNA.

Mice and rats are the preferred species for testing whether chemicals are mutagens, carcinogens or lead to reproductive toxicity, but since there seem to be a marked difference between rodents and humans in the capacity to repair oxidative DNA damage, great care should be taken when drawing conclusions from animal studies. Therefore, we have proposed the use of *Ogg1*$^{-/-}$ mice as a model for humans when studying genotoxic effects of environmental agents in testicular cells. In this study *Ogg1*$^{-/-}$ mice were applied to study the formation of oxidative DNA lesions following exposure to BaP *in vivo*, and to monitor the expression of BaP-metabolising genes. We also studied the repair of Fpg-sensitive lesions *in vivo* in both *Ogg1*$^{-/-}$ and *Ogg1*$^{+/+}$ mice exposed to X-rays, as a part of characterising *Ogg1*$^{-/-}$ mice as model for genotoxic response in human male germ cells.

Repair pathways in male germ cells not discussed here are reviewed by Baarends and co-workers (2001).

## 1.5 Aims

Our main aim in the present work has been to study the role of environmental mutagens on male reproductive health. The genotoxic effects of one specific substance, BaP, were studied, using a variety of experimental approaches. We applied and characterised repair deficient mice as a model for human male germ cell genotoxicity. The study involved large-scale animal experiments, and relevant methods thus had to be developed. Our aims were:

1. Establishing a method for isolating and preserving nuclei - instead of primary cells - suitable for analysis of DNA damage induced *in vivo* in large animal experiments, using the comet assay.

2. Investigating whether *in vivo* exposure of *Ogg1*$^{-/-}$ and *Ogg1*$^{+/+}$ mice to BaP lead to induction of oxidative DNA damage.

3. Investigating the role of selected genes involved in BaP-metabolism in *Ogg1*$^{-/-}$ mice and *Ogg1*$^{+/+}$ mice, by measuring their gene expression following BaP-exposure *in vivo.*

4. Measuring the *in vivo* repair of oxidative DNA damage in *Ogg1*$^{-/-}$ and *Ogg1*$^{+/+}$ mice exposed to X-rays.

5. Adding to the characterisation of *Ogg1*$^{-/-}$ mice as a model for human male germ cell genotoxicity.

# 2 Materials and Methods

All media and solutions used are described in Appendix B.

## 2.1 Mice

### 2.1.1 Breeding and care

*Ogg1*$^{-/-}$ null mice in a mixed background of C57BL/6 and 129SV were generated by Klungland and co-workers (1999) and kindly given to us. The *Ogg1*$^{-/-}$ mice were crossed with Big Blue® C57BL/6 homozygous mice purchased from Stratagene (La Jolla, California, USA). The *Ogg1*$^{-/-}$ mice were backcrossed for 9 generations with Big Blue® C57BL/6 mice to achieve isogenic strains with identical background (C57BL/6). Maintenance of the mouse line was performed by littermate intercrossing of heterozygotes. Homozygotic mice were bred for experiments. The mice used for this study were of generation 2 after backcrossing. The genotypes of the mice were identified by conventional PCR-genotyping (see chapter 2.2). Breeding and care were performed at the Norwegian Institute of Public Health, Oslo, Norway. Breeding trios contained one male and two females, the females were from the same litter. Litters were separated at 17 days, males and females were housed separately. The mice were housed in air flow IVC racks (Thoren Maxi-Miser System) or filter cabinets (Scantainer, Scanbur BK AS, Nittedal, Norway) in plastic disposable cages on Nestpack (Datesand Ltd., Manchester, UK) bedding. The room had 12 hour light/dark cycle, 6-10 air changes per hour, controlled humidity (55±5%) and temperature (19-23°C). Water and diet were given *ad libitum*. The mice were given a breeding/maintenance diet (2018SX Teklad Global 18% Protein Extruded Rodent Diet, Harland Teklad, Madison, Wisconsin, USA) or SDS RM 3 (E) (breeding) and SDS RM 1 (maintenance) from Special Diets Services, Witham, Great Britain. The male mice used in this study were 8-12 weeks old, and were sacrificed with carbon dioxide ($CO_2$). Both *Ogg1*$^{-/-}$ Big Blue (*Ogg1*$^{-/-}$) and *Ogg1*$^{+/+}$ Big Blue (*Ogg1*$^{+/+}$) male mice were used.

### 2.1.2 Organs

The liver, lung and one testicle were quick-frozen on dry ice immediately after dissection from the mice and stored at -80 °C. The tunica albuginea of the testicle was removed before freezing. The other testicle with epididymis, a piece of the lung and the liver were transferred

to ice-cold RPMI 1640 medium with FCS. The organs were kept on ice at all times. The tunica albuginea and epididymis were removed from the testicle before isolation of nuclei. From the reproductive organs only the testicle was used for isolating nuclei, the cauda epididymis, caput epididymis and vas deferens were dissected using a cold lamp and microscope, and quick-frozen on dry ice before storage at -80ºC. The liver and lung were chosen as somatic cell controls, and the lung is also a known target organ for BaP-exposure. The liver is the principal detoxifying organ of BaP.

## 2.2 Genotyping

To identify the genotype of the mice, conventional genotyping was performed. The *Ogg1*$^{-/-}$ sequence is larger than the *Ogg1*$^{+/+}$ sequence due to the inserted *Neo* cassette used to disrupt *Ogg1*. This size difference facilitates identification of the genotypes of the mice. The mice can have one, two or no copies of the disrupted gene, being heterozygous (*Ogg1*$^{+/-}$), *Ogg1*$^{-/-}$ or *Ogg1*$^{+/+}$, respectively. DNA was isolated from ear cartilage and polymerase chain reaction (PCR) was conducted with specified primers (Table 2-1). PCR was performed on a DNA template, with two primers that flank the sequences of interest. The PCR reaction was multiplexed, meaning that both reactions were performed simultaneously in the same tube. The reaction are performed in cycles; high temperature (~94ºC) is required for denaturising the DNA strands, lower temperature (~50-64ºC) is used to allow the primers to anneal to the template, and finally the temperature is set to the optimum temperature for the DNA polymerase (~72ºC). The polymerase extends the primers by incorporating the dNTPs. The cycle is repeated as many times as desired. The PCR products were analysed by polyacrylamide gel electrophoresis.

**Table 2-1 The primers used for genotyping of *Ogg1*$^{-/-}$ and *Ogg1*$^{+/+}$ mice.**

| Name | Primer | Gene | Sequence |
|---|---|---|---|
| Primer 1 | Forward | *Ogg1* | 5'-ATGAGGACCAAGCTAGGTGAC-3' |
| Primer 2 | Reverse | *Ogg1*$^{+/+}$ | 5'-GCCTCACAATCAACTTATCCC-3' |
| Primer 3 | Reverse | *Ogg1*$^{-/-}$ | 5'-ATCTGCGTGTTCGAATTCGCC-3' |

Procedure:

Isolation of DNA:

1. Ear cartilage was collected in Eppendorf tubes and kept on ice.
2. 60 µl TE with 0.05% SDS was added and the mix was heated to 95°C for 10 minutes on a heating block.
3. The samples were cooled on ice, and quickly centrifuged. 0.2 µg/µl Proteinase K was added to digest the proteins, and the ear cartilage was homogenised using a pestil until no cartilage pieces were visible. Then the mix was incubated for 4 - 16 hours in a water bath at 55°C.
4. After incubation the mixture was vortexed and heated to 95°C for 15-20 minutes and diluted 1:50 (ranged from 1:10 to 1:200) with distilled water. The DNA was kept at 4ºC until PCR was performed.

Preparation of mastermix:

5. The mastermix was prepared according to Table 2-2.

**Table 2-2 Mastermix for genotyping of ear cartilage.**

| **Components** | **Concentration of stock solutions** | **Volume (µl) per 10 µl DNA sample** | **Final concentrations** |
|---|---|---|---|
| Gold buffer | 10 x | 2.5 | 1 x |
| dNTPs (dATP, dGTP, dCTP, dTTP) | 2 mM | 2.5 | 0.2 mM |
| 25 mM $MgCl_2$ | 25 mM | 2.0 | 2 mM |
| Primer 1 | 100 µM | 2.5 | 10 µM |
| Primer 2 | 100 µM | 2.5 | 10 µM |
| Primer 3 | 100 µM | 2.5 | 10 µM |
| Triton X-100 | 10% | 0.3 | 0.12% |
| AmpliTaq Gold® DNA polymerase | 5 U/µl | 0.3 | 0.06 U/µl |
| **Volume of mastermix** | | 15.1 | |
| **Volume of mastermix + DNA template** | | 25.1 | |

PCR:

6. Mastermix (15.1 µl) and ear cartilage DNA (10 µl of a suitable dilution) was combined. Distilled water was used for negative controls (10 µl).
7. The PCR was carried out according to this program using an Eppendorf Mastercycler Gradient.
    a. Step 1: 1 cycle
        i. 94°C for 10 minutes
    b. Step 2: 35 cycles
        i. 94°C for 45 seconds
        ii. 61°C for 1 minute
        iii. 72°C for 2 minutes
    c. Step 3: Hold at 4°C

### 2.2.1 Analysis of PCR products by polyacrylamide gel electrophoresis (PAGE)

1. 15% polyacrylamide gels were casted in 1x TAE-buffer.
2. 2 µl 6X loading buffer dye combined with 3 µl GeneRuler 100 bp DNA size marker was loaded into the first well.
3. 2 µl 6X loading buffer dye and 10 µl PCR product or negative control were mixed loaded in the following wells.
4. The gel electrophoresis was run in 1x TAE-buffer, at 150 volt for 1 hour.
5. DNA was visualised by UV-light after the gels had been stained with SYBR® Green (0.5 µg/µl) for 10 minutes and subsequently washed in $dH_2O$.
6. Images of the gels were taken using a gel documentation instrument (IS2000RT, Kodak 1D 3.6 NE software).
7. Interpretation of the results; see Figure 2-1. The band with highest molecular weight (300 bp) represent *Ogg1*$^{-/-}$, whereas the band with the lowest molecular weight (250 bp) represent *Ogg1*$^{+/+}$. Wells displaying both bands represent *Ogg1*$^{+/-}$.

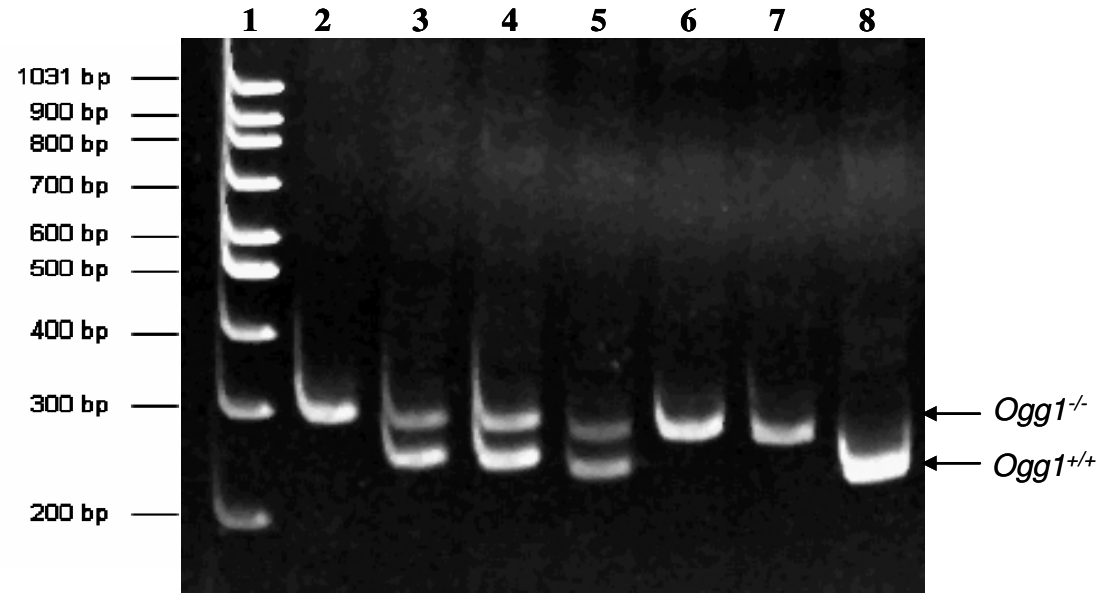


**Figure 2-1 PAGE of Ogg1 PCR. The band at 250 bp correspond to *Ogg1*$^{+/+}$ genotype, the band at 300 bp corresponds to the *Ogg1*$^{-/-}$ sequence, and the band at 300 bp corresponds to the disrupted Ogg1 sequence (*Ogg1*$^{-/-}$). Presence of both bands corresponds to *Ogg1*$^{+/-}$ mice. DNA from *Ogg1*$^{+/+}$ mice are present in lane 8, *Ogg1*$^{-/-}$ mice in lane 2, 6 and 7, and *Ogg1*$^{+/-}$ mice are present in lanes 3, 4 and 5.**

## 2.3 Isolation of nuclei from tissue

Nuclei were isolated based on a method (Brunborg *et al.* 1988) for isolation of nuclei from tissues such as the lung, testis, liver, kidney and the brain, originally developed for DNA damage analysis using alkaline elution. A unit used to squeeze the nuclei from the tissue was custom made for this specific technique. It is a stainless steel cylindrical tube (15 mm in diameter) with a stainless steel screen of 0.4 mm fitted inside. A modified plastic plunger that fits the cylindrical tube is used to force the tissue through the screen, similar to using a syringe. The nuclei used in this study were isolated from fresh tissue, but pilot studies were conducted showing that nuclei could also be frozen and analysed later. This method is quick and easy to perform, and is convenient for large scale *in vivo* animal studies. The formerly used methods for isolating primary cells make use of enzymes such as collagenase and trypsin to remove tissue around the germ cells, but in our method no enzymes were used. By omitting these enzymatic digestion steps, the DNA damage present would persist in the nuclei, as opposed to partly being removed by DNA repair during the digestion steps. The nuclei were subjected to DNA damage and repair analyses using the comet assay, and for determination of DNA damage levels using analytical methods (the results of which are not included in this thesis).

Procedure:

The buffer and nuclei were kept on ice, in dim light and processed quickly to eliminate interference with existing DNA damage levels and integrity of the nuclei.

1. A small piece of tissue of about 0.5 cm in diameter was used. The tissue was placed in 1 ml Merchants buffer and minced with scissors a few times.
2. The tissue was transferred to the unit and forced through the screen by pressing the plunger a couple of times. This was repeated to as many times as necessary to ensure that all tissue has been transferred, the cylinder were rinsed to reduce loss of nuclei.
3. The suspension of released nuclei, cells and tissue fragments was filtered through a 100 μm nylon filter, and centrifuged at 214 x g for 5 minutes at 4 °C.
4. The pellet was resuspended in 0.5-1 ml Merchant's buffer, and filtered once more through a 100 μm nylon filter. The filtrate contained the crude nuclei.
5. The number of nuclei could be estimated by counting using a light microscope. The suspension was diluted to a suitable concentration for the comet assay (approximately 1.3 x $10^6$ nuclei/ml).

The nuclei suspensions were either used immediately or frozen at -20ºC as described in 2.3.1.

### 2.3.1 Freezing and thawing of nuclei

Freezing:

The procedure was conducted on ice and in dim light.

1. The samples were added FCS (Foetal Calf Serum) to a concentration of 15% and DMSO to a concentration of 10%, and were mixed well by inverting the tubes.
2. The tubes were rapidly put into a -20ºC freezer for short time storage, or a freezer unit "Mr. Frosty" (5100 Cryo 1 °C Freezing Container, Nalgene Labware) was used to freeze at -80°C (cooling rate; -1°C/ minute).

Thawing:

Everything was kept on ice and in dim light.

1. The suspension was thawed in the hand until the frozen suspension could be transferred into 5 ml ice cold Merchants buffer. After complete thawing the suspension was immediately centrifuged at 214 x g for 5 minutes at 4°C.
2. The supernatant was removed and the pellet resuspended in Merchants buffer at equal or lower volumes as the initial sample.

## 2.4 *In vivo* and *in vitro* exposure of mice and nuclei

Mice were exposed for BaP *in vivo* to investigate the possible induction of DNA lesions in male germ cells and control tissues. Mice were exposed to X-rays *in vivo* to measure *in vivo* repair of oxidative DNA damage. Nuclei exposed to X-rays or to RO 12-9786 were used to establish the essay conditions.

### 2.4.1 *In vitro* exposure of nuclei to X-rays

X-rays mostly create SSBs and oxidative base damage such as 8-oxoG. Nuclei kept on ice and in dim light. The nuclei were irradiated in Eppendorf tubes placed directly on the X-ray tube window, with a 0.5 mm Cu film as filter. The X-ray source was a Phillips MG300 X-ray unit (Germany) operated at 10 mA and 260 kV. The dose rate was 10 Gy/minute, as measured by Fricke's chemical dosimetry.

### 2.4.2 *In vitro* exposure of nuclei to Ro 12-9786 plus visible light

During the development of new drugs for treating anxiety, many compounds are normally discarded due to unacceptable toxicity such as mutagenic effects (Will *et al.* 1999; Gocke *et al.* 2003). Two such compounds, Ro 12-9786 and Ro 19-8022, developed by Roche, proved to specifically induce oxidative base damage in presence of light, and these have later been extensively used in experimental systems to induce 8-oxoG. Here is oxidative DNA damage induced by Ro 12-9786, in the presence of visible light.

Procedure:
Samples and buffer was kept on ice and in dim light.

1. Treated samples: 1000 µl nuclei suspension was mixed with 2.50 µl 1.2 mM Ro 12-9786 (1:400).
2. Negative control samples: 1000 µl nuclei suspension was mixed with 2.50 µl DMSO (1:400 – Ro 12-9786 was dissolved in DMSO, here the nuclei is exposed to a equal concentration of the vehicle only).
3. The samples were allowed to stay for 1 minute, after which they were irradiated for 5 minutes with cold visible light (Schott KL 1500 electronic).
4. The nuclei were kept in small beakers (5 ml) or Petri dishes in Merchants buffer, 10 cm from the fibre optic light guide.

5. The exposure was stopped by adding 1.5 times more Merchants buffer than treatment volume (here 1500 µl) and centrifuged at 482 x g at 4 °C. The supernatant was removed, and the pellet was resuspended in Merchants buffer at its initial volume (here 1000 µl).

### 2.4.3 *In vivo* exposure of mice to BaP

#### 2.4.3.1 Dissolving BaP in corn oil

BaP is both toxic and carcinogenic and hence the required precautions were taken.

Procedure:

1. BaP were weighed in a glass vial inside a ventilation cabinet. Corn oil was added to obtain a concentration of 7.5 mg BaP/ml corn oil. The bottle was placed in a water bath at 30 °C with shaking for about 1 hour to dissolve.
2. Remaining undissolved material was dissolved by using a magnetic stirrer and letting it stir for 1 hour or until everything is dissolved.
3. The vial with dissolved BaP was covered with aluminium foil and stored within a dedicated container in the dark at room temperature in a ventilated security cabinet.

#### 2.4.3.2 BaP-exposure of mice

BaP dissolved in corn oil (see chapter 2.4.3.1) was administrated by i.p. injection, performed by trained personnel. The volume of BaP injected was according to the body weight and the dose. The mice were administered a single dose of 150 mg BaP/kg bodyweight, or the vehicle (corn oil). The mice were sacrificed using $CO_2$ at different time points (1, 3, 5 and 17 days) after exposure, and testes, epididymis, liver and lung were removed. The mice were housed as described in chapter 2.1.1, but they were kept in separated disposable cages after exposure.

The experimental design is shown in Figure 2-2 with the number of mice sacrificed at each time point. The control mice were administered corn oil or nothing at all (unexposed controls).

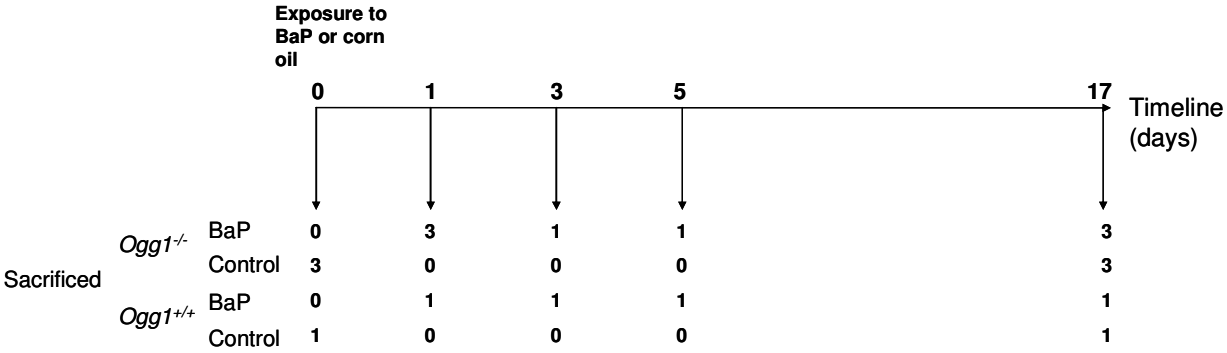


**Figure 2-2 Experimental design of the BaP study. All mice were exposed at time point zero, and sacrificed at different time points (days) after exposure. They were injected i.p. with 150 mg/kg bodyweight BaP or corn oil.**

### 2.4.4 *In vivo* exposure to X-rays

One animal at a time was put in a plastic container, with a diameter of ~10.5 cm, and was irradiated 30 cm above the irradiation source, as described in 2.4.1. The dose rate was 0.70 Gy/minute; mice treated with 10 Gy were therefore exposed for 14 minutes and 20 seconds. The animals were sacrificed using $CO_2$ at different time points (hours) following irradiation (Figure 2-3). Control mice were not irradiated, but otherwise treated as the other animals. The mice were kept in separate cages after exposure with water and diet *ad libitum*.

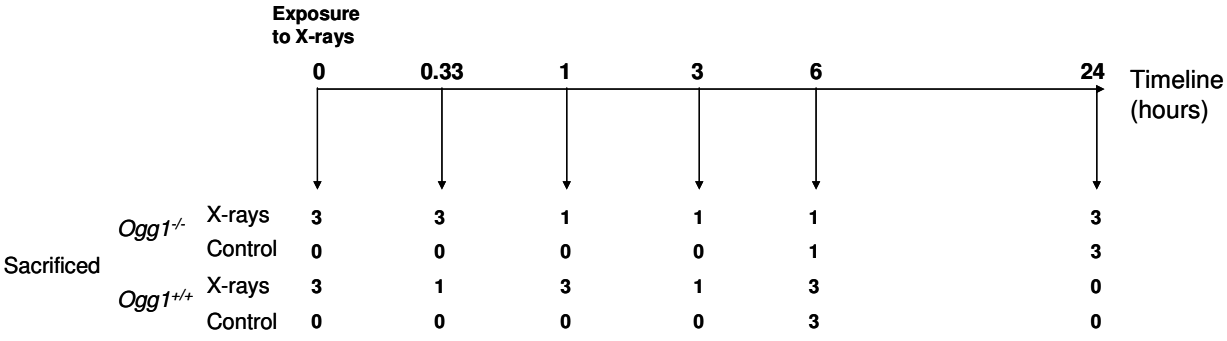


**Figure 2-3 Experimental design for the study of *in vivo* repair of oxidative DNA damage.**

## 2.5 The alkaline single cell gel electrophoresis (comet) assay

The comet assay is a simple and effective technique for measuring DNA strand breaks in single eukaryotic cells (Ostling and Johanson 1984; Singh *et al.* 1988; Olive *et al.* 1992). Cells exposed to a genotoxic agent are embedded in agarose, after which proteins are removed and the DNA is unwound. DNA SSBs are visualised by alkaline gel electrophoresis whereby

nicked DNA generates a tail. In the living cell, the DNA is organised in nucleosomes. DNA is wound around a histone core that creates a negative supercoiling. After the histones are removed and thereby disrupting of the nucleosome, the supercoiled DNA is still intact. SSBs relaxes the supercoiling and enables the relaxed loop to travel under the electrophoretic field. DNA is negatively charged and the relaxed loops will travel towards the positive pole.

A modified version of the assay includes repair enzymes like Fpg and Nth from *E. coli*. The enzymes recognise specific DNA damage and cleave the DNA backbone at such specific sites, making a strand break that is detected in the assay. The sensitivity of the comet assay is thus markedly increased. Fpg, as an example, recognises oxidised purines such as 8-oxoG.

One of the more recent modifications to the comet assay in our laboratory is the use of Gelbond® films, which are easier to handle and more practical than glass slides. The nuclei are moulded in agarose gel on the Gelbond® film, on its hydrophilic side. Twelve agarose gels were casted per film, which is more effective than the three gels per glass slide. Furthermore, the films can be stored for longer time periods before (and after) scoring when the gels are fixed in ethanol and dried.

Procedure:

Every step was performed in dim light.

1. Low melting agarose (0.75%), the lysis solution and electrophoresis buffer was prepared. The agarose was kept at 37 °C, whereas lysis solution and electrophoresis buffer were kept at 4 °C.
2. The cells or nuclei were mixed with the agarose (1:10) and moulded (60 µl) on the films with the help of a casting frame. The films were placed on a cold metal plate for moulding. Eight technical replicates were moulded for each sample; four were designated for treatment with Fpg and four were designated as controls.
3. The films were placed in lysis solution for 1-24 hours, after which they were rinsed in $dH_2O$ and placed in Enzyme Reaction buffer first for 10 minutes and then for 50 minutes in fresh Enzyme Reaction buffer at 4°C.
4. Crude Fpg extract was thawed and added to preheated Enzyme reaction buffer (0.2 mg/ml BSA), giving a final concentration of 1 µg/ml. The films were placed in the preheated Enzyme reaction buffer with or without enzyme and put at 37°C for 1 hour.

5. The films were placed in Electrophoresis buffer (pH 13.2) at 4 °C for unwinding of DNA for 5 minutes and then 35 minutes in fresh buffer.
6. Gel electrophoresis was performed in Electrophoresis buffer at 8°C for 20 minutes at 20 V and approx. 300 mA, with an approximate voltage drop of 1.1 V/cm over the platform.
7. The films were neutralised for 5 minutes twice in fresh neutralising buffer at room temperature.
8. Then the films were rinsed in $dH_2O$ for one minute, placed in absolute ethanol for 5 minutes, and then in > 70% ethanol for 1.5 hour to fix the films.
9. The films were allowed to dry, and were stored in a dark place at room temperature until staining (up to several months).
10. Scoring: The comets were stained using 30 µl SYBR® Gold (1000X stock in DMSO) in 25 ml TE-buffer per film for 20 minutes, after which they were stored moist, dark and cold (8°C) when not scored (scoring within three days). After scoring the films were allowed to air-dried and stored dry at room temperature.

### 2.5.1 Scoring of comets

We used an image analysis software called "Comet assay IV" from Perceptive Instruments. The microscope was Olympus BX51 (Japan) with an A312f camera (Basler Vision Technologies, Germany), and Olympus Burner with a Mercury Short-Arc HBO® 100 W/2 lamp (Osram, Germany). The comets were selected by the operator (without selectively avoiding certain comets) and the system calculates the total intensity, per cent DNA in the head, per cent DNA in the tail and tail moment for each comet. The comets were stained with SYBR® Gold, which binds to DNA and emit fluorescence. There are several dyes available, such as ethidium bromide, DAPI and SYBR® Green, but we used SYBR Gold due to its sensitivity and lower quenching. The system measures the tail from the middle of the head, and estimates per cent tail intensity in the tail relative to the head. The scoring is preferably made without manual interference, but when the system sets the middle of the head erroneously, we can manually set it to the visually right position. Overlapping nuclei were not scored. For testis nuclei we tried to avoid elongated spermatids by their distinct shape and small size. The scoring is performed blindly; treatment of samples were not known, only whether the film was treated with Fpg or not. The results are reported as per cent tail intensity (% DNA in the tail).

## 2.6 Gene expression analysis using real-time reverse transcriptase (RT) PCR

To investigate the response of BaP-metabolising genes in mice exposed to BaP, gene expression analysis was conducted using real-time RT PCR. With real-time RT PCR expression of selected genes can be studied. To do that total RNA was isolated, reverse transcribed to cDNA and real-time PCR performed.

### 2.6.1 Isolation of RNA

Isolation of RNA from tissue was done according to the GeneElute™ Mammalian Total RNA Kit (product code RTN70) from Sigma. RNA was isolated from testis and liver tissue of unexposed mice and mice exposed to BaP or to the vehicle (Figure 2-2). Tissues were prepared as described in chapter 2.1.2.

Procedure:
All steps were carried out in room temperature except for the tissue harvest and the lysis steps.

1. **Preparation**
    a. Step 1: Preparation of tissue
        i. Up to 40 mg of tissue per preparation could be used. It was important to weigh the tissue without letting it thaw before coming in contact with the Lysis Solution, to prevent RNA degradation.
        ii. The tissue was transferred to an Eppendorf tube containing 500 µl of Lysis Solution/2-ME Mixture.
    b. Step 2: Lysing of tissue and inactivation with RNases
    In this step cells are lysed and RNases are inactivated to prevent RNA digestion.
        i. The tissue was homogenised the tissue quickly and thoroughly with a small pestle until no visible pieces remained. The lysate can be stored at -70°C for several months.
    c. Step 3: Filtration of lysate
    Filtration removes cellular fragments and shears DNA.
        i. The lysate was transferred into a GeneElute Filtration Column and centrifuged at maximum speed (14100 x g) for 2 minutes

ii. The filtered lysate was used further and the filtration column discarded.

d. Step 4: Preparement for binding of RNA to column
   i. 500 µl of 70% ethanol solution was added to the filtered lysate and the sample was mixed by vortexing.

## 2.7 RNA isolation

e. Step 1: Loading onto columns
   i. Up to 700 µl of the ethanol containing lysate were pipetted into a GeneElute Binding Column after which it was centrifuged at 14100 x g for 15 seconds.
   ii. The collection tube and the column were kept whereas the flow-through liquid was discarded. The column was returned to the collection tube, and the remaining ethanol/lysate mixture was added to the column and centrifuged at 14100 x g for 15 seconds.
   iii. The flow-through liquid was discarded, and the RNA was bound to the column.

f. Step 2: First column wash
   i. 500 µl Wash Solution 1 was transferred to the column. It was centrifuged at 14100 x g for 15 seconds and the flow through liquid was discarded.

g. Step 3: Second column wash
   i. The column was transferred to a fresh collection tube, 500 µl of ethanol-diluted Wash Solution 2 was added to the column and it was centrifuged at 14100 x g for 15 seconds.
   ii. Then the flow-through liquid was discarded.

h. Step 4: Third column wash
   i. 500 µl of ethanol-diluted Wash Solution 2 was added to the column, it was centrifuged at 14100 x g for 2 minutes and then the flow-through liquid was discarded.
   ii. To ensure that the binding column was dry, an optional spin at 14100 x g for 1 minute was performed. The column must be free of ethanol-containing liquid before elution of RNA.

i. Step 5: Elution of RNA

i. The binding column was transferred to a fresh collection tube, 50 µl of Elution Solution was added to the column and then it was centrifuged at 14100 x g for 1 minute.
ii. If more than 50 µg of RNA was expected, the elution was repeated with new 50 µl Elution Solution. The RNA was always kept on ice after elution and stored at -70ºC for longer time periods.

2. Quantification and purity of total RNA were measured using the NanoDrop™ 1000 Spectrophotometer (Thermo Scientific).

### 2.7.1 Quantity and purity assessment with NanoDropTM 1000 Spectrophotometer

The samples were measured according to the manual of the NanoDrop1000 software.

1. The system was initiated with a distilled water sample.
2. "RNA-40" was chosen for RNA samples, whereas "DNA-50" was chosen for DNA and "other-38" was chosen for cDNA.
3. A blank measurement was conducted using 1.5 µl from the solution the sample was diluted in, and then 1.5 µl of each sample was used for the sample measurements.
4. The system measured absorbance at 260 nm and 280 nm and gave directly the concentration of the sample in ng/µl.
5. The Sample Retention System was cleaned with distilled water.

### 2.7.2 RNA quality measurement using 2100 Bioanalyser (Agilent Technologies)

In addition to measuring the quantity and purity of RNA, the quality of RNA can be measured using gel electrophoresis with 2100 Bioanalyzer.

Procedure (according to the 2100 Bioanalyser Manual):

1. Making the running gel
    a. The gel was centrifuged at 1500 x g for 15 minutes and 65 µl aliquots were prepared.
    b. 3 µl of the dye was added to one aliquot, it was vortexed and centrifuged at 13000 x g for 10 minutes. Then the gel-dye mix was equilibrated at room temperature for 30 minutes, protected from light.
2. 5 µl of each RNA-sample was heated at 70 °C for 2 minutes, to unfold secondary structures.

3. Setting up the Agilent 2100 Bioanalyzer
    a. The electrodes were rinsed with 350 µl of RNaseZAP for 1 minute and then with 350 µl of RNase-free water for 10 seconds to avoid contamination.
4. Setting up the chip priming station
    a. A new syringe was placed into the clip, arranged into the luer lock adapter and the whole construction was screwed to the chip priming station. The clip lever was then slided to the top position.
5. Loading the chip (Agilent RNA 6000 Nano Kit)
    a. A new RNA Nano chip was placed in the priming station and 9 µl gel-dye was loaded in the appropriate well marked "G".
    b. The chip priming station was closed with the plunger of the syringe placed at 1 ml and the plunger was pressed until the clip was holding it.
    c. Waited for exactly 30 seconds and released then the plunger from the clip. The plunger moved back, waited new 5 seconds and pulled then the plunger back to 1 ml mark.
    d. 9 µl of the gel-dye mix was added in the two other wells marked for gel-dye mix.
    e. 5 µl marker was added to all 12 sample wells and the ladder well, and 1 µl ladder was added to the well marked with "ladder" and 1 µl sample in all sample wells.
    f. The chip was vortexed for 60 seconds at 2400 rpm on an IKA Vortex Mixer.
    g. The chip was runned in the Agilent 2100 Bioanalyzer.

### 2.7.3 Reverse transcription of RNA to cDNA

RT of mRNA to cDNA was conducted according to the High-Capacity cDNA Reverse Transcription Kits (Applied Biosystems, 200 reactions, without RNase inhibitor). The RNA was reverse transcribed to cDNA because PCR depends on DNA template to synthesise double stranded products. Here random primers were used, but gene specific priming or oligo(dT) primers can also be used. Random primers are capable of priming cDNA synthesis at many points along the RNA template. Priming at many points simultaneously ensures the efficiency of the cDNA synthesis and that the whole sequence of interest are synthesised (Sambrook and Russell 2001).

Procedure:

Everything was kept on ice at all times of the procedure, which was conducted according to the kit.

1. 500 ng total RNA was reverse transcribed into cDNA using 96-well reaction plate. Diluted RNA can be stored in -70 °C before reverse transcription.
2. Mastermix was prepared according to the kit (Table 2-3).

**Table 2-3. Mastermix for cDNA reverse transcription, modified from Applied Biosystem High-Capacity cDNA Reverse Transcription Kits.**

| **Component** | **Volume (µl) (for 40 µl reaction)** | **End concentration (for 40 µl reaction)** |
|---|---|---|
| 10 x RT buffer | 4.0 | 1 x |
| 25 x dNTP mix (100 mM) | 1.6 | 1 x |
| 10 x RT random primers | 4.0 | 1 x |
| MultiScribe™ Reverse Transcriptase (50 U/µl) | 2.0 | 2.5 U/µl |
| Nuclease-free $H_2O$ | 8.4 | |
| **Total mastermix volume** | 20.0 | |

3. 20 µl (for a total of 40 µl reaction) of the diluted RNA (500 ng/µl) sample was added to a 96-well reaction plate. 20 µl prepared mastermix was then added in each well, and mixed by pipetting a couple of times.
4. The plate was centrifuged briefly to remove air bobbles and to spin down the content.
5. The reverse transcription was runned on a thermal cycler (Eppendorf Mastercycler Gradient) (Table 2-4).

**Table 2-4. Thermal cycler program.**

| | **Step 1** | **Step 2** | **Step 3** | **Step 4** |
|---|---|---|---|---|
| **Temperature** | 25 °C | 37 °C | 85 °C | 4 °C |
| **Time** | 10 minutes | 120 minutes | 5 seconds | ∞ |

6. Quantification and purity of cDNA were conducted using the NanoDrop™ 1000 Spectrophotometer, according to the procedure previously described (chapter 2.7.1).
7. cDNA was stored at -20 °C. Made sure that the samples were not thawed and frozen unnecessary, ensuring less degradation of the cDNA samples.

### 2.7.4 Real-time PCR

Real-time PCR is essentially the same as ordinary PCR (described in chapter 2.2), the difference lays mainly in how the results are extracted. To obtain results from traditionally PCR (end-point PCR) gel electrophoresis have to be performed after the PCR, but when conducting real-time PCR the results are obtained "real-time" during measurement of the kinetics of the reaction. End-point PCR has a poor sensitivity and is time consuming, where as real-time PCR is more sensitive and the results are obtained when the run is finished. Real-time PCR makes use of a fluorescence reporter that binds to the product and reports its presence by fluorescence. There are many fluorescence reporters available, both sequence specific and non-specific. Here SYBR® Green has been used, which is a sequence non-specific asymmetric cyanine dye. It has no fluorescence when it is free in solution, but become fluorescent when binding to the minor groove of DNA. The fluorescence increases as the amount of double stranded PCR product is formed, also undesired primer-dimer products. Therefore a melting curve analysis is conducted at the end; the temperature is gradually increased, the fluorescence decreases gradually as the temperature increases, until the double stranded DNA melts, then the fluorescence drops abruptly. When primer-dimer products are present they are typically shorter than the targeted product, and can therefore be distinguished from the target. The real-time PCR is reviewed by (Kubista *et al.* 2006).

There are several probes on the market, for example TaqMan probes, which are hydrolysis probes with two dyes. The TaqMan probe anneals to a specific sequence of the template and the polymerase cleaves it when it copies the template. When the TaqMan probe is cleaved it stops the energy transfer between the high energy dye (reporter) and an acceptor molecule (quencher), and the fluorescence from the reporter increases. Probes do not detect primer-dimer products, because of the template specificity.

If a single target is detected per sample, there is not much difference in using a dye or a probe. For this relatively simple setup SYBR® Green is the convenient alternative; it is cheaper than TaqMan and eventually unwanted primer-dimer products can be detected.

To avoid unspecific annealing, sequence specific primers are used. We used primers for *Akr1a4*, *Cyp1a1*, *-1a2* and *-1b1*, as well as the housekeeping genes *18S ribosomal RNA* (*rRNA*) and *β-actin*. The housekeeping genes are ubiquitously and are thought to be expressed

at similar levels in all cells. Therefore they are used to correct for methodological variations during the same run. After testing both housekeeping genes, we chose one of the two for all the analyses due to cost and time issues, but the two together would be the best. A Cycle Threshold (CT) value is estimated from a specified threshold after the run are completed. The threshold is set over the background and the cycle number when the signal crosses the threshold is the CT value (Figure 2-4).

Normalisation was performed according to the ΔΔCT-method (Livak and Schmittgen 2001). The samples were normalised to the housekeeping gene first ($\Delta CT = CT_{target} - CT_{housekeeping}$) and then values for the treated samples vs. the control samples were calculated ($\Delta\Delta CT = \Delta CT_{treated} - \Delta CT_{control}$). For expressing the relative change between treated and control $2^{-\Delta\Delta CT}$ values were calculated, and then the fold change values were log2-transformed.

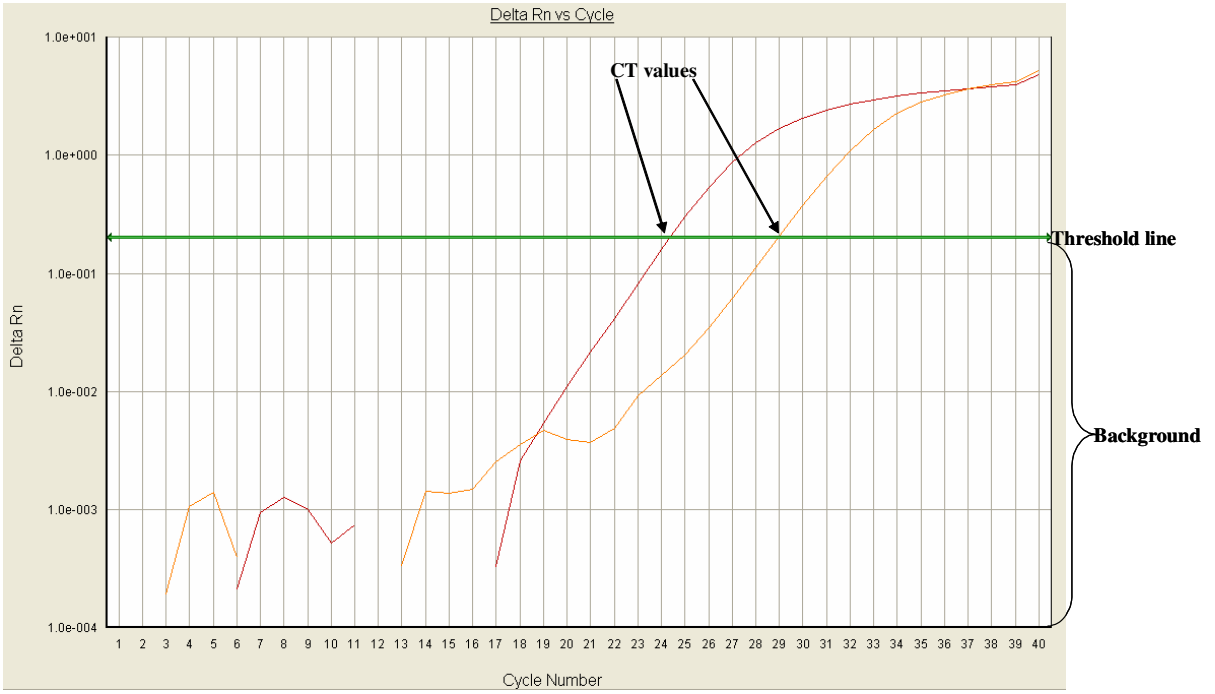


**Figure 2-4 Real-time PCR showed with the threshold line and CT values.**

Real-time PCR procedure:

Thawed cDNA and all solutions were kept on ice at all times. A dilution series with a control and an exposed sample were conducted to find the cDNA dilution appropriate for the selected genes. This ensures that the eventually change of expression of the genes are not lost, as well as having an optimal cDNA concentration for the run.

1. Prepared plates for running
    a. 8 µl $H_2O$ and 2 µl cDNA sample was added to each appropriate wells of a 96-well reaction plate.
    b. 10 µl Power SYBR® Green PCR Mastermix (Applied Biosystems) was mixed with 2 µl TE-buffer diluted primer (QuantiTect Primer assay, Qiagen) and 12 µl were distributed to each appropriate well containing 10 µl $dH_2O$/cDNA sample.
    c. The plate was centrifuged briefly (1 minute) to remove air bubbles and to spin down the content.
2. Running real-time PCR on Applied Biosystems 7500 Fast Real-Time PCR System, Absolute Quantification (Applied Biosystems)
    a. Prepared the run using the 7500 Fast System program
        i. Assay: absolute quantification
        ii. New detectors (gene name) were added
        iii. Stage 1: 1 cycle
            1. 95 °C for 15 seconds
        iv. Stage 2: 40 cycles
            1. Step 1: 95 °C for 15 seconds
            2. Step 2: 60 °C for 1 minute
            3. Step 3: 72 °C for 35 seconds (data collection step)
        v. Dissociation stage (stage 3) was added.
        vi. The run mode was Standard 7500 and the volume of each sample was 22 µl.

## 2.8 Isolation of DNA with DNA extractor WB kit (Wako)

DNA was isolated to measure 8-oxoG and bulky adducts from BaP (BPDE-dG), according to the Wako-kit description in the presence of a strong antioxidant, desferal, to minimise the induction of oxidative DNA damage during DNA isolation. The isolation of DNA is performed here, but the analyses of DNA lesions are beyond the scope of this study.

Procedure:

1. Fresh Lysis solution with 1 mM Desferal was prepared

   a. 100-300 mg tissue: 1.0 ml Lysis solution/1 mM Desferal (5 µl 20mM Desferal to 1.0 ml Lysis solution) was added.
      i. The tissue was homogenised with a Dounce homogeniser (8 times with pestle A and 8 times with pestle B) and then the mix was vortexed for 30 seconds at moderate speed.
   b. Cell pellet ($10^3$-$10^6$ cells); the pellet was suspended in 1.0 ml Lysis solution with Desferal and vortexed for 30 seconds at moderate speed.
2. The mix was centrifuged at 10000 x g for 20 seconds at 4 °C. The supernatant was removed and the pellet was kept intact.
3. The pellet was suspended with 1.0 ml Lysis solution with Desferal and vortexed for 30 seconds at moderate speed.
4. The sample was then centrifuged at 10000 x g for 20 seconds at 4 °C. The supernatant was removed and the pellet was suspended in 200 µl of Enzyme Reaction solution (if this solution was crystallised it could be warmed to 50 °C). 20U RNaseA and 2U $RNaseT_1$ was added, the samples was mixed well by vortexing and incubated at 37 °C for 30 minutes. These enzymes degrade single stranded RNA.
5. 10 µl Proteinase K (16.67 mg/ml) was added, the samples were mixed well by vortexing and incubated at 37 °C for 1 hour. The tubes were inversed several times during the incubation. Proteinase K was added to digest proteins in the mixture.
6. The mix was centrifuged at 10000 x g for 5 minutes at room temperature, and the supernatant was collected with a genomic tip. 300 µl of sodium iodide (NaI) solution was added to the supernatant, and the tube was inverted to mix. NaI is a chaotropic agent, it participate in solubilisation of macromolecules such as proteins, lipids and DNA.
7. 500 µl Isopropanol was added to the mixture, and the tube was mixed well by inversion until DNA precipitated (a whitish material). Isopropanol precipitates DNA.
8. The samples were centrifuged at 10000 x g for 10 minutes at room temperature and the supernatant was gently removed. The tip of sterile paper was used or the tubes were turned upside down to remove any residual liquid.
9. The pellet was rinsed by adding 1 ml of Washing solution A, and mixed thoroughly until the pellet dislocated from the tube wall. The samples were centrifuged at 10000 x g for 5 minutes and the supernatant was carefully removed. This step was then repeated with Washing solution B.

10. The DNA pellet was air dried until no ethanol was left. 500 µl of HPLC grade water was added and the pellet was left to dissolve for a minimum of 16 hours rotating device on moderate speed at ambient temperature.
11. The DNA concentration was determined by UV absorbance at 260 and 280 nm using the NanoDrop™ 1000 Spectrophotometer (chapter 2.7.1).

## 2.9 Statistical methods

At present there is no agreement on a standard statistical method that could be used on comet data, reviewed in (Lovell and Omori 2008). Parametric tests such as the analysis of variance (ANOVA), a generalised linear model (GLM), rely on assumptions of independence, equal variances and normality. However, the ANOVA is robust enough to conduct with some differences in the variances, and with a minor violation of the normality (Lovell and Omori 2008). Comet data have a tendency to fail the normality tests, this applies also often to Log transformation of the data, because the data are left or right skewed. Lesser damaged nuclei tend to skew to the right, but nuclei with much damage tend to skew to the left. Data skewed to the right could be normalised with Log transformation, but this transformation does not normalise left skewed data (Moore and McCabe 2003). Furthermore, Log transformation can result in heterogeneity of variances (Lovell and Omori 2008). A non-parametric test could be performed when the data violate the assumptions of parametric tests, because non-parametric tests do not require a distribution. However, non-parametric tests are slightly less powerful than their parametric equivalents. Non-parametric tests such as Kruskal-Wallis and Mann-Whitney tests have a tendency to be oversensitive in detecting small differences between samples, and hence is not suitable when detecting gentoxic effects (Duez *et al.* 2003).

The statistical analysis of the BaP-data from the comet assay is not straight forward, because the amount of data is large. In this assay the nuclei are scored with a computer program (Perceptive Instruments), each GelBond film contains 12 gels and from each gel 50 nuclei were scored. There were eight technical replicas for each treatment, four that received enzyme treatment and four that only received enzyme reaction buffer. There were scored 200 nuclei from enzyme reaction buffer only and with enzyme treatment, respectively, from each treatment. Nested (hierarchical) ANOVA with Type I sum of squares was applied to the comet data, since the animal should be regarded as the experimental unit and not the comet (Lovell and Omori 2008). Gels and animals were nested and set as random factors, whereas exposure was the fixed factor, and tail intensity (%) was the dependent variable. Day 17 after

BaP-exposure was compared to the 17 day vehicle control. Day 1 following BaP-exposure was also compared to the day 17 vehicle control, but since the day 17 control is a different treatment (days) than 1 day, the comparison is shown just for illustration. At other time points data from one mouse were used, and since the treatment (and hence the mice) is the experimental unit, the analyses were only performed on the time points with three mice. The animals and the gels were nested and set as random parameters, to take into account possible differences between the animals and the technical replicates (the gels). We used univariate ANOVA with Levene's test of equal variances. For *post hoc* comparisons Tamhane's T2 test, which do not assume equal variances, were used, due to the outcome of the Levene's test. Tukey HSD test is an alternative test which assumes equal variances. Levene's test for equality of variances was conducted to check if the variance of the vehicle control was similar to the variances of the exposed groups, or significantly different from each other. The variances in the control group and the exposed groups should be similar (p *above* 0.05).

On the real-time RT PCR data logistic regression was applied to the dilution series to ensure that the parallels were linear (a high $R^2$). The real-time data were normalised to the unexposed control, but statistical analyses were not conducted because only day 1 and day 17 following BaP-exposure comprised three animals, and those time points are not suitable for comparisons.

Statistical analyses on the repair data (where there were three animals in the group) were conducted with a Mann-Withney U test, which is a non-parametric version of the independent-samples t-test. The repair data was not nested and median values was used.

The statistical program used was SPSS version 16.0 for Windows, except for the logistic regression where Microsoft Office Excel 2003 for Windows was used. Results were regarded significantly different from the control at a significance level below 0.05.

# 3 Results

In this chapter a colour theme was applied to all figures where it was appropriate (Figure 3-1).

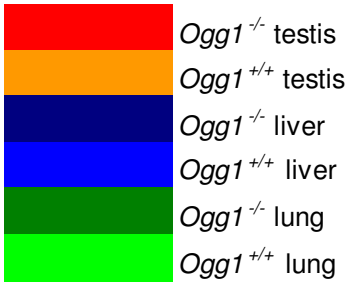


**Figure 3-1 The main colour theme used in the present work.**

## 3.1 Methodological advances to the comet assay

One part of this project was to investigate whether nuclei are suitable for use in the comet assay, which would facilitate more rapid preparation of samples from *in vivo* experiments. This would again give room for expansion of the number of samples per experiment as well as extending the possibility of interlaboratory collaborations. The mechanical isolation of nuclei did not lead to significant oxidative DNA damage due to the isolation procedure in itself compared to conventional isolation of primary cells, which has been the standard procedure in our laboratory. By mechanical isolation there is no discrimination between different cell types, so in addition to the germ cell nuclei, some somatic nuclei are also present in the sample and are scored in the comet assay. This is however also the case for primary male germ cells isolated by enzymatic digestion.

The possibility of freezing the nuclei is very useful when performing large-scale animal studies or for interlaboratory collaborations. Therefore suitable freezing and thawing conditions of the nuclei were established (Figure 3-2).

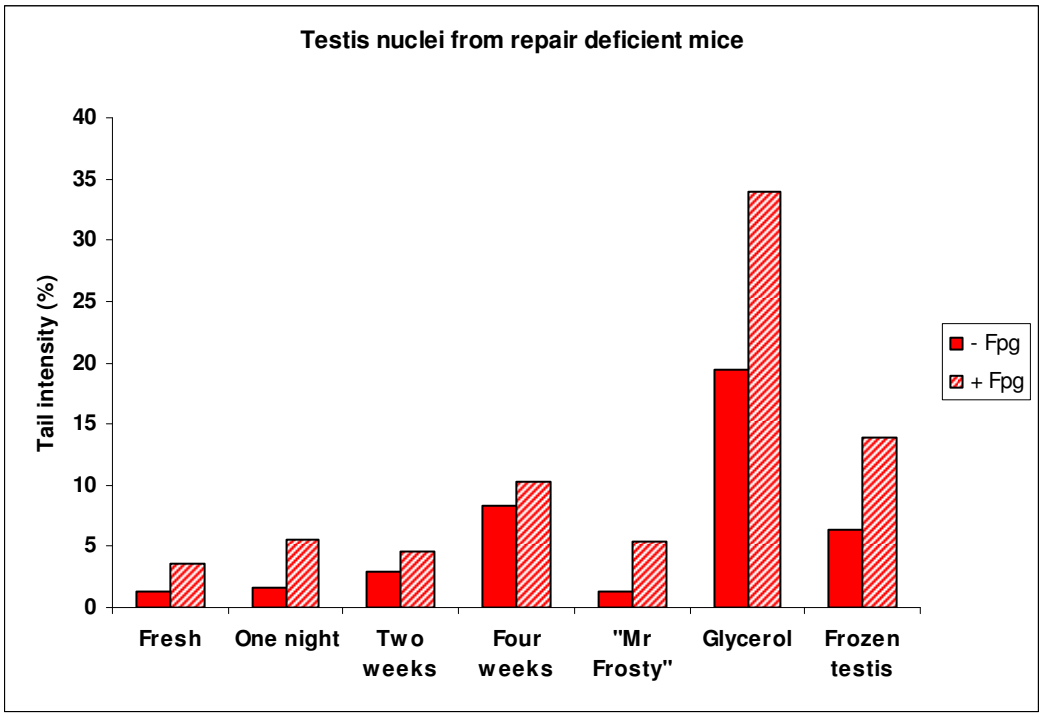


**Figure 3-2 DNA damage in testis samples freshly prepared or frozen, and stored using different protocols. Tail intensities of freshly isolated nuclei from *Ogg1*$^{-/-}$ mice that were thawed after one night, two weeks and four weeks at - 20ºC and nuclei frozen in standard freezing medium or in 50% glycerol in the "Mr Frosty" unit, both for one night, are presented. Finally nuclei freshly isolated from frozen testis tissue are presented. Per cent tail intensity (intensity of the tail relative to the comet head) is used as a measure of DNA damage. Full bars; nuclei not treated with Fpg, striped bars; nuclei treated with Fpg.**

Freezing the nuclei at - 20°C in standard freezing medium with DMSO and FCS for up to two weeks, did not lead to any significant induction of oxidative DNA damage compared to fresh nuclei. When the suspensions were left for four weeks at - 20ºC, higher levels of oxidative DNA damage were measured (Figure 3-2). Marginal levels of DNA damage induced during experiments could be masked or not revealed with such initial levels of DNA in treated samples.

A special freezing unit ("Mr Frosty") was tested to find optimal freezing conditions; this unit has a cooling rate of minus 1°C/minute until - 80°C is reached. Keeping nuclei for 24 hours in "Mr Frosty" did not induce significant levels of DNA damage (Figure 3-2). However, this experiment was only performed once and requires conformation. Furthermore, glycerol (50%) was tested as freezing medium in the "Mr Frosty" unit. Glycerol induced significant levels of DNA damage (Figure 3-2).

A third approach for storage at - 80ºC was to freeze the nuclei first for 1 hour at - 20ºC, and then transfer them to - 80ºC where they were stored for three days. This approach lead to the induction of significant levels of DNA damage (Figure 3-3).

For some experiments it can be useful to start by freezing tissues directly after sacrificing the mice. We wanted to investigate whether it was possible to isolate nuclei with satisfactory low levels of DNA damage for use in comet experiments from frozen tissue. Nuclei isolated from an already snap frozen testis stored at - 80ºC, had acquired increased levels oxidative DNA damage (Figure 3-2). This procedure was only conducted once and requires conformation.

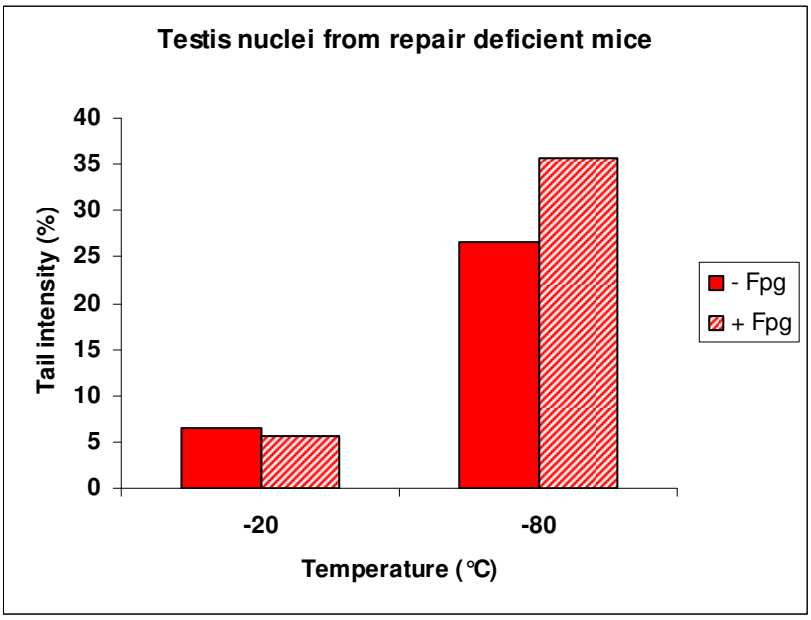


**Figure 3-3 DNA damage in nuclei from *Ogg1*$^{-/-}$ testis frozen at - 20ºC (-20) compared to nuclei frozen at – 20ºC for one hour and then moved to - 80ºC (-80). Both samples were stored for three days, before processing. Refer to Figure 3 1 for legend details.**

Some of the approaches were used for liver nuclei also, with very similar results as with testis nuclei (Figure 3-4). *Ogg1*$^{-/-}$ mice liver spontaneously accumulate higher levels of oxidative base damage, as is shown in freshly isolated liver nuclei (Figure 3-4). Freezing the nuclei directly at - 20ºC in standard freezing medium with DMSO and FCS for up to two weeks did not lead to the induction of significant higher levels of DNA damage compared to freshly isolated nuclei, neither did freezing of the nuclei in the "Mr Frosty" unit.

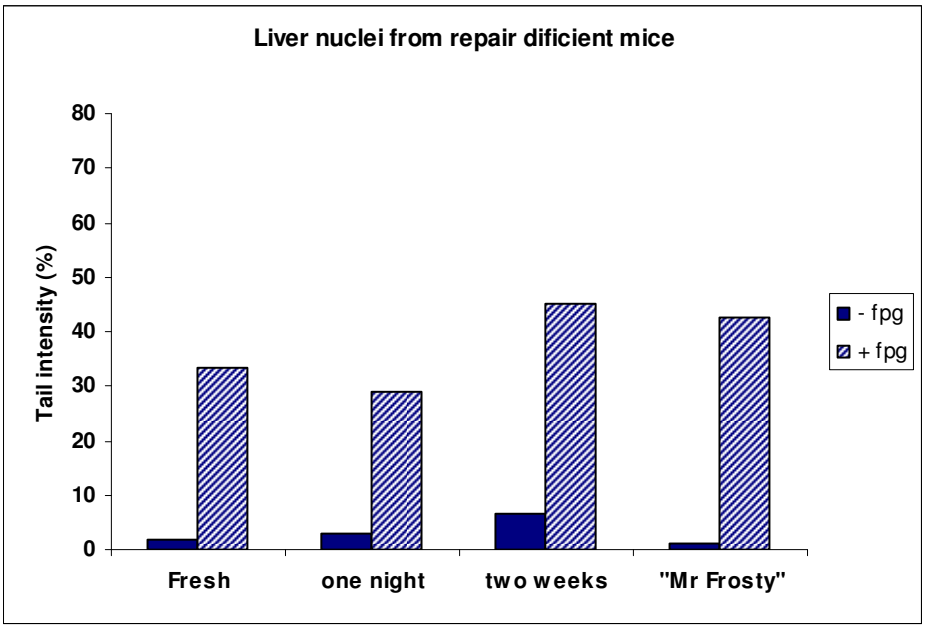


**Figure 3-4 DNA damage in liver nuclei from *Ogg1*$^{-/-}$ mice from freshly isolated nuclei, and nuclei frozen for one night, two weeks or in the "Mr Frosty" unit over night. Refer to Figure 3-2 for legend details.**

The next level of investigation of the suitability of nuclei in comet assays was to expose them to agents to ensure that nuclei respond in a similar way as primary cells. The photosensitiser Ro 12-9786 ± visible light and X-rays were chosen. The former is known to induce high numbers of 8-oxoG relative to the number of SSBs, whereas X-rays induce a definitive number of SSBs per unit dose that is useful for calibration of the comet assay. X-rays induce base damage and SSBs in a 1:1 relationship. As expected, exposure to Ro 12-9786 plus visible light predominantly induced Fpg-sensitive sites (+ Fpg), whereas Ro 12-9786 without light did not induce significant levels of DNA damage (Figure 3-5). X-rays lead to a near linear induction of SSBs, with an increment in tail intensity of approximately 2.3 units per Gy. X-rays induced lower levels of Fpg-sensitive sites relative to SSBs (- Fpg) compared to Ro 12-9786 plus visible light, as expected (Figure 3-5).

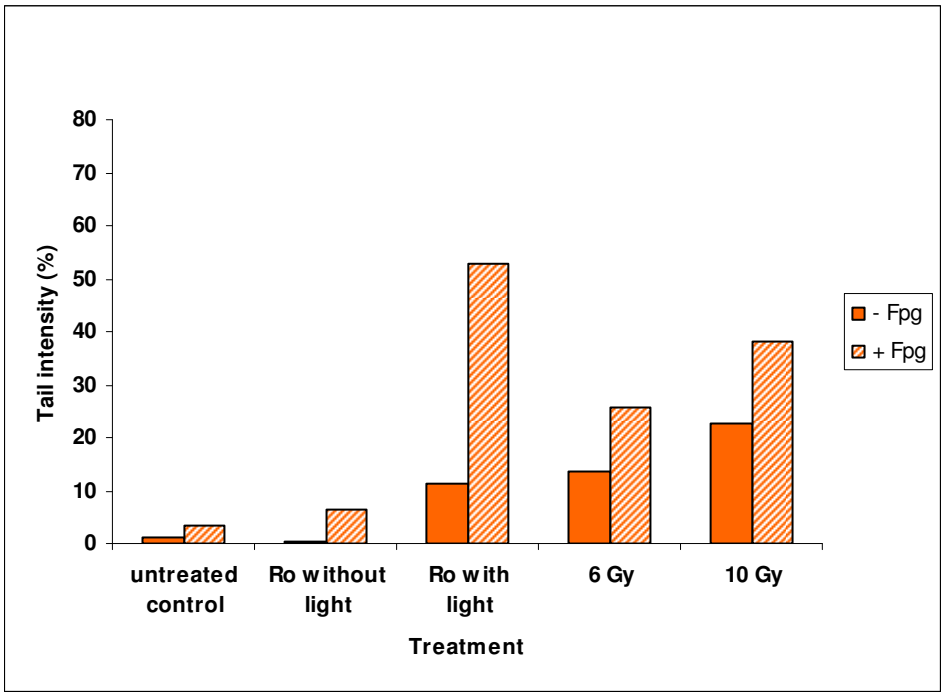


**Figure 3-5 DNA damage in *Ogg1*$^{+/+}$ testis nuclei exposed *in vitro* to Ro 12-9786 plus visible light or to X-ray (Gy). See Figure 3-2 for legend details.**

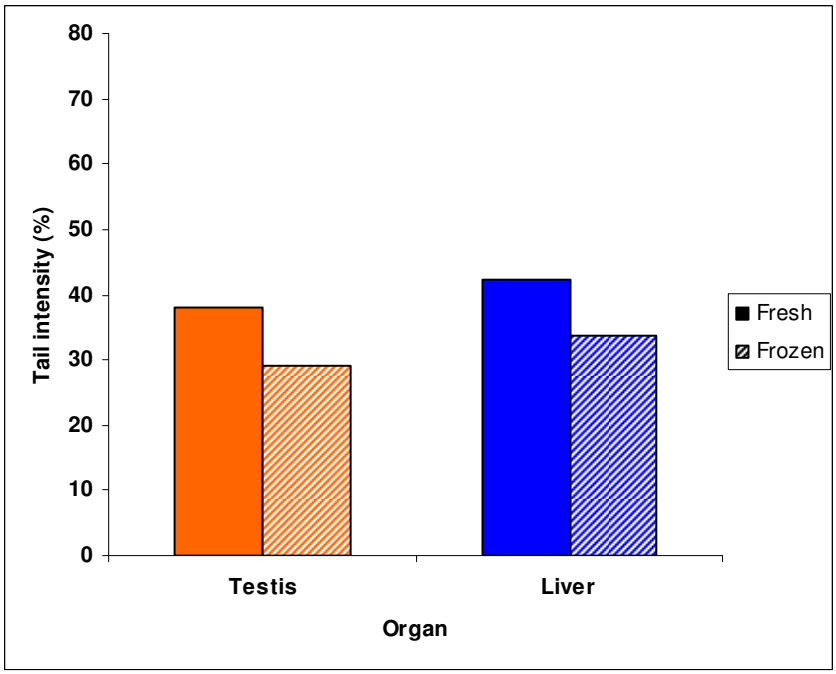


**Figure 3-6 Difference in oxidative DNA damage levels between fresh (filled bar) and frozen nuclei (striped bar) from *Ogg1*$^{+/+}$ testis and liver after *in vitro* exposure to X-rays (10 Gy). All data are comets treated with Fpg.**

Freshly isolated testicular and liver nuclei irradiated with X-rays (10 Gy) casted in agarose immediately, or frozen at - 20ºC for a few days until molding, was tested in the comet assay to establish conditions for *in vivo* studies of DNA repair following X-ray exposure. There was a small decrease in Fpg-sensitive sites in the samples that had been frozen after the irradiation with X-rays (Figure 3-6), probably due to loss of cells.

We concluded that nuclei are useful for use in the comet assay. Furthermore, the marginally lower level of Fpg-sensitive sites in the frozen nuclei were acceptable for use in the *in vivo* repair assay, whereas for measuring oxidative damage induced by BaP exposure *in vivo*, fresh nuclei were required.

## 3.2 Induction of oxidative DNA damage following *in vivo* exposure to BaP

### 3.2.1 *Ogg1*$^{-/-}$ mice

One of the aims of this project was to study the possible induction of oxidative DNA damage following *in vivo* BaP exposure in male germ cells of *Ogg1*$^{-/-}$ and *Ogg1*$^{+/+}$ mice. The mice were exposed to 150 mg BaP/kg bodyweight by i.p. administration and sacrificed at day 1, 3, 5 and 17 after exposure (Figure 2-2 in Materials and Methods). One unexposed control (0 control) and mice exposed to the vehicle only (corn oil 17 days) were included. There was an initial reduction in Fpg-sensitive sites at day 3 in testicular cells from *Ogg1*$^{-/-}$ mice compared to the background level, after which the level of Fpg-sensitive sites increased to a level above background at day 17 (Figure 3-7). Oxidative damage is thus induced as a consequence of BaP-exposure in male germ cells.

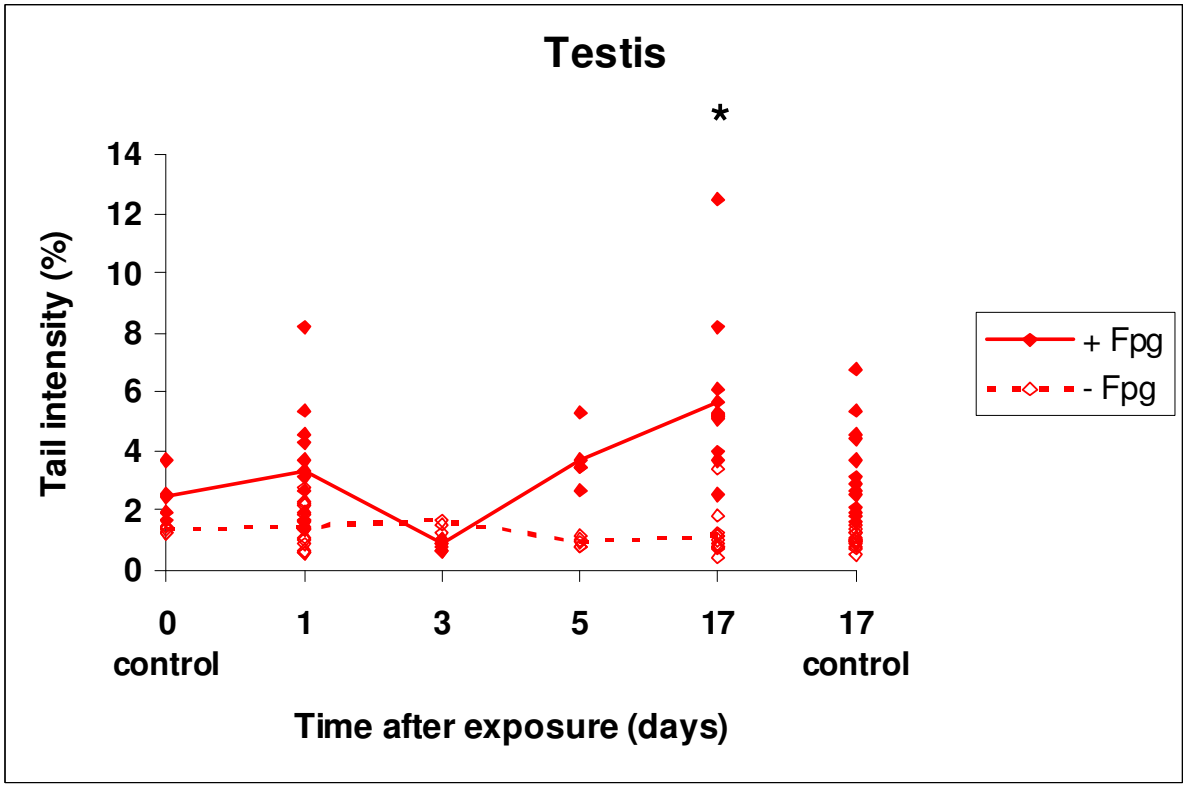


**Figure 3-7 Fpg-sensitive sites in testicular nuclei from *Ogg1*$^{-/-}$ mice exposed to BaP. Median values for each technical replicate (four per animal) were plotted, samples treated with Fpg (+ Fpg) with filled dots and those without Fpg treatment (- Fpg) with open dots. The control at 0 days (0 control) is unexposed, whereas the controls 17 days after exposure (17 control) were exposed to the vehicle (corn oil) only. The bold continuous line represents the mean of nuclei treated with Fpg and the dotted line represents the mean without Fpg treatment. For day 1, 17 and 17 control vehicle consists of three animals, the other time points consists of only one animal. The asterix indicate that the treatment is significantly different from the vehicle.**

The results are based on 4 technical replicates from 12 individual mice; 1 unexposed control (0 control), exposed mice (1 and 17 days = 3 mice, 3 and 5 days = 1 mouse) and 3 mice exposed to the vehicle only for 17 days (17 control). The distribution of the *Ogg1*$^{-/-}$ data for the testis, liver and lung are shown as boxplots in Appendix A (Figure 6-1). The distribution is not normal due to skewed data; especially for the testis. Log transformation did not make a significant difference to the data. The homogeneity of the variances was tested with the Levene's test of equal variances. The p-values were < 0.001 for the testis and the lung, and 0.197 for the liver (Table 3-1), indicating that only data for the liver did not violate the assumption of equal variances. The variances for the testis and lung were significantly different, and hence violated one of the assumptions of the ANOVA. On the other hand, since the ANOVA is regarded as robust and the assumption of independent cases is most important reviewed in (Lovell and Omori 2008) and the non-parametric alternative is less sensitive and

not convenient with nested data, we performed the ANOVA on our data. The ANOVA showed that the different animals and the gels represent a very low fraction of the total variance (Table 3-1), indicating that the gels and the animals in one treatment group is not significantly different from each other. The Tukey HSD test, which assumes equal variances, and Tamhane test, which do not assume equal variances, are *post hoc* comparison tests which patterns in the data not specified a priori may be detected. All results that came out significant in the Tukey HSD test were also significant with the Tamhane test. Since the variances of testis and lung data were not equal, and there was no difference in the significance between the two *post hoc* tests, it was appropriate to use the Tamhane test for all tissues (Table 3-1). The test showed that at day 17 following BaP-exposure, the data for testis nuclei was significantly different from the vehicle control and from day 1 following BaP-exposure ($p < 0.001$). For curiosity, since the following comparison violates statistical rules, the results from day 1 after BaP-exposure were not significantly different from the vehicle control (Table 3-1).

Nuclei of liver and lung were also studied as somatic controls. A similar pattern was observed as in testicular nuclei with an initial reduction followed by an increase in Fpg-sensitive sites, but the time course for each organ was dissimilar (Figure 3-8). The decrease was most pronounced at a later time point in the liver (5 days) than in the testis (3 days) or lung (1 day). This transient reduction is statistically significantly different from the 17 day corn oil control, tested at 1 day after exposure for both liver and lung ($p < 0.001$, Table 3-1). No significant increase in Fpg-sensitive sites were measured for liver at day 17 following BaP-exposure compared to the 17 vehicle ($p = 0.094$, Table 3-1), but there is a trend towards increasing levels of Fpg-sensitive sites. However, lung nuclei 17 days after exposure exhibit significantly higher levels of Fpg-sensitive sites than the 17 day vehicle control ($p = 0.006$, Table 3-1), showing that Fpg-sensitive sites are indeed induced in the lung after *in vivo* exposure to BaP.

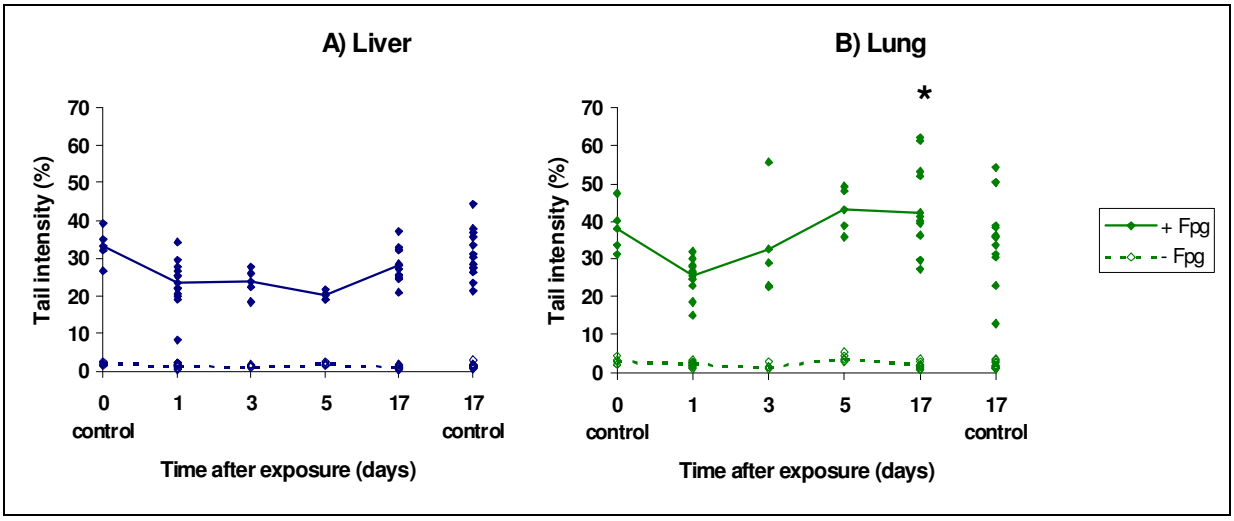


**Figure 3-8 Fpg-sensitive sites in nuclei of liver (A) and lung (B) from *Ogg1*$^{-/-}$ mice exposed to BaP. See Figure 3-7 for legend details. Note the different Y-scale.**

**Table 3-1 *Ogg1*$^{-/-}$ statistics summary. The ANOVA was performed with Levene's test of equality of variances and the *post hoc* Tamehane test. p-values are given for the tests (significance level 0.05).**

| | Equality of variances | Variance (% of the total variance explained by animals and gels) | 17 days BaP vs 17 control | 1 day BaP vs 17 control | 1 day BaP vs 17 days BaP |
|---|---|---|---|---|---|
| **Testis** | < 0.001 | 1.59 (animals)<br>2.96 (gels) | < 0.001 | 0.474 | < 0.001 |
| **Liver** | 0.197 | 7.31 (animals)<br>0.16 (gels) | 0.094 | < 0.001 | < 0.001 |
| **Lung** | < 0.001 | 8.32 (animals)<br>0.38 (gels) | 0.006 | < 0.001 | < 0.001 |

Taken together, we observed an increase in Fpg-sensitive sites in the testis and the lung at 17 days after BaP-exposure, that were both significant ($p < 0.001$). In the liver there is a trend

towards increasing levels of Fpg-sensitive sites at day 17 after BaP-exposure, that nearly reached statistical confidence (p = 0.094).

### 3.2.2 *Ogg1*$^{+/+}$ mice

*Ogg1*$^{+/+}$ mice were also exposed to BaP in order to function as controls. There was no apparent induction of Fpg-sensitive sites in the testis or the somatic organs at any time point (Figure 3-9 and Figure 3-10).

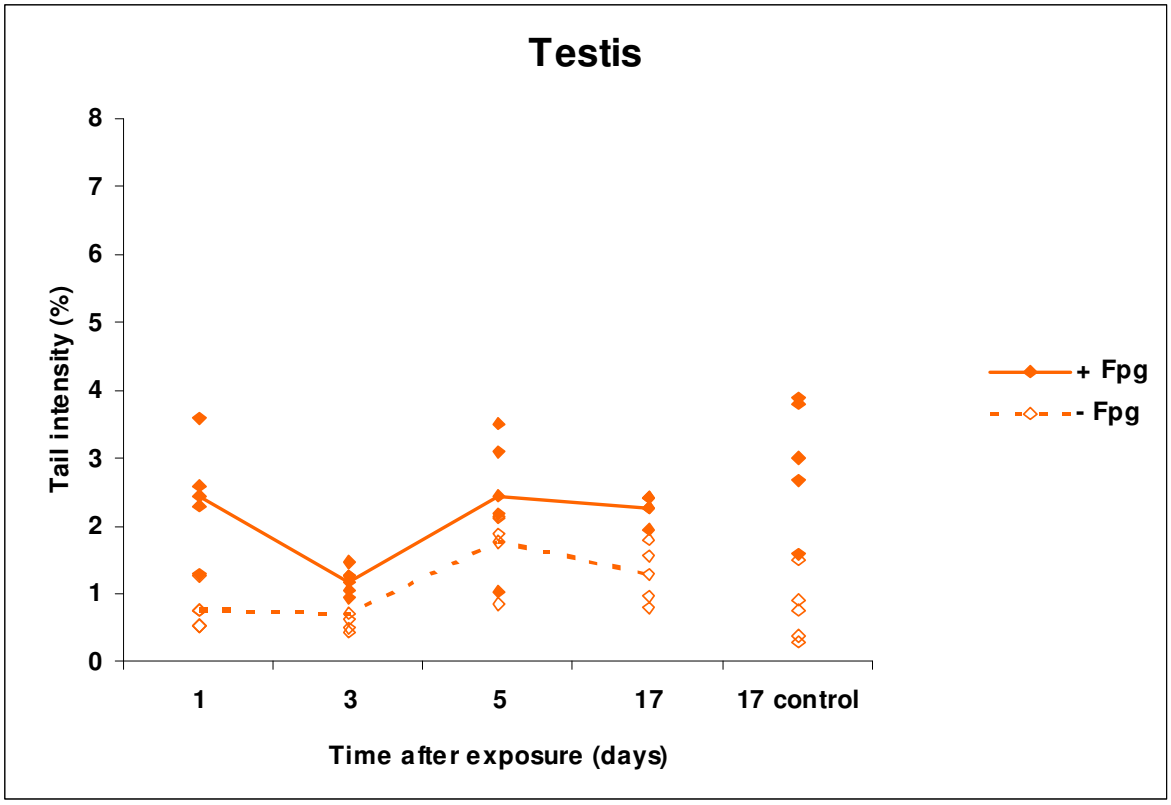


**Figure 3-9 Fpg-sensitive sites in testis nuclei from *Ogg1*$^{+/+}$ mice exposed to BaP. Median values for each technical replicate (four per animal) were plotted, samples treated with Fpg (+ Fpg) with filled dots and those without Fpg treatment (- Fpg) with open dots. The control 17 days after BaP-exposure (17 control) were exposed to the vehicle (corn oil) only. The bold continuous line represents the mean of nuclei treated with Fpg and the dotted line represents the mean without Fpg treatment. It was only one animal per time point.**

However, in the testis there was a temporary decrease in Fpg-sensitive sites at day 3 after BaP-exposure that returned to the initial level at day 5 after BaP-exposure (Figure 3-9). In liver and lung (Figure 3-10) there were no apparent increases in Fpg-sensitive sites after BaP exposure either, but also for these organs there was a transient reduction of Fpg-sensitive sites

at day 3 after BaP-exposure, followed small elevation of both single strand breaks (-Fpg) and Fpg-sensitive sites at day 5 after BaP exposure. A similar small increase in single strand breaks was also observed for *Ogg1*$^{-/-}$ liver and lung (Figure 3-8).

The experiment with *Ogg1*$^{+/+}$ mice consists of one animal per time point for all organs, implicating that statistical analysis was not allowed as the animal is regarded as the experimental unit.

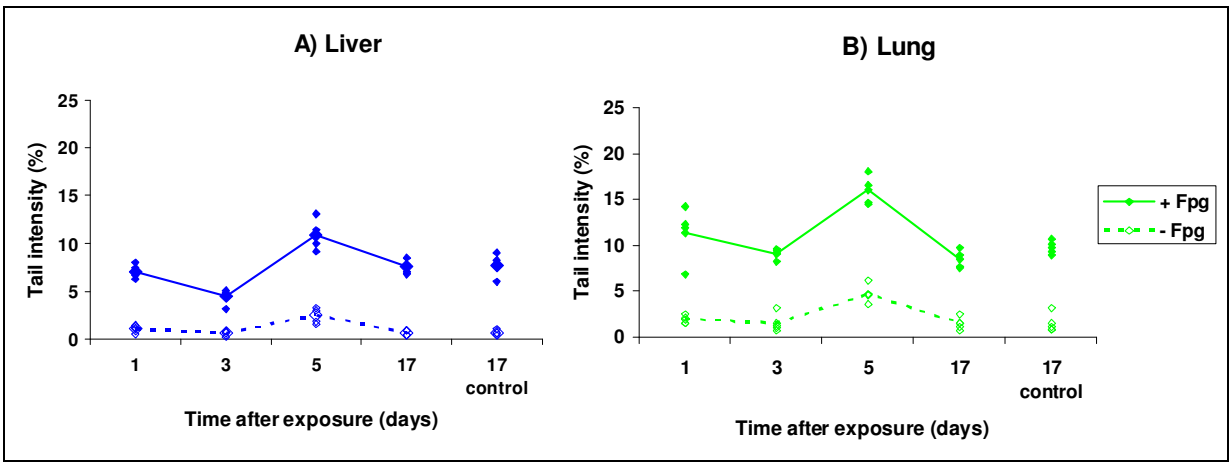


**Figure 3-10 Fpg-sensitive sites in liver (A) and lung (B) nuclei from *Ogg1*$^{+/+}$ mice exposed to BaP. See Figure 3-9 for legend details.**

## 3.3 Gene expression of selected genes involved in BaP-metabolism in *Ogg1*$^{-/-}$ and *Ogg1*$^{+/+}$ mice

The genotoxic effects of BaP are exerted by its metabolites. Knowledge of the response of the genes involved in this process would increase the understanding of the effects of BaP *in vivo*. Hence total RNA was isolated from testis and liver from the *Ogg1*$^{-/-}$ and *Ogg1*$^{+/+}$ mice involved in the BaP-experiment. cDNA was generated and real-time PCR was conducted for *Akr1a4*, *Cyp1a1*, *Cyp1a2* and *Cyp1b1* as well as housekeeping genes as controls.

### 3.3.1 Total RNA and cDNA quantity and purity

The quantity and purity of the total RNA and cDNA samples were analysed using a NanoDrop ND-1000 Spectrophotometer. RNA and DNA absorb at 260 nm and the concentrations of the samples were estimated in the NanoDrop software according to the absorbance at 260 nm. The 260/280- and 260/230 ratios of absorbance were calculated. A 260/280 ratio of around 1.8 for DNA and 2.0 for RNA indicate pure samples, whereas ratios

lower than these values indicate the presence of protein, phenol or other contaminants that absorb light at 280 nm. A 260/230 ratio above 2.0 indicate pure samples. A 260/230 ratio below 2.0 indicate contaminants, such as carbohydrates, salts and phenol, that absorb at 230 nm.

Mean and standard deviation values were calculated for all the total RNA samples from testis and liver and are presented in Table 3-2. The results show that purities and concentrations of the samples were satisfactory. The cDNA samples had a 260/230 ratio of 2.3 ± 0.01 and a 260/280 ratio at 1.8 ± 0.01 in both tissues, which is satisfactory.

**Table 3-2 Mean and standard deviation (SD) values of the purities and amounts of all total RNA samples from testis and from liver.**

| Tissue | Tissue (mean mg ± SD) | 260/230 (mean ± SD) | 260/280 (mean ± SD) | Amount (mean µg ± SD) |
|---|---|---|---|---|
| **Testis** | 25.9 ± 3.9 | 2.2 ± 0.1 | 2.1 ± 0.02 | 49.1 ± 9.2 |
| **Liver** | 27.4 ± 4.5 | 2.0 ± 0.2 | 2.1 ± 0.03 | 43.2 ± 16.8 |

To ensure that the procedure of isolating RNA did not reduce the quality of the RNA, the integrity was analysed in one testis and one liver sample from a control animal using Bioanalyzer (Agilent Technologies). The quality was good, above 8 measured as RNA integrity number (RIN). The RIN number is calculated by the Bioanalyzer 2100 software, based on the shape of the curve in the electropherogram. The classification range from 1 to 10, in where 1 represents the most degraded RNA and 10 represent the most intact RNA.

### 3.3.2 Gene expression analyses

#### 3.3.2.1 Housekeeping gene expression

500 ng total RNA were reverse transcribed into cDNA, which were used in the gene expression analyses. Housekeeping genes are expressed ubiquitously, and usually have similar expression levels in all cells. Thus two housekeeping genes, *18S rRNA* and *β-actin* (*actb*), were tested. The one with the most stable expression in all samples were chosen to normalise for variations between runs in the real-time PCR analyses. In this project *18S rRNA*

was selected due (Figure 3-11), but the expression of *β-actin* was as stable as *18S rRNA* (data not shown).

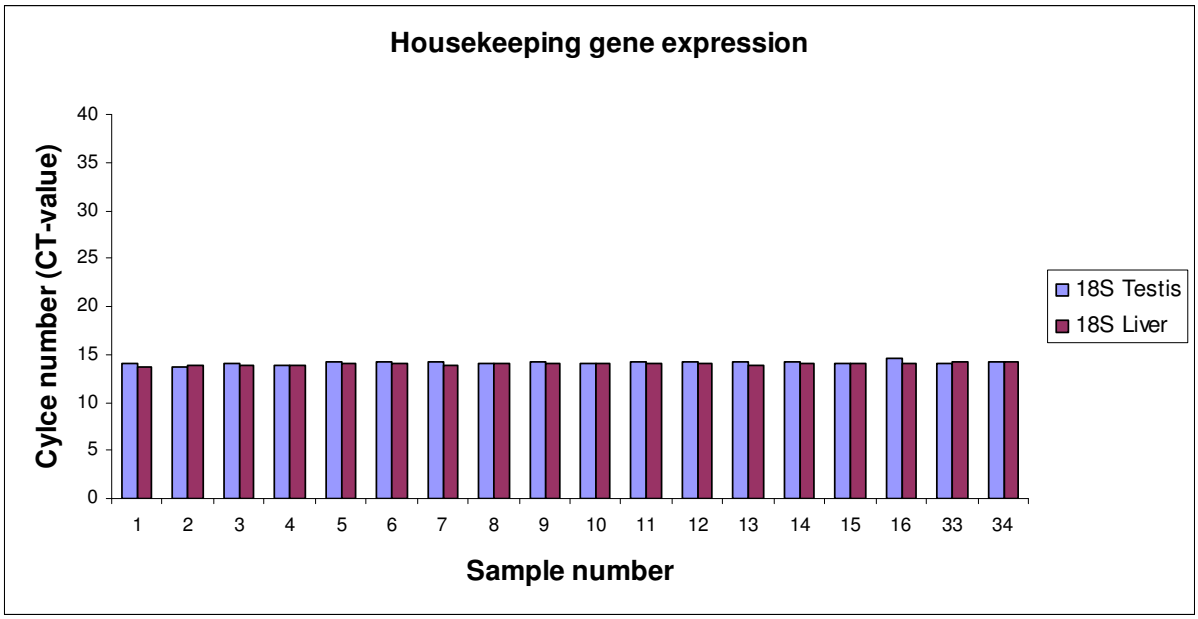


**Figure 3-11 Housekeeping gene 18S expression in all samples from testis and liver. The CT-value represented the cycle number where the amount of PCR-product crossed the threshold line.**

### 3.3.2.2 Dilution series

Dilution series were performed, to find suitable dilutions of cDNA and to ensure that there are equal amplification efficiencies for all genes (Figure 3-12 and Figure 3-13) in order to function as a quantitative assay. Equal efficiency is required for the ΔΔCT-method. The dilution series were performed on one untreated control sample and one 17 days after BaP-exposed sample (data is not shown for the exposed sample), with primers for *m18S*, *mβ-actin*, *mAkr1a4* and *mCyp1a1*. 1 ng/µl cDNA which corresponds to a total of 0.2 ng per well was chosen and used in all further analysis. Logarithmic regression lines, ($R^2$ testis ≈ 0.87 – 0.99; $R^2$ liver ≈ 0.90 – 0.99), were acceptable; there is little variation between parallels.

Throughout this gene expression study dissociation curves was performed to rule out problems such as primer-dimer products. We did not observe any primer-dimer products.

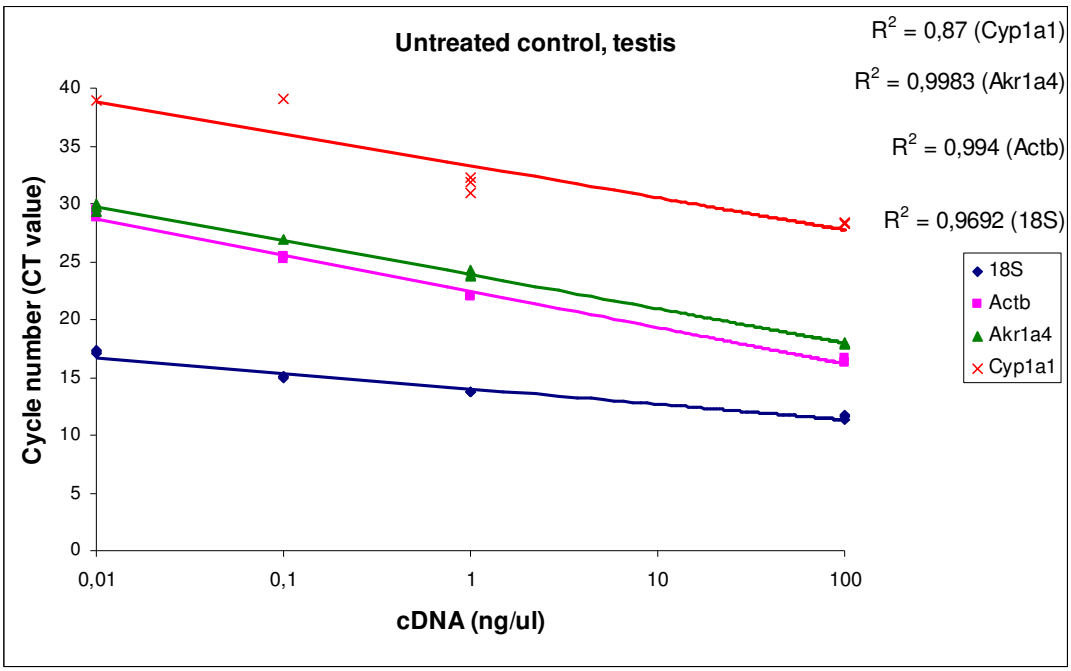


**Figure 3-12 Dilution curves for one unexposed control sample from testis. X-axis is logarithmic with amount of cDNA used (ng/µl), and the Y-axis shows the CT-value. Regression lines are shown with the $R^2$ numbers.**

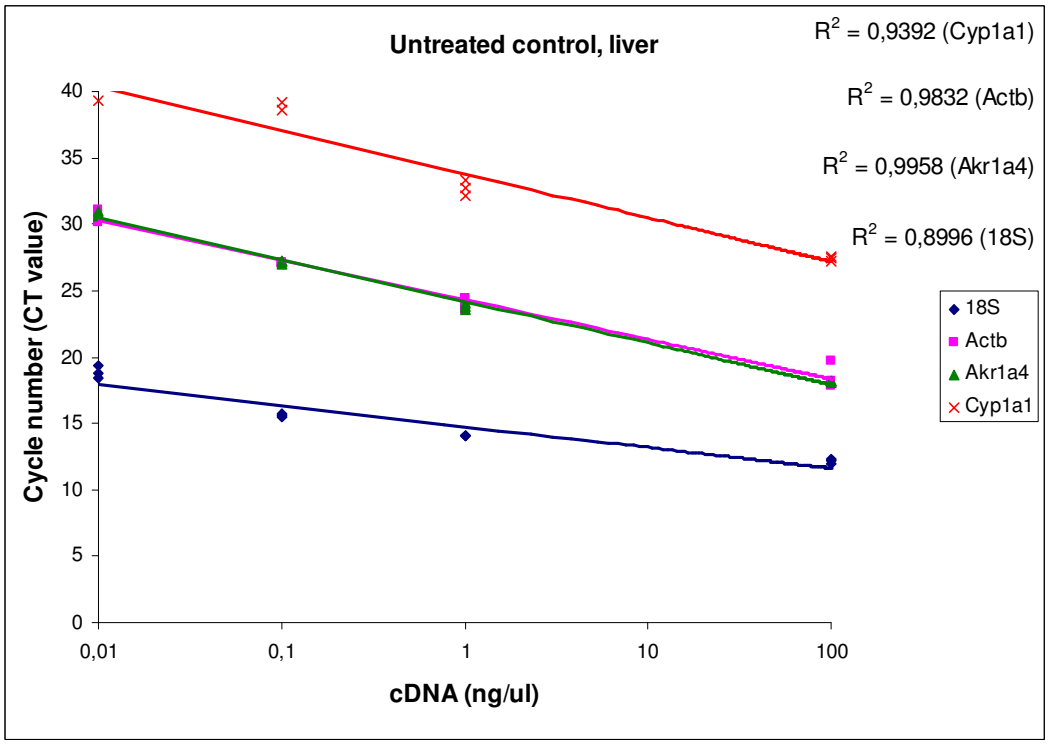


**Figure 3-13 Dilution curves for one unexposed control sample from liver. X-axis is logarithmic with amount of cDNA used (ng/µl), and the Y-axis shows the CT-value. Regression lines are shown with the $R^2$ numbers.**

The relative gene expression was investigated for *Akr1a4*, *Cyp1a1*, *-1a2* and *Cyp1b1* in the testis and liver of the BaP-exposed animals and untreated controls (Figure 3-14 to Figure 3-17). The Cyp genes metabolise BaP to its epoxide, which then can give rise to BPDE-DNA adducts. Akr1a4 is the mouse homologue of AKR1A1 that metabolise BaP to *o*-quinones with concomitant generation of ROS. We wanted to study the expression of these genes following *in vivo* exposure of mice to BaP, to examine if the induced levels of DNA damage (in particular oxidative DNA damage) correspond to altered expression of the genes involved in BaP-metabolism. The figures show relative gene expression (log2 transformed fold change relative to the untreated control) for testis and liver samples. All samples were normalised relative to the unexposed control (day 0) (ΔΔCT). Two of the *Ogg1*$^{-/-}$ liver samples were not labelled properly (one 17 day vehicle control sample and one day 17 after BaP-exposure sample were both labelled with identical names), and were hence excluded from the dataset. Data from 17 days after BaP exposure in liver thus comprises two animals.

### 3.3.2.3 *Akr1a4* expression

In the testis of *Ogg1*$^{-/-}$ mice there was a weak gradual induction with a maximum at 5 days after BaP exposure (~2 fold), and a somewhat more pronounced induction (~2.5 fold) of *Akr1a4* in the liver at 5 days after BaP exposure (Figure 3-14 A).

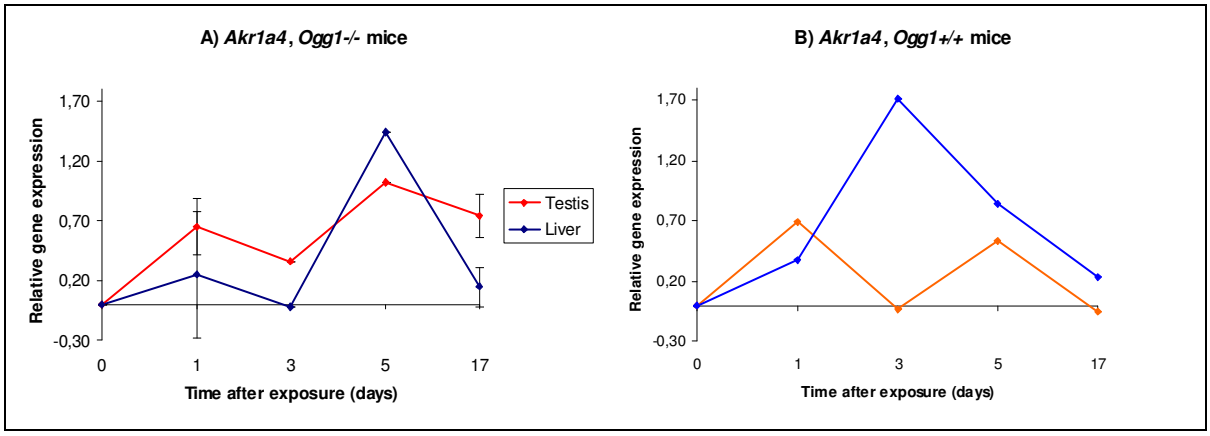


**Figure 3-14 *Akr1a4* expression in testicular (red) and liver (blue) from both *Ogg1*$^{-/-}$ (A) and *Ogg1*$^{+/+}$ (B) mice. The relative gene expression is presented as log2 transformed fold change relative to unexposed control (day 0). Time after exposure to BaP is shown in days.**

The levels in the testis at day 17 after BaP-exposure were reduced marginally compared to day 5 after BaP-exposure, whereas the levels for the liver dropped markedly at 17 days after

exposure to a level similar to that of unexposed mice. The response pattern was different in *Ogg1*$^{+/+}$ mice; the data was variable in the testis, showing a possible weak induction in the testis, whereas in the liver there was a clear induction (~3.3 fold, Figure 3-14 B) that appeared at an earlier time point (day 3) compared to the *Ogg1*$^{-/-}$ mice (day 5). Taken together, *Akr1a4* is induced by BaP in the testis, at least in *Ogg1*$^{-/-}$ mice. There are differences in *Akr1a4* gene expression responses in the testis compared to the liver, as well as between *Ogg1*$^{-/-}$ and *Ogg1*$^{+/+}$ mice.

### 3.3.2.4 *Cyp1a1, -1a2* and *-1b1* expression

In the testis the relative gene expression varied between the genes studied. The relative gene expression in the liver of *Cyp1a1*, *-1a2* and *-1b1*, showed similar patterns to each other; the genes were highly induced at day 1 after BaP-exposure and returned approximately to baseline at day 17 after BaP-exposure (Figure 3-15 to Figure 3-17).

The expression of *Cyp1a1* was very similar in both *Ogg1*$^{-/-}$ (Figure 3-15 A) and *Ogg1*$^{+/+}$ (Figure 3-15 B) mice. The relative gene induction was high for testis (~16 fold) and even higher in liver (~4000 fold) at day 1 after BaP exposure, after which it decreased to near baseline at day 17 after BaP exposure in both tissues.

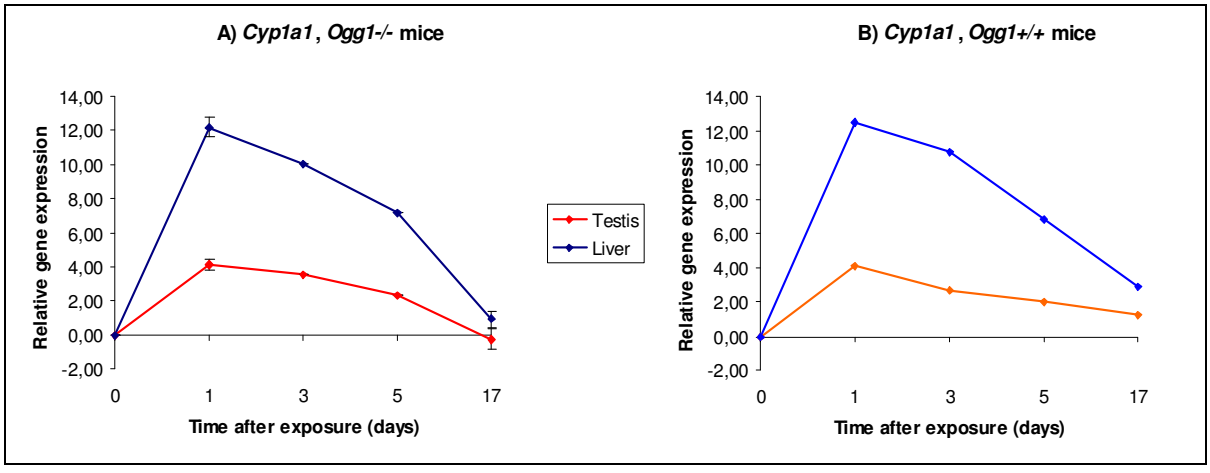


**Figure 3-15 *Cyp1a1* expression in testis and liver from *Ogg1*$^{-/-}$ (A) and *Ogg1*$^{+/+}$ (B) mice. See Figure 3-14 for legend details.**

*Cyp1a2* was weakly induced in *Ogg1*$^{-/-}$ testis following BaP-exposure, with no induction in *Ogg1*$^{+/+}$ testis (Figure 3-16). In the testis from *Ogg1*$^{-/-}$ mice (Figure 3-16 A) the induction (~4 fold) was highest at day 5 after BaP-exposure, and returned to control levels at day 17 after BaP-exposure. In *Ogg1*$^{+/+}$ mice however, there was a reduction (~4 fold) in the expression at

day 17 after exposure (Figure 3-16 B). In the liver the expression patterns were similar to that of the other genes, with highest induction (~ 23 fold) at day 1 after BaP exposure, followed by a decrease, although in *Ogg1*$^{+/+}$ liver the reduction was not returned to control levels at day 17 after BaP exposure. Taken together, we observed differences in *Cyp1a2* expression between *Ogg1*$^{-/-}$ and *Ogg1*$^{+/+}$ mice exposed to BaP, both for testis and liver.

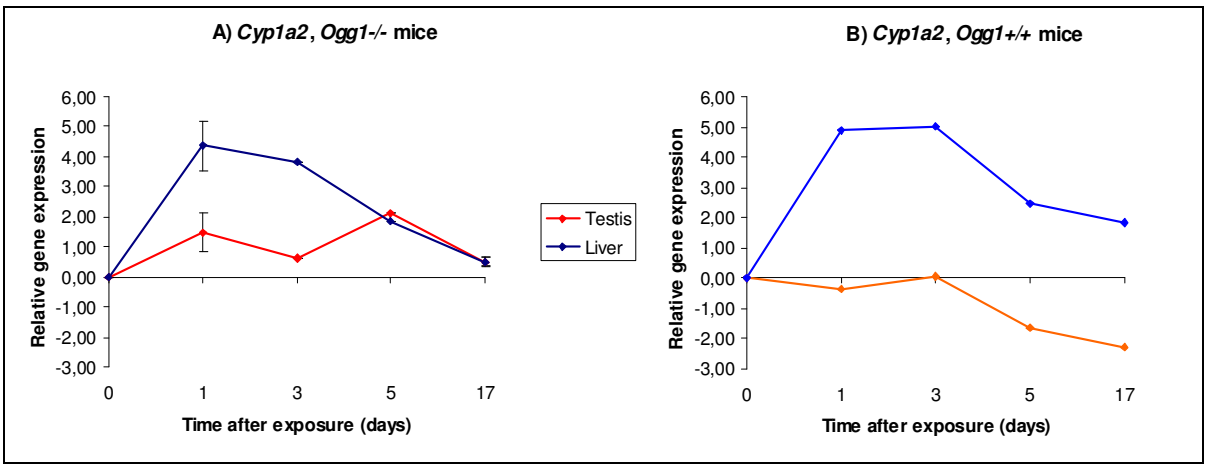


**Figure 3-16 *Cyp1a2* expression in liver and testis from *Ogg1*$^{-/-}$ (A) and *Ogg1*$^{+/+}$ (B) mice. See Figure 3-14 for legend details.**

*Cyp1b1* was not induced in either *Ogg1*$^{-/-}$ or *Ogg1*$^{+/+}$ testis according to our results (Figure 3-17). The liver expression pattern was similar to that of other Cyp-genes with a marked induction (~23 fold) at day 1 after BaP-exposure, which gradually decreased until it reached baseline for *Ogg1*$^{+/+}$ and nearly baseline for *Ogg1*$^{-/-}$ liver at day 17 after BaP-exposure.

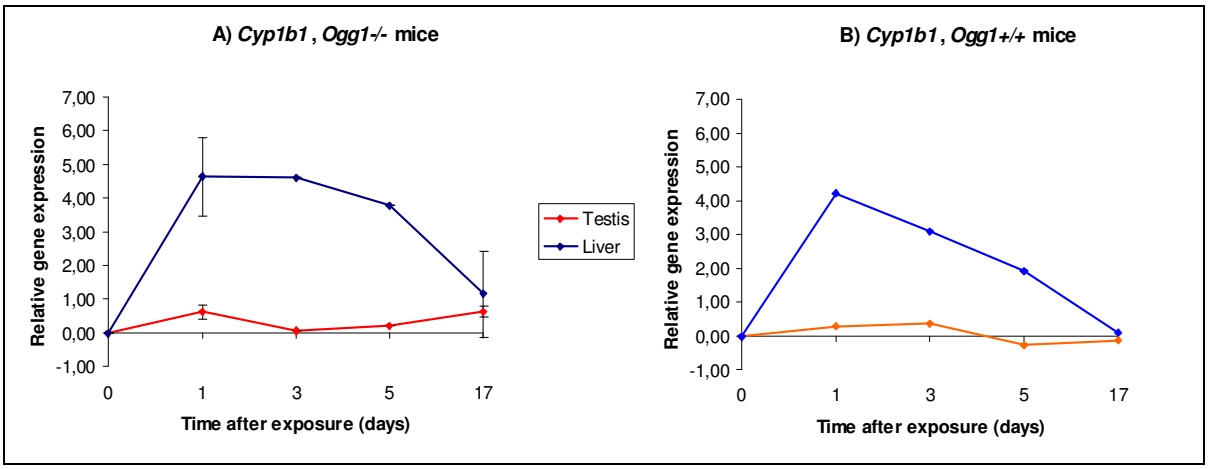


**Figure 3-17 *Cyp1b1* expression in testis and liver from *Ogg1*$^{-/-}$ (A) and *Ogg1*$^{+/+}$ (B) mice. See Figure 3-14 for legend details.**

The constitutive levels of all genes were also established Table 3-3, 2^-ΔCT values of unexposed controls normalised with the housekeeping gene *β-actin* were used. The table shows that in testis *Akr1a4* is highest constitutive expressed, whereas in liver both *Akr1a4* and *Cyp1a2* is expressed in high amounts. *Cyp1a1* and *Cyb1a2* are not expressed in high amounts constitutively in either tissue. There are no obvious differences between *Ogg1*$^{-/-}$ and *Ogg1*$^{+/+}$ mice in either testis or liver control tissues.

**Table 3-3 Constitutive expression of all genes in tissues of both mice genotypes. The values represent 2^-ΔCT values of unexposed controls normalised with the housekeeping gene *β-actin*.**

| Organ | Genotype | *Akr1a4* | *Cyp1a1* | *Cyp1a2* | *Cyp1b1* |
|---|---|---|---|---|---|
| **Testis** | ***Ogg1*$^{-/-}$** | 5.23 | 0.01 | 0.03 | 0.70 |
| | ***Ogg1*$^{+/+}$** | 5.23 | 0.02 | 0.08 | 1.06 |
| **Liver** | ***Ogg1*$^{-/-}$** | 72.89 | 0.03 | 19.53 | 0.01 |
| | ***Ogg1*$^{+/+}$** | 72.89 | 0.04 | 14.80 | 0.05 |

## 3.4 Repair of oxidative DNA damage following *in vivo* exposure of *Ogg1*$^{-/-}$ and *Ogg1*$^{+/+}$ mice to X-rays

As a part of the characterisation of *Ogg1*$^{-/-}$ mice as a model for measuring the potential of environmental agents to induce oxidative damage in male germ cells of humans, repair of oxidative DNA damage *in vivo* was measured in *Ogg1*$^{-/-}$ and *Ogg1*$^{+/+}$ mice. The mice were exposed to 10 Gy of X-rays and were allowed to repair for different time periods following exposure (Figure 3-18 and Figure 3-19). The animals were sacrificed and organs were put on ice within three minutes. The results show that *Ogg1*$^{-/-}$ mice exhibit no detectable repair of Fpg-sensitive sites in mice testis, liver or lung (Figure 3-18). As expected, SSBs were efficiently repaired (Figure 3-18, dashed line). Furthermore, there was a small increase of Fpg-sensitive sites in the *Ogg1*$^{-/-}$ lung.

The data is presented as relative repair normalised using Fpg-sensitive sites at 0 hours as 100% damage (0% repair). This normalisation was conducted to correct for methodological differences since each animal was processed separately. Statistical analyses were performed on time points with three animals (see Figure 2-3 in Materials and Methods), as the animal is

regarded as the experimental unit. Since median values were for the normalisation, a non-parametric method, Mann-Whithey U test, was used for statistical testing. The Mann-Whitney U test is the non-parametric alternative for the independent-sample t-test. For *Ogg1*$^{-/-}$ mice the 20 minutes time point rather than the 0 hour time point was used for comparisons. After X-ray exposure a lower relative number of Fpg-sensitive sites compared to SSBs is measured at time zero than theoretically expected in the comet assay. This is probably due to the clustered nature of DNA damage induced by X-rays, and the fact that Fpg enzyme activity is inhibited by clustered damage (David-Cordonnier *et al.* 2001; Olsen *et al.* 2003; Pearson *et al.* 2004). Hence the initial level of Fpg-sensitive sites is probably underestimated at time zero. As soon as the SSBs are repaired more relevant levels can be measured in this assay. As previously observed and discussed (Olsen *et al.* 2003), there seems to be a smaller radiation-induced increase in Fpg-sensitive sites than expected relative to SSBs, for all tissues in both *Ogg1*$^{-/-}$ mice and *Ogg1*$^{+/+}$ at 0 h time point, probably caused by clustered DNA damage.

For *Ogg1*$^{-/-}$ mice the 20 minutes time point was used to compare the capacities for repair of Fpg-sensitive sites, since at that time a majority of SSBs induced are repaired (approximately 50%). The increase of Fpg-sensitive sites in the lung at 24 hours of repair was significantly higher than at 20 minutes ($p = 0.05$, Table 3-4). In the liver 24 hours of repair was not significantly different from 20 minutes of repair ($p = 0.275$, Table 3-4). The level of Fpg-sensitive sites was unchanged in the testis from 20 minutes to 24 hours ($p = 0.513$, Table 3-4). For *Ogg1*$^{+/+}$ mice, zero hours time point was compared to 6 hours time point even though the zero time point is lower than expected (clustered damage). The comparison was done because we had three animals at zero time point, but only one at 20 minutes, and at 20 minutes almost all damage is repaired.

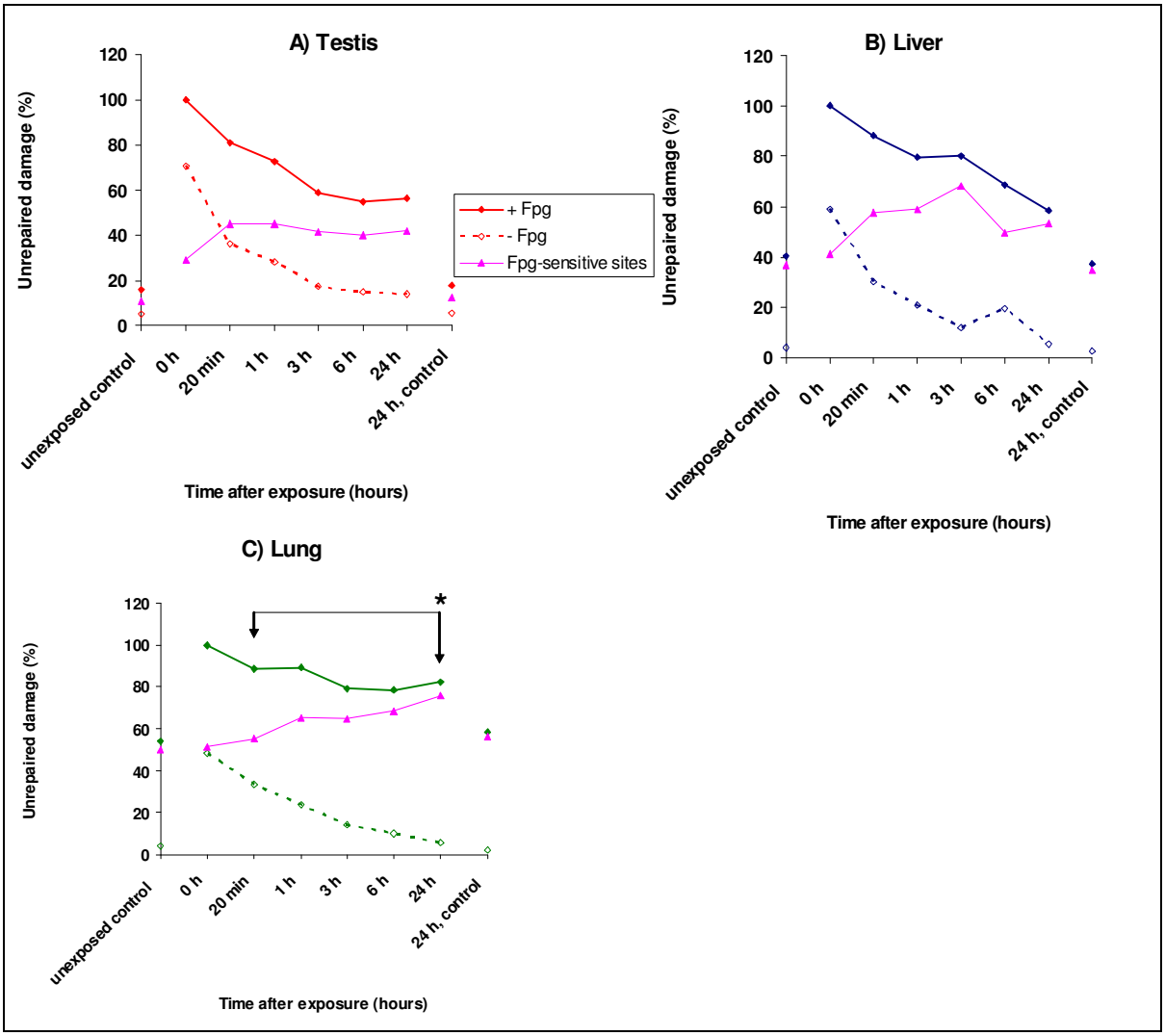


**Figure 3-18 No oxidative DNA damage repair in testis (A), liver (B) and lung (C) nuclei from *Ogg1*$^{-/-}$ mice exposed to X-rays (10 Gy) (pink line). Relative levels of unrepaired DNA damage (%) is plotted against time following exposure (hours). The 24 hour controls are sham exposed controls. The asterix indicate that 24 hours of repair are significantly different from 20 minutes of repair.**

In the experiments with the *Ogg1*$^{+/+}$ mice (Figure 3-19) more than 50% of the oxidative DNA damage in the testis and the liver were removed during the first 20 minutes, after which the remaining lesions were removed more slowly. In the testis the net levels of Fpg-sensitive sites at 6 hours of repair were significantly lower from those of 0 hours of repair in the testis ($p = 0.05$, Table 3-4), but this was not the case in the liver ($p = 0.827$, Table 3-4), probably due to the variations in the experiment. All data from the lung was excluded from this study due to experimental errors.

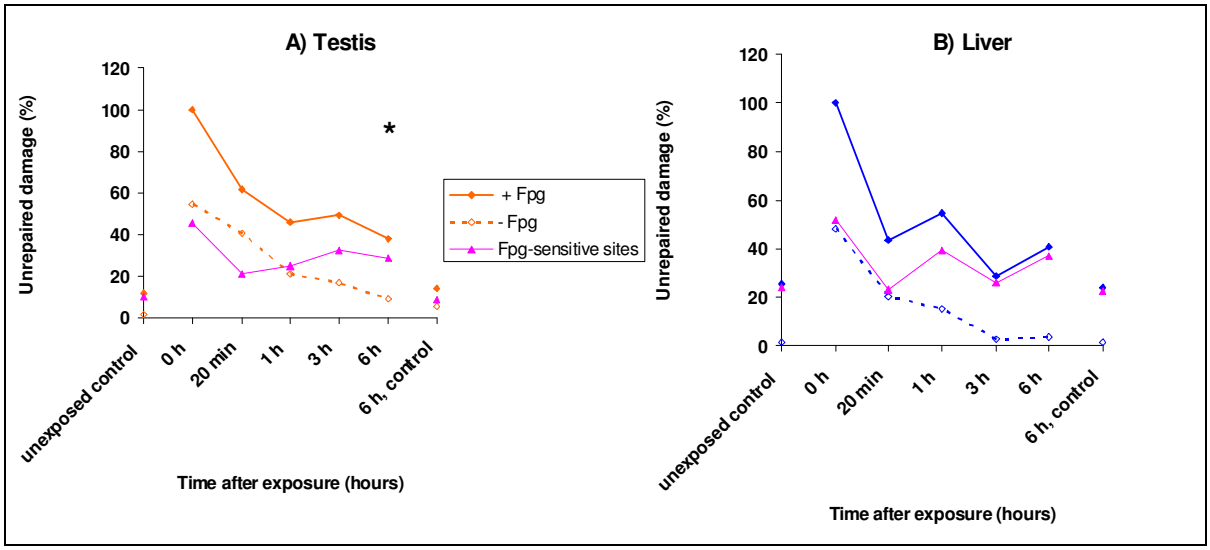


**Figure 3-19 Repair of Fpg-sensitive sites (pink line) in testis (A) and liver (B) of *Ogg1*$^{+/+}$ mice. The 6 hour control is sham exposed controls The asterix indicate that 6 hours of repair is significantly different from 0 hours of repair. Refer to Figure 3-18 for legend details.**

**Table 3-4 Summary of statistical analyses in *in vivo* repair of X-ray damage in *Ogg1*$^{-/-}$ and *Ogg1*$^{+/+}$ mice. The Mann-Whitney U test was used, and the significance level was set as 0.05. The table presents 2-tailed p-values.**

| | ***Ogg1*$^{-/-}$ (20 minutes vs 24 hours)** | ***Ogg1*$^{+/+}$ (0 hours vs 6 hours)** |
|---|---|---|
| **Testis** | 0.513 | 0.05 |
| **Liver** | 0.275 | 0.827 |
| **Lung** | 0.05 | - |

# 4 Discussion

Environmental agents cause oxidative DNA damage such as 8-oxoG in the genome of male germ cells, that have negative effects on male reproduction. Human spermatozoa sometimes possess high levels of DNA damage, which can interfere with the male ability to reproduce (Sun *et al.* 1997; Irvine *et al.* 2000). It has been shown that a decrease in sperm quality and number is correlated with spermatozoa that contain 8-oxoG lesions (Ni *et al.* 1997; Shen *et al.* 1997; Lopes *et al.* 1998; Irvine *et al.* 2000). This again interferes with both *in vivo* and *in vitro* fertilisation ability (Lopes *et al.* 1998; Sakkas *et al.* 1998). Further implications are abortions, congenital malformations and disease in the offspring (Ahmadi and Ng 1999; Zenzes *et al.* 1999b). Smoking has been shown to induce increased levels of oxidative DNA damage such as 8-oxoG lesions in the sperm, abnormal sperm and reduced fecundity (Zitzmann *et al.* 2003). BaP, which is found at high levels in cigarette smoke, represents an environmental exposure which is common and which leads to an increased oxidative stress to the whole organism. BaP is metabolised by CYP1A1, -1A2, -1B1, AKR1A1 and AKR1C1-1C4 into its DNA damaging metabolites. The CYP-enzymes produce BPDE which forms stable adducts with DNA. The AKRs metabolise BaP into *o*-quinones and during this process ROS are produced, which in turn give rise to 8-oxoG in DNA (Penning *et al.* 1996; Quinn and Penning 2008; Park *et al.* 2008b).

Our laboratory has shown that human testicular cells poorly repair oxidative DNA lesions such as 8-oxoG. Rodent testicular cells repair oxidative DNA lesions such as 8-oxoG effectively, whereas humans do not (Olsen *et al.* 2003). Furthermore, male germ cells also exhibit a low NER function (Brunborg *et al.* 1995; Jansen *et al.* 2001). These findings indicate that great care should be taken in extrapolating results from rodents to man, when studying genotoxic effects in male germ cells. *Ogg1*$^{-/-}$ mice are proposed as an more suitable model than wild type (*Ogg1*$^{+/+}$)mice for studying genotoxic effects in human male germ cells, since this model exhibit similar repair deficiencies of 8-oxoG as human testicular cells.

In this study we found that BaP induced statistically increased levels of oxidative DNA damage in the testis of *Ogg1*$^{-/-}$ mice at day 17 after BaP-exposure. DNA damage was also induced in somatic tissues like the liver (not significant) and lung. Such induction did not occur in *Ogg1*$^{+/+}$ mice. The gene expression data supported the observed increased levels of oxidised base damage in the testis. Results from the *in vivo* repair experiment showed that repair of Fpg-sensitive sites was indeed not detectable in the testis, liver or lung of *Ogg1*$^{-/-}$

mice following exposure to X-rays, indicating to significant back-up repair by alternative repair pathways in these tissues. As expected, *Ogg1*$^{+/+}$ mice did repair Fpg-sensitive sites.

## 4.1 Nuclei are useful for *in vivo* genotixicity studies

In our experiments, animals in the BaP-study were exposed to a much higher dose (150 mg/kg), compared to what is expected in the general environment, where the upper limit for products such as smoked meat are 5 µg/kg wet weight (European Community, Commission Regulation (EC) No 208/2005 of 4 February 2005). Higher exposures to humans may be expected in cases where specific populations are chronically exposed to high levels from food, cigarette smoke, occupational exposures or for individuals who live in the vicinity of contaminated sites. It is common practice in animal experiments to use high exposures, to ensure that effects can be measured and to reduce the number of animals used. The dose used was below the $LD_{50}$ dose for mice, which is 232 mg/kg (Salamone 1981).

The rapid mechanical processing of tissues to obtain nuclei, combined with freezing, represents a great advantage when conducting large-scale animal studies, collaboration with partners elsewhere, or when samples are to be shipped between laboratories. The nuclei were isolated rapidly - compared to conventional enzymatic isolation procedures to obtain primary cell suspensions. Using the described protocols, nuclei can be isolated from multiple organs and animals simultaneously or within a short time frame. Isolating primary cell suspensions from multiple organs and animals simultaneously is in practice not possible using conventional methods, because they require more handling and are far more time consuming. Time and temperature are important issues when measuring DNA lesions *in vivo*, since many DNA lesions are rapidly repaired at ambient temperatures. The repair of SSBs induced by ionizing radiation has a $T_{1/2}$ of only minutes in most cell types including male germ cells (Olsen *et al.* 2001). Isolating primary cells by enzymatic digestion of tissue makes use of temperatures of 30-37ºC, whereas in the procedure used in this work, all steps are performed within few minutes and at 0ºC. Furthermore, suitable freezing conditions were established (Figure 3-2 - Figure 3-6), which reduces the work load in larger animal studies, and makes inter-laboratory collaboration possible. Comparisons have been performed on conventional isolation method using enzymatic digestion with a mechanical homogenisation technique for isolation of nuclei used in the comet assay (Hu *et al.* 2002). They concluded that the conventional method induced less oxidative DNA damage than the mechanical method. Our mechanical isolation method is not performed in the same way as their homogenisation

method, and we do not observe significantly elevated levels of DNA damage using our method. Hu and co-workers (2002) also compared freezing of cells at – 85ºC in 10% DMSO or with 10% glycerol, and they found that both DMSO and glycerol protected the cells, but there was more DNA damage after freezing in glycerol. We tested 50% glycerol to freeze our nuclei, but this induced significantly higher levels of DNA damage compared to DMSO and FCS (Figure 3-2). Previously our laboratory have used the same mechanical method in alkaline elution studies of DNA damage from *in vivo* treatment of male Wistar rats, as was used in the present work. It was shown that nuclei could be isolated from multiple organs, without introducing extra DNA damage (Brunborg *et al.* 1988; Brunborg *et al.* 1996).

### 4.1.1 A comet assay adapted to *in vivo* studies

The comet assay is a very useful and relatively easy technique for measuring DNA damage in form of strand breaks in single cells. Under alkaline conditions, strand breaks and alkali-labile sites including AP sites are detected. The method is widely used, and it is a central method in our laboratory. It is repeatedly "under the microscope" at the biennial Comet Assay Workshop. A review was recently published by our laboratory and collaborators, discussing several topical issues of the assay (Collins *et al.* 2008). The assay is versatile since mammalian cells of different origins and various DNA lesions can be studied. In the present work, we used a revised protocol involving GelBond® films in stead of glass slides, which significantly adds to the speed and versatility of the assay (Brunborg *et al*., in preparation). When DNA repair enzymes such as the *E. coli* Fpg is introduced, oxidative DNA damage such as 8-oxoG and FaPyG can be studied specifically (David-Cordonnier *et al.* 2001; Olsen *et al.* 2003). The principle behind the use of repair enzymes is that they mediate cleavage of the DNA strand at specific DNA lesions, and thereby allowing the detection of specific DNA lesions as strand breaks, greatly enhancing the sensitivity and specificity of the comet assay. Other DNA repair enzymes that has been used to detect specific DNA lesions includes; T4 endonuclease V (UV-induced pyrimidine dimers; (Collins *et al.* 1997; Jansen *et al.* 2001)), hOGG1 (human homolouge to Fpg, 8-oxoG; (Smith *et al.* 2006)), Endonuclease III (Nth, oxidised pyrimidines; (Collins *et al.* 1993; David-Cordonnier *et al.* 2001; Olsen *et al.* 2003)), 3-metyladenine DNA-glycosylase II (AlkA, 3-methyladenine; (Collins *et al.* 2001)) and Uracil-DNA glykosylase (uracil; (Duthie and McMillan 1997)).

In the present work, we used a commercial scoring system specially developed for the comet assay, "Comet IV" from Perceptive Instruments. Considerable manual interaction was needed

in the scoring process, i.e. the system was not entirely able to define the centre of the cell in each case. Scoring of comets can be performed using several other approaches; 1) classifying the comets visually, in 5 categories, in which category 0 represents undamaged cells and categories 1-4 represent increasing relative tail intensities; 2) automated systems that measure comets with minimal intervention; or 3) by semi automated image analysis using a camera combined with dedicated software. In this study approach 3) was selected, and SYBR® Gold was used as DNA dye. SYBR® Gold is used due to its higher intensity and slower quenching compared to Ethidium Bromide (EtBr). Another benefit with this dye is that it exhibits low intrinsic fluorescence. For our purposes it has one limitation; unlike EtBr it does not seem to differentiate between germ cell types according to their amount of DNA in the cells (Brunborg, personal communication). When scoring cells, the process should preferably be performed with as little intervention as possible, on coded samples, to minimise human bias. In cases when DNA-staining is weaker, the scoring system tends to define the middle of the head erroneously, and intervention is necessary. In the EC FP6 specific-targeted project COMICS (LSHB-CT-2006-037575) establishing an optimal staining method is one important aim; the idea is a simultaneous determination of relative tail intensity in all cells of one sample, based on differential staining of single stranded vs. double stranded DNA (Collins *et al.* 2008). Such a system would be fast and would also reduce human intervention and bias.

There are alternative methods for studying oxidative DNA damage and repair in cellular systems. These include systems such as alkaline elution, but also analytical and immunological methods, in which DNA has to be isolated prior to DNA damage measurement conducted by high performance liquid chromatography electrochemical detection (HPLC-EC), gas chromatography with mass spectrometric detection (GC-MS) or by using specific antibodies. There are differences in sensitivity between methods. European Standards Committee on Oxidative DNA Damage (ESCODD) (Gedik and Collins 2005) compared the sensitivity of HPLC-EC and the comet assay in detection of the background level of 8-oxoG in human lymphocytes. They observed that HPLC-EC is ~12-fold less sensitive than the comet assay in detecting 8-oxoG, but it could be an underestimation of the true background level of 8-oxoG in the comet assay due to the wider specificity of Fpg, i.e. it detects other lesions than 8-oxoG. In the HPLC-EC method, oxidative DNA damage may be induced during the isolation of DNA. The comet assay is independent of isolating DNA and hence circumvent this challenge (Gedik and Collins 2005). An alternative method with similar sensitivity and specificity to the comet assay is alkaline elution (Brunborg *et al.* 1988).

Compared to alkaline elution the comet assay has one advantage in that it allows us to distinguish between different stages (1C, 2C and 4C) of the spermatogenesis when cells or nuclei are stained with EtBr. One difference between the comet assay and alkaline elution is that in the former some cells may not be possible to score, since their DNA is partly degraded, whereas in the latter method the DNA of all cells or nuclei applied to the apparatus decides the result.

The comet assay returns a very high amount of data, because for each technical replicate 50 comets are scored, and we have 8 technical replicates for each mouse. All these data are usually not normally distributed, and the variances are often not equal. There is no general agreement on what statistical method should be used in the analysis of comet assay data; so far no method is taken as optimal, according to a recent review by Lovell and Omori (2008). Furthermore, complicated experiments often require a nested design to uncover possible variations between animals and replicates in the design. Comet data violate two of the assumptions of the parametric method ANOVA, i.e. normality and equal variances. The non-parametric alternative, on the other hand, is less sensitive and does not handle nested designs as well as the ANOVA. The ANOVA can tolerate minor violations of the homogeneity of variances and normality, as long as the data is independent. Using those arguments we chose to perform the ANOVA with a *post hoc* test that did not require equal variances (the Tamhane test), but other methods could also have been used.

## 4.2 BaP induces oxidative DNA damage *in vivo*

As shown in Figure 3-7 and Figure 3-8, oxidative DNA damage was induced in the testis as well as in the lung as a consequence of BaP-exposure in *Ogg1*$^{-/-}$ mice. The increase, measured at day 17 after BaP-exposure, was statistically different from vehicle controls. However, the increase in the liver did not reach significant levels at day 17 after BaP-exposure. To our knowledge this is the first time oxidative damage induced by BaP has been detected in the testis and lung *in vivo*. Most previous studies of induced 8-oxoG damage following BaP exposure were performed with cultivated cells *in vitro* (Briede *et al.* 2004; Elbekai *et al.* 2004; Park *et al.* 2005; Cunniffe *et al.* 2007; Quinn and Penning 2008; Park *et al.* 2008a; Park *et al.* 2008b). But there are not yet many studies that have shown 8-oxoG levels *in vivo*. One *in vivo* study reported elevated 8-oxoG levels in the liver and kidney from female Sprague-Dawley rats after BaP-exposure (75 mg/rat); however, the authors did not observe this increase in the lung. In the liver the 8-oxoG levels were significantly increased after 12 hours, but returned to

control levels after 24 hours, where it remained stable throughout the remaining time (96 hours in total). In the kidney, however, elevated 8-oxoG levels persisted throughout the study (Kim and Lee 1997). In another study, male rats were exposed to 10 mg BAP/kg and sacrificed at 1, 2, 4, 11 and 21 days after exposure. It was not shown an increase in 8-oxoG after exposure, but rather a transient decrease in the liver and lung at day 5 and 11, and this seemed to return towards base levels at day 21 (Briede *et al.* 2004). This is similar to what we have observed (Figure 3-7 - Figure 3-10). Risom and co-workers (2007a) observed elevated levels of 8-oxoG in the lung of *Ogg1*$^{-/-}$ mice after repeated exposures of diesel exhaust particles (20 mg/m$^3$) by 4 x 1.5 hour inhalation, compared to unexposed mice and to *Ogg1*$^{+/+}$ mice. In another study the same authors exposed *Ogg1*$^{-/-}$ and *Ogg1*$^{+/+}$ mice to diesel exhaust particles through the diet (0.8 and 8 mg/kg) for 21 days. They did not observe any elevated levels of 8-oxoG in the organs examined (Risom *et al.* 2007b).

In order to pursue the hypothesis that AKR mediated quinone metabolism results in ROS mediated oxidative damage, we measured expression of selected genes involved in BaP-metabolism, including AKR. Distinct differences in gene expression levels were observed, for both genes, tissues and genotypes. *Akr1a4*, involved in the diol-quinone pathway generating ROS during metabolism of BaP, was expressed in both the testis and the liver of *Ogg1*$^{-/-}$ mice, with highest amounts at day 5 after BaP-exposure (Figure 3-14). The response of the Cyp-genes, which metabolise BaP to BPDE, varied in the testis. *Cyp1a1* increased, *Cyp1a2* increased marginally in *Ogg1*$^{-/-}$ mice as opposed to a decrease in *Ogg1*$^{+/+}$ mice, and *Cyp1b1* did not change due to the treatment. In the testis the expression was generally lower than in the liver. In the liver, *Cyp1a1*, *-1a2* and *-1b1* all reached maximum amounts at an earlier time point (day 1 after BaP-exposure) than *Akr1a4* (Figure 3-14 - Figure 3-17 and Table 4-1). The later induction of *Akr1a4* compared to the Cyp-enzymes could explain why oxidative DNA damage did not become apparent until day 17 after exposure (Figure 3-7 and Figure 3-8). *Akr1a4* is constitutively expressed at high levels in the testis and the liver of *Ogg1*$^{-/-}$ and *Ogg1*$^{+/+}$ mice (Table 3-3). This is consistent with observations made in experiments implying cloning of *Akr1a4*, in which the authors observed that the gene was expressed in high amounts in all tissues examined (Allan and Lohnes 2000). It is also in agreement with those made on the human homologue AKR1A1, where it was observed that the gene was present in all tissues examined including the testis (Barski *et al.* 1999). The high constitutive level of *Akr1a4* in the testis and the further induction of the gene after BaP-exposure, may suggest that metabolism of agents such as BaP via *Akr1a4* is relevant in the testis.

The expression of *Cyp1a1* was greatly induced (4000 fold) in the liver after BaP-exposure (Table 4-1), whereas the constitutive level was low in both organs and both mouse genotypes (Table 3-3). This is in correspondence with the previous observation that *Cyp1a1* has a low constitutive expression, but is highly induced in the testis and the even higher in the liver following BaP-exposure (100mg/kg) of C57BL/6J mice and sacrificing after 72 hours (Shimada *et al.* 2003). In some ways *Cyp1a1* can be regarded as a positive control in our experiments.

**Table 4-1 Summary of the gene expression in liver and testis from *Ogg1*$^{-/-}$ and *Ogg1*$^{+/+}$ mice. The arrows shows if the gene was up- or downregulated in that tissue, and the parentheses give "days after BaP exposure" where the change was highest.**

| Organ | Genotype | *Akr1a4* | *Cyp1a1* | *Cyp1a2* | *Cyp1b1* |
|---|---|---|---|---|---|
| **Testis** | ***Ogg1*$^{-/-}$** | ↑ (5) | ↑ (1) | ↑ (5) | - |
| | ***Ogg1*$^{+/+}$** | ↑ (1/5) | ↑ (1) | ↓ (17) | - |
| **Liver** | ***Ogg1*$^{-/-}$** | ↑ (5) | ↑ (1) | ↑ (1) | ↑ (1) |
| | ***Ogg1*$^{+/+}$** | ↑ (3) | ↑ (1) | ↑ (1) | ↑ (1) |

*Cyp1a2* is reported not to be expressed in any extrahepatic tissues (Landi *et al.* 1999; Choudhary *et al.* 2003; Choudhary *et al.* 2005), but we observed some response in the testis. *Cyp1a2* was upregulated in *Ogg1*$^{-/-}$ mice and downregulated in *Ogg1*$^{+/+}$ mice. We also observed low constitutive levels in the testis of both *Ogg1*$^{-/-}$ and *Ogg1*$^{+/+}$ mice (Table 3-3), compared to a higher level in the liver. These discrepancies could indicate less sensitivity of the analysis method in a previous study. Real-time PCR can be 10 times more sensitive than end-point PCR which was used in that study (Choudhary *et al.* 2003). Furthermore, observations done at mRNA level does not necessary reflect the protein expression of the gene. We have earlier observed that Cyp1a2 proteins is not expressed in the testis of either *Ogg1*$^{-/-}$ or *Ogg1*$^{+/+}$ mice (unpublished).

*Cyp1b1,* on the other hand, was expressed constitutively, but was not induced in the testis in both genotypes. The gene was however induced in the liver of both *Ogg1*$^{-/-}$ and *Ogg1*$^{+/+}$ mice. The constitutive level of this gene is somewhat higher in the testis than in the liver (Table 3-3). Our results are in agreement with a previous study showing that *Cyp1b1* was expressed

at similar levels in the testis before and after BaP-exposure, as opposed to the liver in which an induction was observed (Shimada *et al.* 2003). Altogether, the expression data corroborate the DNA damage induction data since both *Akr* and oxidative damage are being induced in the testis, and also in the lung.

We have shown in the present work that BaP leads to oxidative DNA damage *in vivo*, and our hypothesis is that Akr1a4 is involved in this process. Our results is in agreement with previous work (presented in chapter 1.3.2.1) which has shown that AKRs can mediate ROS and oxidative DNA damage in cells exposed to BaP *in vitro* (Quinn and Penning 2008; Park *et al.* 2008b). Furthermore, PAH *o*-quinones also have the ability to induce the CYP enzymes through the AhR mediated mechanism (Burczynski and Penning 2000; Jiang *et al.* 2005). However, AKRs can effectively compete with CYPs for metabolising BaP, and the dominant pathway depends on the redox state of the cell (Jiang *et al.* 2005; Quinn and Penning 2008).

In $Ogg1^{+/+}$ mice, oxidative DNA damage is repaired continuously as it arises, and thus we did not observe any significant oxidative DNA damage after BaP-exposure (Figure 3-9 and Figure 3-10), as expected. There is some difference in gene expression between $Ogg1^{-/-}$ and $Ogg1^{+/+}$ mice, mainly in the testis (Table 4-1 and Figure 3-14 - Figure 3-17).

Male germ cells seem less sensitive for acquiring oxidative DNA damage than tissues such as lung and liver, since we find that $Ogg1^{-/-}$ mice accumulate more Fpg-sensitive lesions in the liver and lung, compared to the testis (Figure 3-7 and Figure 3-8), and compared to $Ogg1^{+/+}$ mice (Figure 3-8 and Figure 3-10). This shows the relevance of $Ogg1^{-/-}$ for repairing 8-oxoG in the genome. This has previously been reported by others (Klungland *et al.* 1999; 2007a; 2007b).

The transient reduction of oxidative DNA damage in the testis, liver and lung of mice deficient in Ogg1 is a phenomenon that has also has been observed by others (Klungland *et al.* 1999; Briede *et al.* 2004). $Ogg1^{-/-}$ mice have a very low capacity to repair oxidative damage. There are probably backup repair mechanisms, possibly through NEIL1 (Rolseth 2007). This transient reduction may be due to NER in liver and lung, since there are indications that NER can repair oxidative DNA damage as well as adducts (Lin and Sancar 1989; Czeczot *et al.* 1991; Reardon *et al.* 1997; Le Page *et al.* 2000; Osterod *et al.* 2002; Sunesen *et al.* 2002). Alternatively, as BPDE adducts accumulate, they occupy guanines and may disrupt the steady state levels of 8-oxoG. Also, as DNA lesions are accumulating, especially in repair deficient

mice, backup repair via other repair enzymes such as DNA glycosylases is likely to be inhibited by proximate lesions.

### 4.2.1 Oxidative damage induced by X-rays is repaired in the testis of wild-type (*Ogg1*$^{+/+}$) but not *Ogg1*$^{-/-}$ mice

*In vivo* repair of oxidative DNA damage such as 8-oxoG was not detectable in the testis of *Ogg1*$^{-/-}$ mice. In the *Ogg1*$^{+/+}$ mice, however, the repair was significant but not complete within 6 hours (Figure 4-1). This could have several explanations: The time frame may not be sufficient for complete repair of X-ray induced clustered DNA damage; such damage is inherently difficult to repair (Weinfeld *et al.* 2001; Lomax *et al.* 2002; Pearson *et al.* 2004; Cunniffe *et al.* 2007; Hada and Georgakilas 2008). Further, in nuclei preparations there will always be some elongated spermatids that lack the ability to repair; these cells are normally not scored in the comet assay but may affect the results but to what degree cannot be decided at present. Treating the mice with an alternative agent not inducing clustered DNA damage, such as potassium bromate (Arai *et al.* 2006), may shed light on this hypothesis. Instead of a decrease, we observed a significant increase of Fpg sensitive sites in the lung of *Ogg1*$^{-/-}$ mice (Figure 3-18 C)). It is likely that 10 Gy of X-rays could result in an inflammatory response known to give rise to ROS. It has indeed been shown that 5 Gy can rupture lysosomes in T-cells 4 hours after exposure, with ROS formation and damage to the immune system as a consequence (Ogawa *et al.* 2004). A low dose of gamma irradiation (0.04 Gy) *in vivo* can also give rise to an inflammatory response in lymphocytes 4 hours after irradiation (Ibuki and Goto 1999).

In the comet assay the use of Fpg does not visualise the actual level of DNA damage immediately after X-rays exposure (Olsen *et al.* 2003). The Fpg extract detects lower levels of 8-oxoG than is actually induced, which is probably caused by X-rays inducing clustered DNA damage as described in chapter 1.4.3. Previous studies have shown that Fpg is inhibited by the presence of a strand break close to an 8-oxoG lesion (David-Cordonnier *et al.* 2001; Pearson *et al.* 2004). This phenomenon has also been discussed in a recent review on the comet assay (Collins *et al.* 2008).

In a previous study a backup repair activity of Fpg sensitive lesions was observed using an *Ogg1* null mouse embryo fibroblast (MEF) cell line, which the authors associate with NER (Klungland *et al.* 1999). An Ogg1 independent global genomic repair pathway for removing

8-oxoG has also been identified (Le Page *et al.* 2000; Osterod *et al.* 2002; Sunesen *et al.* 2002). In our assay such a backup repair activity was observed neither tissue *in vivo*. NER is already low or non-functional in testicular cells (Jansen *et al.* 2001). This could explain the results for the testis, but not for the lung and the liver in which NER is efficient. The results did not reveal any significant backup of repair of Fpg-sensitive sites in the testis, liver and lung of *Ogg1*$^{-/-}$ mice (Figure 3-18).

In the liver, the repair data were less consistent (Figure 4-1).

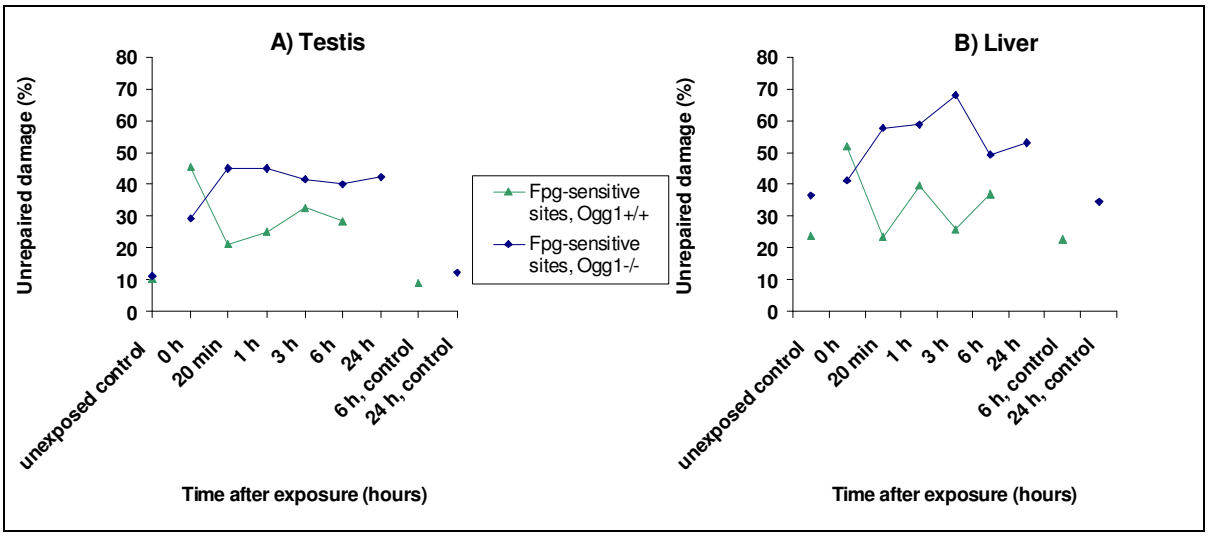


**Figure 4-1 Fpg-sensitive sites in testis (A) and liver (B) from *Ogg1*$^{-/-}$ and *Ogg1*$^{+/+}$ mice exposed to X-ray (10 Gy). Relative levels of unrepaired DNA damage (%) are plotted against time following exposure (hours). The 6 hour and 24 hour controls are sham exposed controls.**

## 4.3 Ogg1 deficient mice constitute a useful model for humans when studying reproductive genotoxicity

As discussed above *Ogg1*$^{-/-}$ mice exhibit defective repair of oxidative DNA damage, such as 8-oxoG and FaPyG sites, similar to what we have previously observed in human male germ cells (Olsen *et al.* 2003). This was the background for the suggestion of *Ogg1*$^{-/-}$ mice as a model for studying genotoxic effects relevant to human testicular cells (Olsen *et al.* 2005; Brunborg *et al.* 2007). One of the aims of this project was to further elucidate whether this model is appropriate for the study of genotoxic effects of chemicals and agents on human male germ cells. For this purpose we studied *in vivo* repair of oxidative damage induced by X-rays, as well as induction of oxidative DNA damage, and gene expression of selected genes,

after BaP-exposure of *Ogg1*$^{-/-}$ and *Ogg1*$^{+/+}$ mice. First of all, we found that the *Ogg1*$^{-/-}$ mice spontaneously accumulate higher levels of oxidative DNA damage than the *Ogg1*$^{+/+}$ mice. This was particularly evident in the liver and lung (Figure 3-8 and Figure 3-10). The testis, on the other hand, accumulates significantly lower numbers of oxidative DNA damage spontaneously; this finding was however different from our previous observations in isolated primary testicular cells from *Ogg1*$^{-/-}$ that do accumulate increased levels of oxidative lesions (Brunborg *et al.* 2007). This discrepancy may be caused by introduction of oxidative lesions during isolation of primary cells. Secondly, repair of Fpg-sensitive sites *in vivo* is non-existent in *Ogg1*$^{-/-}$ mice using our methods, but efficient in *Ogg1*$^{+/+}$ mice (Figure 3-18 and Figure 3-19). This is consistent with the deficient repair of oxidised purines previously observed in human testicular cells (Olsen *et al.* 2003). Furthermore, *Akr1a4* are induced as a response to BaP in the testis, supporting the finding that BaP leads to the induction of oxidative DNA damage in the testis. Gene expression studies of selected genes for proteins involved in BaP-metabolism indicate that there are differences between *Ogg1*$^{-/-}$ and *Ogg1*$^{+/+}$ mice in *Akr1a4* and *Cyp1a2* expression, but not in *Cyp1a1* and *Cyp1b1* expression (Figure 3-14 to Figure 3-17). These differences are probably not significant when testing for genotoxicity, since the homeostasis of DNA lesion induction and removal is already disturbed, small changes in the expression is expected and is probably acceptable for extrapolations from rodents to humans. Some species differences between rodents and higher mammals in metabolising BaP may exist and should be taken into consideration. Microsomes from liver and testis of rodents and higher mammals were incubated with BaP, giving a significantly higher *in vitro* metabolism of BaP in the monkey compared to the mouse (Smith *et al.* 2007). Furthermore, the rodents had significantly lower concentrations of the metabolites than higher mammals, but significantly higher relative amounts of BaP 4,5-diol and 7,8-diol (the substrates for Akrs) to the other metabolites. This is another argument for a thorough evaluation of *Ogg1*$^{-/-}$ mice as model for human reproductive genotoxicity.

## 4.4 Conclusions

The established method for isolating and preserving nuclei for immediate or later use in the comet assay proved to be successful. Acceptable low levels of DNA damage were introduced during the isolation and freezing procedures. The method proved convenient in both large-scale animal studies and inter-laboratory collaborations that require shipping. The method is already being used by others in our laboratory.

Our results indicate that BaP leads to oxidative DNA damage in the testis and lung *in vivo*, and this could explain some of the oxidative DNA damage detected in sperm of smoking men, associated with reproductive challenges. Both *Akr1a4* and *Cyp1a1* are induced in the testis, suggesting that both BPDE and *o*-quinones are being metabolised in this organ after BaP-exposure. The impaired capacity to repair oxidised bases in the testes of *Ogg1*$^{-/-}$ mice, and the absence of significant backup activity, suggest that oxidative lesions persist to the mature sperm. This is also likely to occur in human testicular cells due to their repair deficiency for oxidative DNA lesions, and suggests that life style factors such as smoking may lead to oxidative DNA lesions in male sperm, known to be associated with reproductive difficulties.

The absence of *in vivo* repair of Fpg-sensitive sites in the testis, liver or lung of *Ogg1*$^{-/-}$ mice, as opposed to *Ogg1*$^{+/+}$ mice, following exposure to X-rays indicate no significant back-up repair by alternative repair pathways in the *Ogg1*$^{-/-}$ mice.

From the results presented in this work together with our previous findings (Olsen *et al.* 2003), the *Ogg1*$^{-/-}$ mouse model seems like a good alternative for studying genotoxic effects from environmental agents on testicular cells.

## 4.5 Future work

An immediate follow-up of this study is to confirm the presence (and persistence) of oxidative DNA damage levels by alternative and analytical methods using extracted DNA. Some of the data in the present work are scarce and could not be confirmed within the scope of a master thesis. A functional assay for total AKR-activity in the testis would extend the understanding of the importance of AKRs following BaP exposure. Furthermore, the *Ogg1*$^{-/-}$ mouse as a model for human testicular cells with respect to genotoxicity needs further validation.

# 5 Reference List


Aburatani, H., Hippo, Y., Ishida, T., Takashima, R., Matsuba, C., Kodama, T., Takao, M., Yasui, A., Yamamoto, K., and Asano, M. (1997). Cloning and characterization of mammalian 8-hydroxyguanine-specific DNA glycosylase/apurinic, apyrimidinic lyase, a functional mutM homologue. *Cancer Res.* **57,** 2151-6.

Adami, H. O., Bergstrom, R., Mohner, M., Zatonski, W., Storm, H., Ekbom, A., Tretli, S., Teppo, L., Ziegler, H., Rahu, M., and . (1994). Testicular cancer in nine northern European countries. *Int. J. Cancer* **59,** 33-8.

Adler, I. D. (1996). Comparison of the duration of spermatogenesis between male rodents and humans. *Mutat. Res.* **352,** 169-72.

Ahmadi, A., and Ng, S. C. (1999). Fertilizing ability of DNA-damaged spermatozoa. *J Exp Zool.* **284,** 696-704.

Aitken, R. J., and De Iuliis, G. N. (2007). Origins and consequences of DNA damage in male germ cells. *Reprod. Biomed. Online.* **14,** 727-33.

Aitken, R. J., Koopman, P., and Lewis, S. E. (2004). Seeds of concern. *Nature* **432,** 48-52.

Aitken, R. J., and Krausz, C. (2001). Oxidative stress, DNA damage and the Y chromosome. *Reproduction.* **122,** 497-506.

Allan, D., and Lohnes, D. (2000). Cloning and developmental expression of mouse aldehyde reductase (AKR1A4). *Mech. Dev.* **94,** 271-5.

Anway, M. D., Cupp, A. S., Uzumcu, M., and Skinner, M. K. (2005). Epigenetic transgenerational actions of endocrine disruptors and male fertility. *Science* **308,** 1466-9.

Arai, K., Morishita, K., Shinmura, K., Kohno, T., Kim, S. R., Nohmi, T., Taniwaki, M., Ohwada, S., and Yokota, J. (1997). Cloning of a human homolog of the yeast OGG1 gene that is involved in the repair of oxidative DNA damage. *Oncogene* **14,** 2857-61.

Arai, T., Kelly, V. P., Minowa, O., Noda, T., and Nishimura, S. (2006). The study using wild-type and Ogg1 knockout mice exposed to potassium bromate shows no tumor induction despite an extensive accumulation of 8-hydroxyguanine in kidney DNA. *Toxicology* **221,** 179-86.

Archibong, A. E., Ramesh, A., Niaz, M. S., Brooks, C. M., Roberson, S. I., and Lunstra, D. D. (2008). Effects of benzo(a)pyrene on intra-testicular function in F-344 rats. *Int. J. Environ. Res. Public Health* **5,** 32-40.

Aspinwall, R., Rothwell, D. G., Roldan-Arjona, T., Anselmino, C., Ward, C. J., Cheadle, J. P., Sampson, J. R., Lindahl, T., Harris, P. C., and Hickson, I. D. (1997). Cloning and characterization of a functional human homolog of Escherichia coli endonuclease III. *Proc. Natl. Acad. Sci. U. S. A* **94,** 109-14.

ATSDR (1995) 'Toxicological profile for polycyclic aromatic hydrocarbons (PAHs) (Update).' (U.S. Department of Health and Human Services, Atlanta, Georgia, U.S.)

Baarends, W. M., van der, L. R., and Grootegoed, J. A. (2001). DNA repair mechanisms and gametogenesis. *Reproduction.* **121,** 31-9.

Baird, W. M., Hooven, L. A., and Mahadevan, B. (2005). Carcinogenic polycyclic aromatic hydrocarbon-DNA adducts and mechanism of action. *Environ. Mol. Mutagen.* **45,** 106-14.

Balu, N., Padgett, W. T., Lambert, G. R., Swank, A. E., Richard, A. M., and Nesnow, S. (2004). Identification and characterization of novel stable deoxyguanosine and deoxyadenosine adducts of benzo[a]pyrene-7,8-quinone from reactions at physiological pH. *Chem. Res. Toxicol.* **17,** 827-38.

Balu, N., Padgett, W. T., Nelson, G. B., Lambert, G. R., Ross, J. A., and Nesnow, S. (2006). Benzo[a]pyrene-7,8-quinone-3'-mononucleotide adduct standards for 32P postlabeling analyses: detection of benzo[a]pyrene-7,8-quinone-calf thymus DNA adducts. *Anal. Biochem.* **355,** 213-23.

Bandaru, V., Blaisdell, J. O., and Wallace, S. S. (2006). Oxidative DNA glycosylases: recipes from cloning to characterization. *Methods Enzymol.* **408,** 15-33.

Bandaru, V., Sunkara, S., Wallace, S. S., and Bond, J. P. (2002). A novel human DNA glycosylase that removes oxidative DNA damage and is homologous to Escherichia coli endonuclease VIII. *DNA Repair (Amst)* **1,** 517-29.

Barnes, D. E., and Lindahl, T. (2004). Repair and genetic consequences of endogenous DNA base damage in mammalian cells. *Annu. Rev. Genet.* **38,** 445-76.

Barski, O. A., Gabbay, K. H., and Bohren, K. M. (1999). Characterization of the human aldehyde reductase gene and promoter. *Genomics* **60,** 188-98.

Bart, J., Groen, H. J., van der Graaf, W. T., Hollema, H., Hendrikse, N. H., Vaalburg, W., Sleijfer, D. T., and de Vries, E. G. (2002). An oncological view on the blood-testis barrier. *Lancet Oncol.* **3,** 357-63.

Barton, T. S., Robaire, B., and Hales, B. F. (2005). Epigenetic programming in the preimplantation rat embryo is disrupted by chronic paternal cyclophosphamide exposure. *Proc. Natl. Acad. Sci. U. S. A* **102,** 7865-70.

Bjelland, S., and Seeberg, E. (2003). Mutagenicity, toxicity and repair of DNA base damage induced by oxidation. *Mutat. Res.* **531,** 37-80.

Bjoras, M., Luna, L., Johnsen, B., Hoff, E., Haug, T., Rognes, T., and Seeberg, E. (1997). Opposite base-dependent reactions of a human base excision repair enzyme on DNA containing 7,8-dihydro-8-oxoguanine and abasic sites. *EMBO J* **16,** 6314-22.

Blaisdell, J. O., and Wallace, S. S. (2001). Abortive base-excision repair of radiation-induced clustered DNA lesions in Escherichia coli. *Proc. Natl. Acad. Sci. U. S. A* **98,** 7426-30.

Bostrom, C. E., Gerde, P., Hanberg, A., Jernstrom, B., Johansson, C., Kyrklund, T., Rannug, A., Tornqvist, M., Victorin, K., and Westerholm, R. (2002). Cancer risk assessment, indicators, and guidelines for polycyclic aromatic hydrocarbons in the ambient air. *Environ. Health Perspect.* **110 Suppl 3,** 451-88.

Briede, J. J., Godschalk, R. W., Emans, M. T., De Kok, T. M., Van, A. E., Van, M. J., Van Schooten, F. J., and Kleinjans, J. C. (2004). In vitro and in vivo studies on oxygen free radical and DNA adduct formation in rat lung and liver during benzo[a]pyrene metabolism. *Free Radic. Res.* **38,** 995-1002.

Brunborg, G., Duale, N., Haaland, J. T., Bjørge, C., Søderlund, E., Dybing, E., Wiger, R., and Olsen, A. K. (2007). DNA Repair Capacities in Testicular Cells of Rodents and Man. In 'Male-mediated Developmental Toxicity'. (Eds D. Anderson and M. H. Brinkworth) pp. 273-85. (The Royal Society of Chemistry: Cambrigde, UK).

Brunborg, G., Holme, J. A., and Hongslo, J. K. (1995). Inhibitory effects of paracetamol on DNA repair in mammalian cells. *Mutat. Res.* **342,** 157-70.

Brunborg, G., Holme, J. A., Soderlund, E. J., Omichinski, J. G., and Dybing, E. (1988). An automated alkaline elution system: DNA damage induced by 1,2-dibromo-3-chloropropane in vivo and in vitro. *Anal. Biochem.* **174,** 522-36.

Brunborg, G., Soderlund, E. J., Holme, J. A., and Dybing, E. (1996). Organ-specific and transplacental DNA damage and its repair in rats treated with 1,2-dibromo-3-chloropropane. *Chem. Biol. Interact.* **101,** 33-48.

Burczynski, M. E., and Penning, T. M. (2000). Genotoxic polycyclic aromatic hydrocarbon ortho-quinones generated by aldo-keto reductases induce CYP1A1 via nuclear translocation of the aryl hydrocarbon receptor. *Cancer Res.* **60,** 908-15.

Casarett, L. J., Klaassen, C. D., and Doull, J. (2001). 'Casarett and Doull's Toxicology: the basic science of poisons.' (McGraw-Hill: New York).

Cavalieri, E. L., and Rogan, E. G. (1995). Central role of radical cations in metabolic activation of polycyclic aromatic hydrocarbons. *Xenobiotica* **25,** 677-88.

Chandley, A. C. (1991). On the parental origin of de novo mutation in man. *J. Med. Genet.* **28,** 217-23.

Chang, J. S., Selvin, S., Metayer, C., Crouse, V., Golembesky, A., and Buffler, P. A. (2006). Parental smoking and the risk of childhood leukemia. *Am. J. Epidemiol.* **163,** 1091-100.

Cheng, K. C., Cahill, D. S., Kasai, H., Nishimura, S., and Loeb, L. A. (1992). 8-Hydroxyguanine, an abundant form of oxidative DNA damage, causes G----T and A----C substitutions. *J Biol Chem.* **267,** 166-72.

Choudhary, D., Jansson, I., Schenkman, J. B., Sarfarazi, M., and Stoilov, I. (2003). Comparative expression profiling of 40 mouse cytochrome P450 genes in embryonic and adult tissues. *Arch. Biochem. Biophys.* **414,** 91-100.

Choudhary, D., Jansson, I., Stoilov, I., Sarfarazi, M., and Schenkman, J. B. (2005). Expression patterns of mouse and human CYP orthologs (families 1-4) during development and in different adult tissues. *Arch. Biochem. Biophys.* **436,** 50-61.

Clemmesen, J. (1997). Is pregnancy smoking causal to testis cancer in sons? A hypothesis. *Acta Oncol.* **36,** 59-63.

Collins, A. R. (2005). Assays for oxidative stress and antioxidant status: applications to research into the biological effectiveness of polyphenols. *Am. J. Clin. Nutr.* **81,** 261S-7S.

Collins, A. R., Dusinska, M., and Horska, A. (2001). Detection of alkylation damage in human lymphocyte DNA with the comet assay. *Acta Biochim. Pol.* **48,** 611-4.

Collins, A. R., Duthie, S. J., and Dobson, V. L. (1993). Direct enzymic detection of endogenous oxidative base damage in human lymphocyte DNA. *Carcinogenesis* **14,** 1733-5.

Collins, A. R., Mitchell, D. L., Zunino, A., de, W. J., and Busch, D. (1997). UV-sensitive rodent mutant cell lines of complementation groups 6 and 8 differ phenotypically from their human counterparts. *Environ. Mol. Mutagen.* **29,** 152-60.

Collins, A. R., Oscoz, A. A., Brunborg, G., Gaivao, I., Giovannelli, L., Kruszewski, M., Smith, C. C., and Stetina, R. (2008). The comet assay: topical issues. *Mutagenesis* **23,** 143-51.

Crow, J. F., and Denniston, C. (1981). The mutation component of genetic damage. *Science* **212,** 888-93.

Cunniffe, S. M., Lomax, M. E., and O'Neill, P. (2007). An AP site can protect against the mutagenic potential of 8-oxoG when present within a tandem clustered site in E. coli. *DNA Repair (Amst)* **6,** 1839-49.

Czeczot, H., Tudek, B., Lambert, B., Laval, J., and Boiteux, S. (1991). Escherichia coli Fpg protein and UvrABC endonuclease repair DNA damage induced by methylene blue plus visible light in vivo and in vitro. *J. Bacteriol.* **173,** 3419-24.

David-Cordonnier, M. H., Laval, J., and O'Neill, P. (2001). Recognition and kinetics for excision of a base lesion within clustered DNA damage by the Escherichia coli proteins Fpg and Nth. *Biochemistry* **40,** 5738-46.

Dizdaroglu, M., Karahalil, B., Senturker, S., Buckley, T. J., and Roldan-Arjona, T. (1999). Excision of products of oxidative DNA base damage by human NTH1 protein. *Biochemistry* **38,** 243-6.

Dubrova, Y. E., Hickenbotham, P., Glen, C. D., Monger, K., Wong, H. P., and Barber, R. C. (2008). Paternal exposure to ethylnitrosourea results in transgenerational genomic instability in mice. *Environ. Mol. Mutagen.* **49,** 308-11.

Duez, P., Dehon, G., Kumps, A., and Dubois, J. (2003). Statistics of the Comet assay: a key to discriminate between genotoxic effects. *Mutagenesis* **18,** 159-66.

Duthie, S. J., and McMillan, P. (1997). Uracil misincorporation in human DNA detected using single cell gel electrophoresis. *Carcinogenesis* **18,** 1709-14.

Ehmcke, J., Wistuba, J., and Schlatt, S. (2006). Spermatogonial stem cells: questions, models and perspectives. *Hum. Reprod. Update.* **12,** 275-82.

Eide, L., Luna, L., Gustad, E. C., Henderson, P. T., Essigmann, J. M., Demple, B., and Seeberg, E. (2001). Human endonuclease III acts preferentially on DNA damage opposite guanine residues in DNA. *Biochemistry* **40,** 6653-9.

Elbekai, R. H., Korashy, H. M., Wills, K., Gharavi, N., and El-Kadi, A. O. (2004). Benzo[a]pyrene, 3-methylcholanthrene and beta-naphthoflavone induce oxidative stress in hepatoma hepa 1c1c7 Cells by an AHR-dependent pathway. *Free Radic. Res.* **38,** 1191-200.

Falnes, P. O., Johansen, R. F., and Seeberg, E. (2002). AlkB-mediated oxidative demethylation reverses DNA damage in Escherichia coli. *Nature* **419,** 178-82.

Friedberg E.C., Walker, G. C., Siede W., Wood R.D., Schultz R.A., and Ellenberger T. (2006). 'DNA repair and mutagenesis.' (ASM Press: Washington, D.C.).

Gandy, J., Primiano, T., Novak, R. F., Kelce, W. R., and York, J. L. (1996). Differential expression of glutathione S-transferase isoforms in compartments of the testis and segments of the epididymis of the rat. *Drug Metab Dispos.* **24,** 725-33.

Gedik, C. M., and Collins, A. (2005). Establishing the background level of base oxidation in human lymphocyte DNA: results of an interlaboratory validation study. *FASEB J.* **19,** 82-4.

Gelboin, H. V. (1980). Benzo[alpha]pyrene metabolism, activation and carcinogenesis: role and regulation of mixed-function oxidases and related enzymes. *Physiol Rev.* **60,** 1107-66.

Gocke, E., Chetelat, A. A., Csato, M., McGarvey, D. J., Jakob-Roetne, R., Kirchner, S., Muster, W., Potthast, M., and Widmer, U. (2003). Phototoxicity and photogenotoxicity of nine pyridone derivatives. *Mutat. Res.* **535,** 43-54.

Goodhead, D. T. (1994). Initial events in the cellular effects of ionizing radiations: clustered damage in DNA. *Int. J. Radiat. Biol.* **65,** 7-17.

Ha, H. C., Yager, J. D., Woster, P. A., and Casero, R. A., Jr. (1998). Structural specificity of polyamines and polyamine analogues in the protection of DNA from strand breaks induced by reactive oxygen species. *Biochem. Biophys. Res. Commun.* **244,** 298-303.

Hada, M., and Georgakilas, A. G. (2008). Formation of clustered DNA damage after high-LET irradiation: a review. *J. Radiat. Res. (Tokyo)* **49,** 203-10.

Hattemer-Frey, H. A., and Travis, C. C. (1991). Benzo-a-pyrene: environmental partitioning and human exposure. *Toxicol. Ind. Health* **7,** 141-57.

Hazra, T. K., Izumi, T., Boldogh, I., Imhoff, B., Kow, Y. W., Jaruga, P., Dizdaroglu, M., and Mitra, S. (2002a). Identification and characterization of a human DNA glycosylase for repair of modified bases in oxidatively damaged DNA. *Proc. Natl. Acad. Sci. U. S. A* **99,** 3523-8.

Hazra, T. K., Kow, Y. W., Hatahet, Z., Imhoff, B., Boldogh, I., Mokkapati, S. K., Mitra, S., and Izumi, T. (2002b). Identification and characterization of a novel human DNA glycosylase for repair of cytosine-derived lesions. *J. Biol. Chem.* **277,** 30417-20.

Hecht, N. B. (1990). Regulation of 'haploid expressed genes' in male germ cells. *J. Reprod. Fertil.* **88,** 679-93.

Hilbert, T. P., Chaung, W., Boorstein, R. J., Cunningham, R. P., and Teebor, G. W. (1997). Cloning and expression of the cDNA encoding the human homologue of the DNA repair enzyme, Escherichia coli endonuclease III. *J. Biol. Chem.* **272,** 6733-40.

Holstein, A. F., Schulze, W., and Davidoff, M. (2003). Understanding spermatogenesis is a prerequisite for treatment. *Reproductive Biology and Endocrinology* **1,** 107.

Hsu, G. W., Ober, M., Carell, T., and Beese, L. S. (2004). Error-prone replication of oxidatively damaged DNA by a high-fidelity DNA polymerase. *Nature* **431,** 217-21.

Hu, M. L., Chuang, C. H., Sio, H. M., and Yeh, S. L. (2002). Simple cryoprotection and cell dissociation techniques for application of the comet assay to fresh and frozen rat tissues. *Free Radic. Res.* **36,** 203-9.

Ibuki, Y., and Goto, R. (1999). Contribution of inflammatory cytokine release to activation of resident peritoneal macrophages after in vivo low-dose gamma-irradiation. *J. Radiat. Res. (Tokyo)* **40,** 253-62.

Irvine, D. S., Twigg, J. P., Gordon, E. L., Fulton, N., Milne, P. A., and Aitken, R. J. (2000). DNA integrity in human spermatozoa: relationships with semen quality. *J. Androl* **21,** 33-44.

Jacobsen, R., Moller, H., Thoresen, S. O., Pukkala, E., Kjaer, S. K., and Johansen, C. (2006). Trends in testicular cancer incidence in the Nordic countries, focusing on the recent decrease in Denmark. *Int. J. Androl.* **29,** 199-204.

Jansen, J., Olsen, A. K., Wiger, R., Naegeli, H., de, B. P., van Der, H. F., Holme, J. A., Brunborg, G., and Mullenders, L. (2001). Nucleotide excision repair in rat male germ cells: low level of repair in intact cells contrasts with high dual incision activity in vitro. *Nucleic Acids Res.* **29,** 1791-800.

Jez, J. M., Bennett, M. J., Schlegel, B. P., Lewis, M., and Penning, T. M. (1997a). Comparative anatomy of the aldo-keto reductase superfamily. *Biochem. J.* **326 ( Pt 3),** 625-36.

Jez, J. M., Flynn, T. G., and Penning, T. M. (1997b). A new nomenclature for the aldo-keto reductase superfamily. *Biochem. Pharmacol.* **54,** 639-47.

Ji, B. T., Shu, X. O., Linet, M. S., Zheng, W., Wacholder, S., Gao, Y. T., Ying, D. M., and Jin, F. (1997). Paternal cigarette smoking and the risk of childhood cancer among offspring of nonsmoking mothers. *J. Natl. Cancer Inst.* **89,** 238-44.

Jiang, H., Shen, Y. M., Quinn, A. M., and Penning, T. M. (2005). Competing roles of cytochrome P450 1A1/1B1 and aldo-keto reductase 1A1 in the metabolic activation of (+/-)-7,8-dihydroxy-7,8-dihydro-benzo[a]pyrene in human bronchoalveolar cell extracts. *Chem. Res. Toxicol.* **18,** 365-74.

Jorgensen, N., Carlsen, E., Nermoen, I., Punab, M., Suominen, J., Andersen, A. G., Andersson, A. M., Haugen, T. B., Horte, A., Jensen, T. K., Magnus, O., Petersen, J. H., Vierula, M., Toppari, J., and Skakkebaek, N. E. (2002). East-West gradient in semen quality in the Nordic-Baltic area: a study of men from the general population in Denmark, Norway, Estonia and Finland. *Hum. Reprod.* **17,** 2199-208.

Kim, K. B., and Lee, B. M. (1997). Oxidative stress to DNA, protein, and antioxidant enzymes (superoxide dismutase and catalase) in rats treated with benzo(a)pyrene. *Cancer Lett.* **113,** 205-12.

Klotz, T., Vorreuther, R., Heidenreich, A., Zumbe, J., and Engelmann, U. (1996). Testicular tissue oxygen pressure. *J. Urol.* **155,** 1488-91.

Klungland, A., Rosewell, I., Hollenbach, S., Larsen, E., Daly, G., Epe, B., Seeberg, E., Lindahl, T., and Barnes, D. E. (1999). Accumulation of premutagenic DNA lesions in mice defective in removal of oxidative base damage. *Proc Natl Acad Sci U S A* **96,** 13300-5.

Klungland, A., and Bjelland, S. (2007). Oxidative damage to purines in DNA: role of mammalian Ogg1. *DNA Repair (Amst)* **6,** 481-8.

Knuckles, M. E., Inyang, F., and Ramesh, A. (2001). Acute and subchronic oral toxicities of benzo[a]pyrene in F-344 rats. *Toxicol. Sci.* **61,** 382-8.

Kovacic, P., and Wakelin, L. P. (2001). Review: DNA molecular electrostatic potential: novel perspectives for the mechanism of action of anticancer drugs involving electron transfer and oxidative stress. *Anticancer Drug Des* **16,** 175-84.

Krokan, H. E., Nilsen, H., Skorpen, F., Otterlei, M., and Slupphaug, G. (2000). Base excision repair of DNA in mammalian cells. *FEBS Lett.* **476,** 73-7.

Kubista, M., Andrade, J. M., Bengtsson, M., Forootan, A., Jonak, J., Lind, K., Sindelka, R., Sjoback, R., Sjogreen, B., Strombom, L., Stahlberg, A., and Zoric, N. (2006). The real-time polymerase chain reaction. *Mol. Aspects Med.* **27,** 95-125.

Landi, M. T., Sinha, R., Lang, N. P., and Kadlubar, F. F. (1999). Human cytochrome P4501A2. *IARC Sci. Publ.* 173-95.

Larsen, E., Meza, T. J., Kleppa, L., and Klungland, A. (2007). Organ and cell specificity of base excision repair mutants in mice. *Mutat. Res.* **614,** 56-68.

Le Page, F., Klungland, A., Barnes, D. E., Sarasin, A., and Boiteux, S. (2000). Transcription coupled repair of 8-oxoguanine in murine cells: the ogg1 protein is required for repair in nontranscribed sequences but not in transcribed sequences. *Proc. Natl. Acad. Sci. U. S. A* **97,** 8397-402.

Li, G. M. (2008). Mechanisms and functions of DNA mismatch repair. *Cell Res.* **18,** 85-98.

Lin, J. J., and Sancar, A. (1989). A new mechanism for repairing oxidative damage to DNA: (A)BC excinuclease removes AP sites and thymine glycols from DNA. *Biochemistry* **28,** 7979-84.

Lindahl, T. (1974). An N-glycosidase from Escherichia coli that releases free uracil from DNA containing deaminated cytosine residues. *Proc. Natl. Acad. Sci. U. S. A* **71,** 3649-53.

Lindahl, T. (1993). Instability and decay of the primary structure of DNA. *Nature* **362,** 709-15.

Livak, K. J., and Schmittgen, T. D. (2001). Analysis of relative gene expression data using real-time quantitative PCR and the 2(-Delta Delta C(T)) Method. *Methods* **25,** 402-8.

Lomax, M. E., Gulston, M. K., and O'Neill, P. (2002). Chemical aspects of clustered DNA damage induction by ionising radiation. *Radiat. Prot. Dosimetry.* **99,** 63-8.

Lopes, S., Jurisicova, A., Sun, J. G., and Casper, R. F. (1998). Reactive oxygen species: potential cause for DNA fragmentation in human spermatozoa. *Hum. Reprod.* **13,** 896-900.

Lovell, D. P., and Omori, T. (2008). Statistical issues in the use of the comet assay. *Mutagenesis* **23,** 171-82.

Lu, R., Nash, H. M., and Verdine, G. L. (1997). A mammalian DNA repair enzyme that excises oxidatively damaged guanines maps to a locus frequently lost in lung cancer. *Curr. Biol.* **7,** 397-407.

Luna, L., Bjoras, M., Hoff, E., Rognes, T., and Seeberg, E. (2000). Cell-cycle regulation, intracellular sorting and induced overexpression of the human NTH1 DNA glycosylase involved in removal of formamidopyrimidine residues from DNA. *Mutat. Res.* **460,** 95-104.

McCoull, K. D., Rindgen, D., Blair, I. A., and Penning, T. M. (1999). Synthesis and characterization of polycyclic aromatic hydrocarbon o-quinone depurinating N7-guanine adducts. *Chem. Res. Toxicol.* **12,** 237-46.

Michaels, M. L., and Miller, J. H. (1992). The GO system protects organisms from the mutagenic effect of the spontaneous lesion 8-hydroxyguanine (7,8-dihydro-8-oxoguanine). *J. Bacteriol.* **174,** 6321-5.

Ministry of the Environment (2004) 'FOR 2004-06-01 nr 931: Forskrift om begrensning av forurensning (forurensningsforskriften).'

Minowa, O., Arai, T., Hirano, M., Monden, Y., Nakai, S., Fukuda, M., Itoh, M., Takano, H., Hippou, Y., Aburatani, H., Masumura, K., Nohmi, T., Nishimura, S., and Noda, T. (2000). Mmh/Ogg1 gene inactivation results in accumulation of 8-hydroxyguanine in mice. *Proc. Natl. Acad. Sci. U. S. A* **97,** 4156-61.

Moore, D. J., and McCabe, G. P. (2003). 'Introduction to the Practice of Statistics.' (W. H. Freeman and Company: New York).

Morland, I., Rolseth, V., Luna, L., Rognes, T., Bjoras, M., and Seeberg, E. (2002). Human DNA glycosylases of the bacterial Fpg/MutM superfamily: an alternative pathway for the repair of 8-oxoguanine and other oxidation products in DNA. *Nucleic Acids Res.* **30,** 4926-36.

Mruk, D. D., Silvestrini, B., Mo, M. Y., and Cheng, C. Y. (2002). Antioxidant superoxide dismutase - a review: its function, regulation in the testis, and role in male fertility. *Contraception* **65,** 305-11.

Nebert, D. W., Dalton, T. P., Okey, A. B., and Gonzalez, F. J. (2004). Role of aryl hydrocarbon receptor-mediated induction of the CYP1 enzymes in environmental toxicity and cancer. *J. Biol. Chem.* **279,** 23847-50.

Nelson, K., and Holmes, L. B. (1989). Malformations due to presumed spontaneous mutations in newborn infants. *N. Engl. J. Med.* **320,** 19-23.

Ni, Z. Y., Liu, Y. Q., Shen, H. M., Chia, S. E., and Ong, C. N. (1997). Does the increase of 8-hydroxydeoxyguanosine lead to poor sperm quality? *Mutat. Res.* **381,** 77-82.

Nikjoo, H., O'Neill, P., Terrissol, M., and Goodhead, D. T. (1999). Quantitative modelling of DNA damage using Monte Carlo track structure method. *Radiat. Environ. Biophys.* **38,** 31-8.

Nishioka, K., Ohtsubo, T., Oda, H., Fujiwara, T., Kang, D., Sugimachi, K., and Nakabeppu, Y. (1999). Expression and differential intracellular localization of two major forms of human 8-oxoguanine DNA glycosylase encoded by alternatively spliced OGG1 mRNAs. *Mol. Biol. Cell* **10,** 1637-52.

O'Connor, T., Ireland, L. S., Harrison, D. J., and Hayes, J. D. (1999). Major differences exist in the function and tissue-specific expression of human aflatoxin B1 aldehyde reductase and the principal human aldo-keto reductase AKR1 family members. *Biochem. J.* **343 Pt 2,** 487-504.

O'Driscoll, M., and Jeggo, P. A. (2006). The role of double-strand break repair - insights from human genetics. *Nat. Rev. Genet.* **7,** 45-54.

Ogawa, Y., Kobayashi, T., Nishioka, A., Kariya, S., Ohnishi, T., Hamasato, S., Seguchi, H., and Yoshida, S. (2004). Reactive oxygen species-producing site in radiation-induced apoptosis of human peripheral T cells: involvement of lysosomal membrane destabilization. *Int. J. Mol. Med.* **13,** 69-73.

Olive, P. L., Wlodek, D., Durand, R. E., and Banath, J. P. (1992). Factors influencing DNA migration from individual cells subjected to gel electrophoresis. *Exp. Cell Res.* **198,** 259-67.

Olsen, A. K., Bjortuft, H., Wiger, R., Holme, J., Seeberg, E., Bjoras, M., and Brunborg, G. (2001). Highly efficient base excision repair (BER) in human and rat male germ cells. *Nucleic Acids Res.* **29,** 1781-90.

Olsen, A. K., Duale, N., Bjoras, M., Larsen, C. T., Wiger, R., Holme, J. A., Seeberg, E. C., and Brunborg, G. (2003). Limited repair of 8-hydroxy-7,8-dihydroguanine residues in human testicular cells. *Nucleic Acids Res.* **31,** 1351-63.

Olsen, A. K., Lindeman, B., Wiger, R., Duale, N., and Brunborg, G. (2005). How do male germ cells handle DNA damage? *Toxicol. Appl. Pharmacol.* **207,** 521-31.

Osterod, M., Hollenbach, S., Hengstler, J. G., Barnes, D. E., Lindahl, T., and Epe, B. (2001). Age-related and tissue-specific accumulation of oxidative DNA base damage in 7,8-dihydro-8-oxoguanine-DNA glycosylase (Ogg1) deficient mice. *Carcinogenesis* **22,** 1459-63.

Osterod, M., Larsen, E., Le, P. F., Hengstler, J. G., Van Der Horst, G. T., Boiteux, S., Klungland, A., and Epe, B. (2002). A global DNA repair mechanism involving the Cockayne syndrome B (CSB) gene product can prevent the in vivo accumulation of endogenous oxidative DNA base damage. *Oncogene* **21,** 8232-9.

Ostling, O., and Johanson, K. J. (1984). Microelectrophoretic study of radiation-induced DNA damages in individual mammalian cells. *Biochem. Biophys. Res Commun.* **123,** 291-8.

Ovrebo, S., Haugen, A., Fjeldstad, P. E., Hemminki, K., and Szyfter, K. (1994). Biological monitoring of exposure to polycyclic aromatic hydrocarbon in an electrode paste plant. *J. Occup. Med.* **36,** 303-10.

Park, J. H., Gelhaus, S., Vedantam, S., Oliva, A. L., Batra, A., Blair, I. A., Troxel, A. B., Field, J., and Penning, T. M. (2008a). The pattern of p53 mutations caused by PAH o-quinones is driven by 8-oxo-dGuo formation while the spectrum of mutations is determined by biological selection for dominance. *Chem. Res. Toxicol.* **21,** 1039-49.

Park, J. H., Gopishetty, S., Szewczuk, L. M., Troxel, A. B., Harvey, R. G., and Penning, T. M. (2005). Formation of 8-oxo-7,8-dihydro-2'-deoxyguanosine (8-oxo-dGuo) by PAH o-quinones: involvement of reactive oxygen species and copper(II)/copper(I) redox cycling. *Chem. Res. Toxicol.* **18,** 1026-37.

Park, J. H., Mangal, D., Tacka, K. A., Quinn, A. M., Harvey, R. G., Blair, I. A., and Penning, T. M. (2008b). Evidence for the aldo-keto reductase pathway of polycyclic aromatic trans-dihydrodiol activation in human lung A549 cells. *Proc. Natl. Acad. Sci. U. S. A* **105,** 6846-51.

Parsons, J. L., Zharkov, D. O., and Dianov, G. L. (2005). NEIL1 excises 3' end proximal oxidative DNA lesions resistant to cleavage by NTH1 and OGG1. *Nucleic Acids Res.* **33,** 4849-56.

Pearson, C. G., Shikazono, N., Thacker, J., and O'Neill, P. (2004). Enhanced mutagenic potential of 8-oxo-7,8-dihydroguanine when present within a clustered DNA damage site. *Nucleic Acids Res* **32,** 263-70.

Pegg, A. E. (2000). Repair of O(6)-alkylguanine by alkyltransferases. *Mutat. Res.* **462,** 83-100.

Penning, T. M. (2004). Aldo-keto reductases and formation of polycyclic aromatic hydrocarbon o-quinones. *Methods Enzymol.* **378,** 31-67.

Penning, T. M., and Drury, J. E. (2007). Human aldo-keto reductases: Function, gene regulation, and single nucleotide polymorphisms. *Arch. Biochem. Biophys.* **464,** 241-50.

Penning, T. M., Ohnishi, S. T., Ohnishi, T., and Harvey, R. G. (1996). Generation of reactive oxygen species during the enzymatic oxidation of polycyclic aromatic hydrocarbon trans-dihydrodiols catalyzed by dihydrodiol dehydrogenase. *Chem. Res. Toxicol.* **9,** 84-92.

Pettersson, A., Akre, O., Richiardi, L., Ekbom, A., and Kaijser, M. (2007). Maternal smoking and the epidemic of testicular cancer--a nested case-control study. *Int. J. Cancer* **120,** 2044-6.

Pettersson, A., Kaijser, M., Richiardi, L., Askling, J., Ekbom, A., and Akre, O. (2004). Women smoking and testicular cancer: one epidemic causing another? *Int. J. Cancer* **109,** 941-4.

Phillips, D. H. (1999). Polycyclic aromatic hydrocarbons in the diet. *Mutat. Res.* **443,** 139-47.

Prieto Alamo, M. J., Jurado, J., Francastel, E., and Laval, F. (1998). Rat 7,8-dihydro-8-oxoguanine DNA glycosylase: substrate specificity, kinetics and cleavagemechanism at an apurinic site. *Nucleic Acids Res.* **26,** 5199-202.

Quinn, A. M., and Penning, T. M. (2008). Comparisons of (+/-)-benzo[a]pyrene-trans-7,8-dihydrodiol activation by human cytochrome P450 and aldo-keto reductase enzymes: effect of redox state and expression levels. *Chem. Res. Toxicol.* **21,** 1086-94.

Radicella, J. P., Dherin, C., Desmaze, C., Fox, M. S., and Boiteux, S. (1997). Cloning and characterization of hOGG1, a human homolog of the OGG1 gene of Saccharomyces cerevisiae. *Proc. Natl. Acad. Sci. U. S. A* **94,** 8010-5.

Ramesh, A., Inyang, F., Hood, D. B., Archibong, A. E., Knuckles, M. E., and Nyanda, A. M. (2001). Metabolism, bioavailability, and toxicokinetics of benzo(alpha)pyrene in F-344 rats following oral administration. *Exp. Toxicol. Pathol.* **53,** 275-90.

Ramesh, A., Inyang, F., Lunstra, D. D., Niaz, M. S., Kopsombut, P., Jones, K. M., Hood, D. B., Hills, E. R., and Archibong, A. E. (2008). Alteration of fertility endpoints in adult male F-344 rats by subchronic exposure to inhaled benzo(a)pyrene. *Exp. Toxicol. Pathol.*

Reardon, J. T., Bessho, T., Kung, H. C., Bolton, P. H., and Sancar, A. (1997). In vitro repair of oxidative DNA damage by human nucleotide excision repair system: possible explanation for neurodegeneration in xeroderma pigmentosum patients. *Proc. Natl. Acad. Sci. U. S. A* **94,** 9463-8.

Riccardi, V. M., Dobson, C. E., Chakraborty, R., and Bontke, C. (1984). The pathophysiology of neurofibromatosis: IX. Paternal age as a factor in the origin of new mutations. *Am. J. Med. Genet.* **18,** 169-76.

Richiardi, L., Bellocco, R., Adami, H. O., Torrang, A., Barlow, L., Hakulinen, T., Rahu, M., Stengrevics, A., Storm, H., Tretli, S., Kurtinaitis, J., Tyczynski, J. E., and Akre, O. (2004). Testicular cancer incidence in eight northern European countries: secular and recent trends. *Cancer Epidemiol. Biomarkers Prev.* **13,** 2157-66.

Risom, L., Haug, T., Wallin, H., Klungland, A., Dybdahl, M., Møller, P., Vogel, U., and Loft, S. (2007a). Repeated inhalations of diesel exhaust particles and oxidatively damaged DNA in young oxoguanine DNA glycosylase (OGG1) deficient mice. *Free Radic Res* **41,** 172-81.

Risom, L., Vogel, U., Wallin, H., Møller, P., Dybdahl, M., and Loft, S. (2007b). Dietary exposure to diesel exhaust particles and oxidatively damaged DNA in young oxoguanine DNA glycosylase 1 deficient mice. *TOXICOLOGY LETTERS* **175,** 16-23.

Roldan-Arjona, T., Wei, Y. F., Carter, K. C., Klungland, A., Anselmino, C., Wang, R. P., Augustus, M., and Lindahl, T. (1997). Molecular cloning and functional expression of a human cDNA encoding the antimutator enzyme 8-hydroxyguanine-DNA glycosylase. *Proc. Natl. Acad. Sci. U. S. A* **94,** 8016-20.

Rolseth, V. DNA glycosylases initiating repair of oxidative DNA lesions in mammalian cells. 2007. Faculty of Medicine, University of Oslo. Ref Type: Thesis/Dissertation

Rosenquist, T. A., Zharkov, D. O., and Grollman, A. P. (1997). Cloning and characterization of a mammalian 8-oxoguanine DNA glycosylase. *Proc. Natl. Acad. Sci. U. S. A* **94,** 7429-34.

Russell L.D., Ettlin R., Sinha Hikim A.P., and Clegg E.D. (1990). Mammalian Spermatogenesis. In 'Histological and Histopathological Evaluation of the Testis'. pp. 1-37. (Cache River Press: Clearwater, Florida).

Sakkas, D., Urner, F., Bizzaro, D., Manicardi, G., Bianchi, P. G., Shoukir, Y., and Campana, A. (1998). Sperm nuclear DNA damage and altered chromatin structure: effect on fertilization and embryo development. *Hum. Reprod.* **13 Suppl 4,** 11-9.

Sakumi, K., Furuichi, M., Tsuzuki, T., Kakuma, T., Kawabata, S., Maki, H., and Sekiguchi, M. (1993). Cloning and expression of cDNA for a human enzyme that hydrolyzes 8-oxo-dGTP, a mutagenic substrate for DNA synthesis. *J. Biol. Chem.* **268,** 23524-30.

Sakumi, K., Tominaga, Y., Furuichi, M., Xu, P., Tsuzuki, T., Sekiguchi, M., and Nakabeppu, Y. (2003). Ogg1 knockout-associated lung tumorigenesis and its suppression by Mth1 gene disruption. *Cancer Res.* **63,** 902-5.

Salamone, M. F. (1981). Toxicity of 41 carcinogens and noncarcenogenic analogs. In 'Evaluation of short-term tests for carcinogens: report of the international collaborative program'. (Eds F. J. De Serres and J. Ashby) pp. 682-5. (Elsevier/North-Holland: New York).

Sambrook, J., and Russell, D. W. (2001). 'Molecular cloning: a laboratory manual.' (Cold Spring Harbor Laboratory Press: Cold Spring Harbor, NY).

Sarker, A. H., Ikeda, S., Nakano, H., Terato, H., Ide, H., Imai, K., Akiyama, K., Tsutsui, K., Bo, Z., Kubo, K., Yamamoto, K., Yasui, A., Yoshida, M. C., and Seki, S. (1998). Cloning and characterization of a mouse homologue (mNthl1) of Escherichia coli endonuclease III. *J. Mol. Biol.* **282,** 761-74.

Schmidt, J. V., and Bradfield, C. A. (1996). Ah receptor signaling pathways. *Annu. Rev. Cell Dev. Biol.* **12,** 55-89.

Sekiguchi, M. (1996). MutT-related error avoidance mechanism for DNA synthesis. *Genes Cells* **1,** 139-45.

SFT . Miljøstatus i Norge, PAH. Norwegian Pollution Control Authority . 22-5-2008. Norwegian Pollution Control Authority. 28-6-2007. Ref Type: Electronic Citation

Shen, H. M., Chia, S. E., Ni, Z. Y., New, A. L., Lee, B. L., and Ong, C. N. (1997). Detection of oxidative DNA damage in human sperm and the association with cigarette smoking. *Reprod. Toxicol.* **11,** 675-80.

Shen, Y. M., Troxel, A. B., Vedantam, S., Penning, T. M., and Field, J. (2006). Comparison of p53 mutations induced by PAH o-quinones with those caused by anti-benzo[a]pyrene diol epoxide in vitro: role of reactive oxygen and biological selection. *Chem. Res. Toxicol.* **19,** 1441-50.

Shimada, T., Sugie, A., Shindo, M., Nakajima, T., Azuma, E., Hashimoto, M., and Inoue, K. (2003). Tissue-specific induction of cytochromes P450 1A1 and 1B1 by polycyclic aromatic hydrocarbons and polychlorinated biphenyls in engineered C57BL/6J mice of arylhydrocarbon receptor gene. *Toxicol. Appl. Pharmacol.* **187,** 1-10.

Silverthorn, D. U., and Ober, W. C. (2007). 'Human physiology: an integrated approach.' (Pearson Benjamin Cummings: San Francisco).

Singh, N. P., McCoy, M. T., Tice, R. R., and Schneider, E. L. (1988). A simple technique for quantitation of low levels of DNA damage in individual cells. *Exp Cell Res* **175,** 184-91.

Skakkebaek, N. E., Rajpert-De, M. E., and Main, K. M. (2001). Testicular dysgenesis syndrome: an increasingly common developmental disorder with environmental aspects. *Hum. Reprod.* **16,** 972-8.

Slupska, M. M., Baikalov, C., Luther, W. M., Chiang, J. H., Wei, Y. F., and Miller, J. H. (1996). Cloning and sequencing a human homolog (hMYH) of the Escherichia coli mutY gene whose function is required for the repair of oxidative DNA damage. *J. Bacteriol.* **178,** 3885-92.

Smith, C. C., O'Donovan, M. R., and Martin, E. A. (2006). hOGG1 recognizes oxidative damage using the comet assay with greater specificity than FPG or ENDOIII. *Mutagenesis* **21,** 185-90.

Smith, T. L., Merry, S. T., Harris, D. L., Joe, F. J., Ike, J., Archibong, A. E., and Ramesh, A. (2007). Species-specific testicular and hepatic microsomal metabolism of benzo(a)pyrene, an ubiquitous toxicant and endocrine disruptor. *Toxicol. In Vitro* **21,** 753-8.

Steinberger, E., and Rodriguez-Rigau, L. J. (1983). The infertile couple. *J. Androl* **4,** 111-8.

Straif, K., Baan, R., Grosse, Y., Secretan, B., El Ghissassi, F., and Cogliano, V. (2005). Carcinogenicity of polycyclic aromatic hydrocarbons. *The Lancet Oncology* **6,** 931-2.

Sun, J. D., Wolff, R. K., and Kanapilly, G. M. (1982). Deposition, retention, and biological fate of inhaled benzo(a)pyrene adsorbed onto ultrafine particles and as a pure aerosol. *Toxicol. Appl. Pharmacol.* **65,** 231-44.

Sun, J. G., Jurisicova, A., and Casper, R. F. (1997). Detection of deoxyribonucleic acid fragmentation in human sperm: correlation with fertilization in vitro. *Biol. Reprod.* **56,** 602-7.

Sunesen, M., Stevnsner, T., Brosh Jr, R. M., Dianov, G. L., and Bohr, V. A. (2002). Global genome repair of 8-oxoG in hamster cells requires a functional CSB gene product. *Oncogene* **21,** 3571-8.

Sutovsky P., and Manandhar G. (2006). Mammalian spermatogenesis and sperm structure: anatomical and compartmental analysis. In 'The Sperm Cell'. (Eds DeJonge C and Barratt C) pp. 1-30. (Cambrigde University Press: Cambrigde).

Takao, M., Kanno, S., Kobayashi, K., Zhang, Q. M., Yonei, S., Van Der Horst, G. T., and Yasui, A. (2002). A back-up glycosylase in Nth1 knock-out mice is a functional Nei (endonuclease VIII) homologue. *J. Biol. Chem.* **277,** 42205-13.

Tani, M., Shinmura, K., Kohno, T., Shiroishi, T., Wakana, S., Kim, S. R., Nohmi, T., Kasai, H., Takenoshita, S., Nagamachi, Y., and Yokota, J. (1998). Genomic structure and chromosomal localization of the mouse Ogg1 gene that is involved in the repair of 8-hydroxyguanine in DNA damage. *Mamm. Genome* **9,** 32-7.

Tiemann-Boege, I., Navidi, W., Grewal, R., Cohn, D., Eskenazi, B., Wyrobek, A. J., and Arnheim, N. (2002). The observed human sperm mutation frequency cannot explain the achondroplasia paternal age effect. *Proc. Natl. Acad. Sci. U. S. A* **99,** 14952-7.

Twigg, J. P., Irvine, D. S., and Aitken, R. J. (1998). Oxidative damage to DNA in human spermatozoa does not preclude pronucleus formation at intracytoplasmic sperm injection. *Hum. Reprod.* **13,** 1864-71.

van der Kemp, P. A., Thomas, D., Barbey, R., de, O. R., and Boiteux, S. (1996). Cloning and expression in Escherichia coli of the OGG1 gene of Saccharomyces cerevisiae, which codes for a DNA glycosylase that excises 7,8-dihydro-8-oxoguanine and 2,6-diamino-4-hydroxy-5-N-methylformamidopyrimidine. *Proc. Natl. Acad. Sci. U. S. A* **93,** 5197-202.

van Hoffen, A., Balajee, A. S., van Zeeland, A. A., and Mullenders, L. H. (2003). Nucleotide excision repair and its interplay with transcription. *Toxicology* **193,** 79-90.

Van Loon, A. A., Den Boer, P. J., Van der Schans, G. P., Mackenbach, P., Grootegoed, J. A., Baan, R. A., and Lohman, P. H. (1991). Immunochemical detection of DNA damage induction and repair at different cellular stages of spermatogenesis of the hamster after in vitro or in vivo exposure to ionizing radiation. *Exp. Cell Res.* **193,** 303-9.

Van Loon, A. A., Sonneveld, E., Hoogerbrugge, J., Van der Schans, G. P., Grootegoed, J. A., Lohman, P. H., and Baan, R. A. (1993). Induction and repair of DNA single-strand breaks and DNA base damage at different cellular stages of spermatogenesis of the hamster upon in vitro exposure to ionizing radiation. *Mutat. Res.* **294,** 139-48.

Verhofstad, N., Linschooten, J. O., van, B. J., Dubrova, Y. E., van, S. H., Van Schooten, F. J., and Godschalk, R. W. (2008). New methods for assessing male germ line mutations in humans and genetic risks in their offspring. *Mutagenesis* **23,** 241-7.

Vogel, F., and Rathenberg, R. (1975). Spontaneous mutation in man. *Adv. Hum. Genet.* **5,** 223-318.

Wallace, S. S. (1994). DNA damages processed by base excision repair: biological consequences. *Int. J. Radiat. Biol.* **66,** 579-89.

Wallace, S. S. (2002). Biological consequences of free radical-damaged DNA bases. *Free Radic. Biol. Med.* **33,** 1-14.

Ward, J. F. (1988). DNA damage produced by ionizing radiation in mammalian cells: identities, mechanisms of formation, and reparability. *Prog. Nucleic Acid Res. Mol. Biol.* **35,** 95-125.

Ward, J. F. (1994). The complexity of DNA damage: relevance to biological consequences. *Int. J. Radiat. Biol.* **66,** 427-32.

Weinfeld, M., Rasouli-Nia, A., Chaudhry, M. A., and Britten, R. A. (2001). Response of base excision repair enzymes to complex DNA lesions. *Radiat. Res.* **156,** 584-9.

Wenger, R. H., and Katschinski, D. M. (2005). The hypoxic testis and post-meiotic expression of PAS domain proteins. *Semin. Cell Dev. Biol.* **16,** 547-53.

Weyand, E. H., and Bevan, D. R. (1986). Benzo(a)pyrene disposition and metabolism in rats following intratracheal instillation. *Cancer Res.* **46,** 5655-61.

WHO (1998). 'Selected non-heterocyclic polycyclic aromatic hydrocarbons.' (World Health Organization: Geneva).

Will, O., Gocke, E., Eckert, I., Schulz, I., Pflaum, M., Mahler, H. C., and Epe, B. (1999). Oxidative DNA damage and mutations induced by a polar photosensitizer, Ro19-8022. *Mutat. Res.* **435,** 89-101.

Xue, W., and Warshawsky, D. (2005). Metabolic activation of polycyclic and heterocyclic aromatic hydrocarbons and DNA damage: a review. *Toxicol. Appl. Pharmacol.* **206,** 73-93.

Yu, D., Berlin, J. A., Penning, T. M., and Field, J. (2002). Reactive oxygen species generated by PAH o-quinones cause change-in-function mutations in p53. *Chem. Res. Toxicol.* **15,** 832-42.

Zenzes, M. T., Bielecki, R., and Reed, T. E. (1999a). Detection of benzo(a)pyrene diol epoxide-DNA adducts in sperm of men exposed to cigarette smoke. *Fertil. Steril.* **72,** 330-5.

Zenzes, M. T., Puy, L. A., Bielecki, R., and Reed, T. E. (1999b). Detection of benzo[a]pyrene diol epoxide-DNA adducts in embryos from smoking couples: evidence for transmission by spermatozoa. *Mol. Hum. Reprod.* **5,** 125-31.

Zitzmann, M., Rolf, C., Nordhoff, V., Schrader, G., Rickert-Fohring, M., Gassner, P., Behre, H. M., Greb, R. R., Kiesel, L., and Nieschlag, E. (2003). Male smokers have a decreased success rate for in vitro fertilization and intracytoplasmic sperm injection. *Fertil. Steril.* **79 Suppl 3,** 1550-4.

# 6 Appendix A

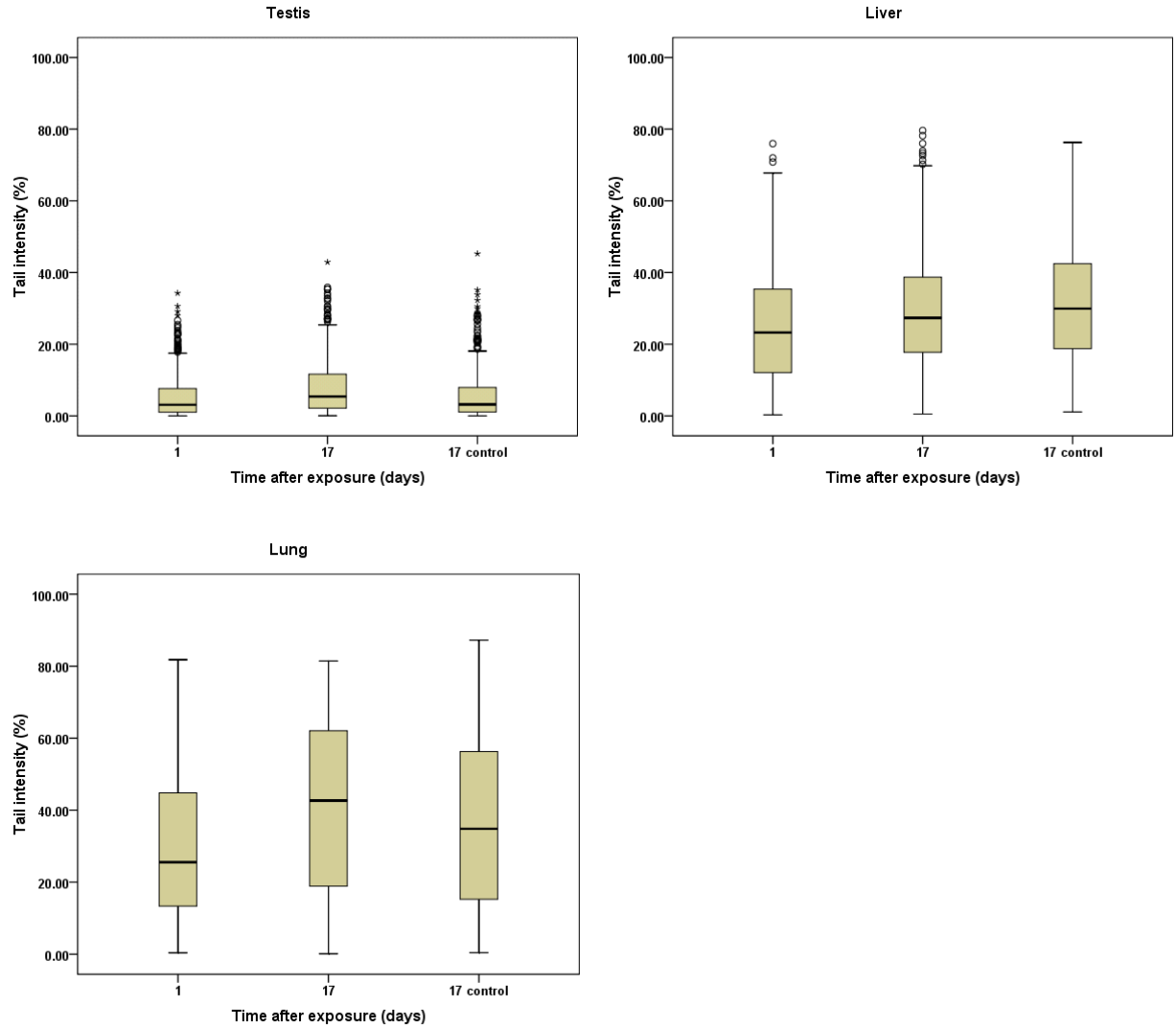


**Figure 6-1 *Ogg1*$^{-/-}$ boxplot. Time after exposure are shown on the x-axis and tail intensity (%) on the y-axis. 1 and 17 days after BaP exposure and 17 days after exposure to vehicle (17 control) shown are the basis for the statistical analysis performed on the *Ogg1*$^{-/-}$ data with three mice. The line across the inside of the box marks the median (50$^{th}$ percentile), the length of the box is the interquartile range (IQR) (25$^{th}$ and 75$^{th}$ percentile, 50% of the cases), the protruding lines (whiskers) goes out to the smallest and largest values (< 1.5 x IQR), the circles represents outliers (> 1.5 x IQR) and asterix (*) represent extreme points (> 3 x IQR).**

# 7 Appendix B

## 7.1 Solutions and media

**0.75% Agarose solution (low melting point)**

Added 0.075 g NuSieve GTG Low melting agarose to 10 ml of 10 mM EDTA-solution, warmed up to boiling point until the Agarose are dissolved and held warm in a warming block at 37 °C.

**15% Acrylamide gel**

50 µl 10 % APS

200 µl 50X TAE

3 ml Long Ranger® Gel Solution

6.8 ml $dH_2O$

5 µl Temed

**10% Ammonium persulfate (APS)**

10 g APS

100 ml $dH_2O$

Storage at -20 °C

**10 mM EDTA-solution (for 0.75% Agarose solution)**

1.86 g $Na_2EDTA$ was dissolved in 500 ml PBS without Ca and Mg and pH was adjusted to 7.4 with NaOH.

**Merchant's buffer**

0.14 M NaCl

1.47 mM $KH_2PO_4$

2.7 mM KCl

8.1 mM $Na_2HPO_4$

10 mM EDTA

Dissolved in sterile $H_2O$, pH adjusted to 7.4 and stored at 4 °C.

**Lysis fluid for Comet (stock)**

2.5 M* NaCl

100 mM* EDTA

10 mM* Tris-base

1%* SLS

Dissolved in $dH_2O$, before SLS was added pH was adjusted to approximately 10 with NaOH pellet. The stock was leaved to stir until everything was dissolved, and then was pH adjusted again to 10 with concentrated HCl or 10N NaOH.

*) This is stock fluid, final concentration was achieved after addition of DMSO and Triton-X

**Lysis fluid for Comet (for four GelBond® films)**

300 ml Lysis fluid stock

10% DMSO (33.3 ml)

1% Triton-X (3.33 ml)

**Neutralising buffer**

0.4 M Tris-base

Dissolved in $dH_2O$ and pH adjusted to 7.5 with concentrated HCl.

**Electrophoresis buffer for Comet**

10 M NaOH

200 mM EDTA

Dissolved in $dH_2O$ and pH adjusted to 13.2 with concentrated HCl.

**Enzyme reaction buffer for Comet**

40 mM Hepes

0.1 M KCl

0.5 mM EDTA

Dissolved in $dH_2O$ and pH adjusted to 7.6 with 7M KOH.

**TE-buffer**

1 mM EDTA

10 mM Tris-HCl

Dissolved in $dH_2O$ and pH adjusted to 8.0.

**RPMI 1640 medium with FCS**

500 ml bottle RPMI 1640 medium with 25 mM Hepes and L-glutamine

10% FCS (foetal calf serum)

0.1 mg/ml Sodium pyruvate

5 mM DL-lactic acid

**Electrophoresis buffer for PCR (5X)**

25 mM Trizma base (15.5 g)

192 mM Glycine (72 g)

Dissolve in 900 ml $dH_2O$

0.1% SDS (50 ml 10% SDS)

Adjust the volume to 1000 ml with $dH_2O$

**Electrophoresis buffer for PCR (1X)**

200 ml 5X Electrophoresis buffer for PCR

800 ml $dH_2O$

**Loading buffer for PCR (6X, 20 ml)**

12% Ficoll-400 (2.4 g)

0.6% EDTA (2.4 ml)

0.15% Bromphenol blue (30 mg)

0.15% Xylene cyanol (30 mg)

**Proteinase K**

10 mg Proteinase K dissolved in 1 ml $dH_2O$

**10% Sodium dodecyl sulfate (SDS)**

10 g SDS

100 ml $dH_2O$

pH adjusted to 7.5

**Ro 12-9786 stock**

1.2 mM Ro 12-9786 diluted in DMSO

**Lysis Solution/2-ME Mixture**

10 µl 2-mercaptoethanol (2-ME) per 1 ml Lysis Solution (1:100)

## 7.2 Products and producers

| Product | Producer | Country |
|---|---|---|
| 2-Mercaptoethanol | Sigma | France |

| | | |
|---|---|---|
| Absolutt alkohol prima (100% ethanol) | Arkus kjemi | Norway |
| Agilent RNA 6000 Nano Kit | Agilent Technologies | USA |
| Ammonium persulphate | BioRad | Canada |
| AmpliTaq Gold® buffer | Applied Biosystems | Switzerland |
| AmpliTaq Gold® DNA polymerase | Applied Biosystems | Switzerland |
| AmpliTaq Gold® $MgM_2$ | Applied Biosystems | Switzerland |
| Benzo(*a*)pyrene | Sigma | USA |
| Bio Whittaker® RPMI 1640 medium | Lonza | Belgium |
| Bovine serum albumine (BSA) | Sigma | USA |
| Bromphenol blue | Sigma | USA |
| Corn Oil | Mills | Norway |
| Desferal | Qiagen | Germany |
| Dimethyl sulphoxide (DMSO) | Merck | Germany |
| Distilled water, DNase, RNase Free | Gibco | USA |
| DL-lactic acid | Sigma | Norway |
| DNA Extractor WB Kit | Wako | Japan |
| Ethylenediaminetetraacetic acid disodium salt dihydrate (EDTA-$Na_2$) | Sigma | USA |
| Ficoll-400 | Sigma | USA |
| Foetal calf serum (FCS) | Gibco | USA |
| Fpg | Locally produced | Norway |
| GelBond® Film | Cambrex | USA |
| GeneElute Mammalian Total RNA Miniprep Kit | Sigma | USA |
| GeneRuler 100 bp DNA ladder and loading buffer | Fermentas | Sweeden |
| Glycerol | Sigma | USA |
| Glycine | Sigma | South Korea |
| Hepes | Sigma | USA |
| High-Capacity cDNA Reverse Transcription Kit, without RNase (200 | Applied Biosystems | USA |

| | | |
|---|---|---|
| reactions) | | |
| Hydrogen chloride (HCl) | Merck | Germany |
| Isopropanol prima | Arcus kjemi | Norway |
| Long Ranger® Gel Solution | Lonza | USA |
| MicroAmp 96-well reaction plate | Applied Biosystems | Singapore |
| Mm_Actb_2_SG QuantiTect Primer Assay (200 reactions) | Qiagen | Germany |
| Mm_Akr1a4_1_SG QuantiTect Primer Assay (200 reactions) | Qiagen | Germany |
| Mm_Cyp1a1_1_SG QuantiTect Primer Assay (200 reactions) | Qiagen | Germany |
| Mm_Cyp1a2_1_SG QuantiTect Primer Assay (200 reactions) | Qiagen | Germany |
| Mm_Cyp1b1_2_SG QuantiTect Primer Assay (200 reactions) | Qiagen | Germany |
| Mm_Rn18s_2_SG QuantiTect Primer Assay (200 reactions) | Qiagen | Germany |
| NuSieve GTG Low Melting Agarose | Cambrex | USA |
| Ogg1 | Sigma Genosys | Canada |
| Ogg1 ko | Sigma Genosys | Canada |
| Ogg1 wt | Sigma Genosys | Canada |
| Pestle (for homogenising tissue) | VWR | UK |
| Phosphate buffer solution (PBS) | Locally produced | Norway |
| Potassium cloride (KCl) | Merck | Germany |
| Potassium dihydrogenphosphate (KH2PO4) | Merck | Germany |
| Potassium hydroxide (KOH) | Merck | Germany |
| Power SYBR® Green PCR Master Mix | Applied Biosystems | UK |
| Proteinase K | Merch | Germany |
| RNace-1t™ Ribonuclease cocktail (RNaseT1 and RNaseA) | Stratagene | Canada |
| Sodium chloride (NaCl) | Merck | Germany |

| | | |
|---|---|---|
| Sodium dodecyl sulphate (SDS) | Fluka | Japan |
| Sodium hydrogenphosphate (Na2HPO4) | Merck | Germany |
| Sodium Hydroxide (NaOH) | Merck | Germany |
| Sodium lauryl sarcosinate (SLS) | Sigma | UK |
| Sodium pyruvate | Sigma | Japan |
| Sterile water | Fresenius Kabi | Norway |
| SYBR® Gold | Invitrogen | USA |
| SYBR® Green | Sigma | USA |
| Temed | BioRad | Canada |
| Trisma® HCl | Sigma | USA |
| Triton-X | Sigma | USA |
| Trizma® base (Tris (hydroxymethyl)-aminomethane, Tris-base) | Sigma | USA |
| Tween20 | BioRad | Canada |
| Xylene cyanole | Sigma | USA |